University of Zagreb
Faculty of Mechanical Engineering and Naval Architecture

Mario Sremec

Experimental Investigation of Influence of Dual-Fuel Engine Operating Parameters on Combustion, Efficiency and Exhaust Gas Emissions

DOCTORAL THESIS

Zagreb, 2018

University of Zagreb
Faculty of Mechanical Engineering and Naval Architecture

Mario Sremec

Experimental Investigation of Influence of Dual-Fuel Engine Operating Parameters on Combustion, Efficiency and Exhaust Gas Emissions

DOCTORAL THESIS

Supervisor: prof. Darko Kozarac, PhD

Zagreb, 2018

Sveučilište u Zagrebu

Sveučilište u Zagrebu
Fakultet strojarstva i brodogradnje

Mario Sremec

Eksperimentalno istraživanje utjecaja radnih parametara dvogorivnog motora na način izgaranja, učinkovitost i emisiju štetnih tvari

DOKTORSKI RAD

Mentor: prof. dr. sc. Darko Kozarac

Zagreb, 2018.

BIBLIOGRAPHY DATA

UDC

Keywords:	dual-fuel, compression ignition, compressed natural gas, methane, alternative fuel, diesel fuel, HCCI combustion mode, combustion parameters
Scientific area:	Technical sciences
Scientific field:	Mechanical engineering
Institution:	Faculty of Mechanical Engineering and Naval Architecture, University of Zagreb
Supervisor:	Darko Kozarac, PhD, professor
Number of pages:	161
Number of figures:	119
Number of tables:	21
Number of references:	111
Date of public defense:	5th December 2018
Committee members:	Zoran Lulić, PhD, full professor Momir Sjerić, PhD, assistant professor Vladimir Medica, PhD
Archieve:	Faculty of Mechanical Engineering and Naval Architecture, University of Zagreb, Croatia

Acknowledgments

First of all, I would like to thank my supervisor, prof. Darko Kozarac, PhD for giving me the opportunity to perform the research outlined in this thesis and for his help and expertise over the last four years.

Next I would like to thank all members of Department of Internal Combustion Engines and Motor Vehicles at Faculty of Mechanical Engineering and Naval Architecture for unselfish help and improving a good working atmosphere during my research and postgraduate study.

The greatest thank goes to my wife Ivana and to my family for the support they have given me during my research.

The research presented in this thesis was supported by the Croatian Science Foundation and Faculty of Mechanical Engineering and Naval Architecture within the project "Experimental Research, Optimization and Characterization of piston engine operation with DUal-Fuel COmbustion - DUFCOROC" IP-2014-09-1089. This support is gratefully appreciated.

Contents

Abstract

The strict regulations related to exhaust gas emissions from internal combustion engines in the transport sector, created by governments around the world, forces manufacturers to improve existing combustion techniques, develop new ones and apply alternative, environmentally more acceptable fuels. In this context, natural gas is recognized as an alternative fuel which can be used both in spark ignition and compression ignition engines with a number of benefits. In recent years, special attention has been given to the research of diesel-natural gas dual-fuel combustion, which has potential to reduce greenhouse gas emissions, as well as harmful exhaust gas emissions. Given that this combustion technique is not fully investigated, but can be easily used in existing diesel engines, there is a need for further improvement, which is the main objective of this work.

The purpose of the research is to experimentally examine possibilities of using compressed natural gas in conventional dual-fuel internal combustion engine, with goals that include achieving maximum efficiency and maintaining exhaust gas emissions on permitted levels. Special attention was given to the improvement of characteristics at low and high loads, where dual-fuel shows some disadvantages compared to the normal diesel operation. By using the fully flexible fuel injection system and exhaust gas recirculation, there were achieved different combustion techniques including: diffusion flame combustion, premixed flame propagation and premixed chemically controlled combustion of homogeneous or stratified mixture. It is shown that adequate injection strategies in combination with other operating parameters can significantly improve exhaust gas emissions from dual-fuel engine. Finally, recommendations for selecting operating parameters at low and high loads are given.

Keywords: dual-fuel, compression ignition, compressed natural gas, methane, alternative fuel, diesel fuel, HCCI combustion mode, combustion parameters

Prošireni sažetak

Osnovni cilj ove disertacije je istraživanje mogućnosti korištenja prirodnog plina (PP) u dvogorivnom (eng. Dual-fuel) motoru s unutarnjim izgaranjem. Dvogorivni motori su modificirani Dieselovi motori kod kojih se prirodni plin koristi kao glavno gorivo, a njegovo izgaranje se inicira ubrizgavanjem male količine dizelskog goriva. Korištenje PP-a uz dizelsko gorivo pogodno je zbog čišćeg izgaranja, široke dostupnosti te potencijala za smanjenje emisije štetnih tvari u ispušnim plinovima.

Glavni cilj istraživanja bio je ispitati ostvarive performanse motora i emisije koje nastaju pri dvogorivnom izgaranju. Prema pregledu literature, takvi motori imaju određenih problema pri niskim i visokim opterećenjima pa je posebna pozornost posvećena istraživanju upravljanja radom u tim radnim područjima. Na postojeći motor eksperimentalnog postava dograđen je potpuno fleksibilan sustav dobave dizelskog goriva koji omogućuje, uz korištenje povrata ispušnih plinova, postizanje različitih tehnika izgaranja koje uključuju: izgaranje difuzijskim plamenom, kombinirano izgaranje difuzijskim i predmješanim turbulentnim plamenom te predmješano kemijski uvjetovano izgaranje homogene ili slojevite smjese. Ostvarenim rezultatima pokazano je da se korištenjem adekvatne strategije ubrizgavanja u kombinaciji s ostalim radnim parametrima može značajno poboljšati izgaranje u dvogorivnom motoru, čime se postižu niže emisije štetnih tvari uz istu ili poboljšanu učinkovitost. Na kraju istraživanja, prikazane su smjernice za izbor radnih parametara na niskom i visokom opterećenju.

Uvod i pregled dosadašnjih istraživanja

Kao rezultat kontinuiranog industrijskog rasta i kontinuiranog rasta broja stanovnika, potrošnja energije u stalnom je porastu, a obzirom da se trendovi porasta svjetske populacije ne mijenjaju, očekuje se nastavak dosadašnjeg trenda povećanja potrošnje energije [1]. Obzirom da se očekuje nastavak upotrebe motora s unutarnjim izgaranjem, i obzirom da se većina svjetskih rezervi nafte nalazi na politički nestabilnim područjima, postoji potreba za sigurnim i održivim izvorima energije [2].

Transport je već neko vrijeme prepoznat kao jedan od većih onečišćivača okoliša pa postoji potreba za smanjenjem njegovog negativnog utjecaja. S tim ciljem su vlade širom

svijeta nametnule niz propisa kojima se nastoji smanjiti emisija štetnih tvari iz motora s unutarnjim izgaranjem korištenih u transportu [5], [6].

Suvremena istraživanja u području motora s unutarnjim izgaranjem usmjerena su prema optimizaciji procesa izgaranja i upotrebi čišćih, ekološki prihvatljivijih goriva. U tom je kontekstu prirodni plin prepoznat kao potencijalna zamjena za konvencionalna tekuća goriva [2]. Glavni sastojak prirodnog plina je metan (CH_4) koji izgara čišće od ostalih konvencionalnih goriva i daje potencijal za smanjenje emisije CO_2 do 25% zbog visokog omjera vodika prema ugljiku [9], [10]. U usporedbi s konvencionalnim tekućim gorivima (benzin i dizelsko gorivo), glavni sastojak prirodnog plina, metan, ima veću oktansku vrijednost, veću donju ogrjevnu vrijednost po jedinici mase (J/kg), veću stehiometrijsku količinu zraka za izgaranje te znatno manju gustoću i molarnu masu [13]. Iako ima veću donju ogrjevnu vrijednost, veća stehiometrijska količina zraka znači da se u cilindru nalazi manja masa goriva po jedinici mase zraka, što znači da je sadržaj energije u cilindru približno jednak kao i pri pogonu s konvencionalnim tekućim gorivima. Zbog znatno manje gustoće od konvencionalnih goriva, prirodni plin za pohranu iste količine energije treba znatno veći spremnik.

Iako bi se, zbog veće oktanske vrijednosti prirodnog plina od benzina, u Ottovom motoru mogli postići viši kompresijski omjeri i time ostvariti i veće iskoristivosti, njegova primjena u takvom motoru ima cijeli niz nedostataka. Da bi se izbjegle povišene temperature i emisije dušikovih oksida svele na dozvoljene vrijednosti, motor treba pogoniti siromašnom smjesom [10], [18]. Zbog manje molekularne mase od konvencionalnih goriva, metan istiskuje više zraka pa je na taj način stupanj punjenja motora manji. Svi ovi nedostaci sprječavaju Ottov motor pogonjen prirodnim plinom da dosegne efikasnosti Dieselovog motora [19]. Važan nedostatak kod primjene u Ottovom motoru s visokim kompresijskim omjerom je i doseg vozila pogonjenog prirodnim plinom, zbog nedostatne infrastrukture za punjenje plina.

Dieselov motor ima znatno veći kompresijski omjer, a time i veći stupanj djelovanja u odnosu na Ottov motor. Prirodni plin se ne može samostalno koristiti u Dieselovom motoru jer teško dolazi do samozapaljenja smjese zbog premalog cetanskog broja [2], [9]. Iz tog se razloga prirodni plin koristi uz dodatak goriva s velikim cetanskim brojem (dizelsko gorivo) [2], [10]. Ovakav tip motora naziva se dvogorivni. U motorima s dvogorivnim načinom izgaranja, mješavina prirodnog plina i zraka neposredno prije gornje mrtve točke pali se plamenom odgovarajuće ubrizgane količine dizelskog goriva (pilot mlaz dizelskog goriva) [2], [9], [10], [13], [19]. Pored konvencionalnog dvogorivnog motora kod kojeg se plin

ubrizgava u usisnu cijev, a dizelsko gorivo izravno u cilindar, postoji i druga izvedba (HPDI, *engl. High Pressure Direct Injection*) kod koje se oba goriva ubrizgavaju direktno u cilindar [31]. Ovaj drugi model izgaranja potpuno je novi i zahtijeva izradu novog motora namijenjenog isključivo HPDI dvogorivnom načinu izgaranja. Istraživanje u sklopu ove disertacije provedeno je na konvencionalnom tipu motora jer se radi o preradi standardnog Dieselovog motora na dvogorivni. Kod ovog tipa motora jednostavan je prelazak na rad s isključivo dizelskim gorivom, što mu daje veliku prednost u korištenju ako se u blizini ne nalazi stanica za punjenje prirodnog plina [2].

Na temelju pregledane literature, može se zaključiti da dvogorivni način izgaranja sadrži karakteristike izgaranja Ottovog i Dieselog motora. Općenito se smatra da se dvogorivni način izgaranja sastoji od tri faze: predmiješano (kemijski kontrolirano) izgaranje dizelskog goriva, izgaranje prirodnog plina u području u kojem izgara dizelsko gorivo i višestruko širenje plamena kroz prostor izgaranja [10].

Dosadašnja eksperimentalna istraživanja pokazala su da je dvogorivni način izgaranja pogodan za smanjenje dušikovih oksida (NO_X) i krutih čestica uz zadržavanje visoke učinkovitosti [26], [31], [38], [40]. Iako je ovakav način izgaranja pokazao veliki potencijal, i dalje postoje određeni nedostatci među kojima su najznačajniji: povećane emisije ugljikovodika (HC) i ugljikovog monoksida (CO) pri niskom opterećenju [26], [31], [38], [40], [41], smanjenje iskoristivosti uz povećanu potrošnju goriva te sklonost samozapaljenju i detonaciji pri visokom opterećenju [10], [42]. Navedeni problemi na niskom opterećenju posljedica su niskih temperatura u cilindru i siromašne smjese, zbog čega je širenje plamena sporije [26], [41], [43]. Neka od mogućih rješenja za rad pri niskom opterećenju su: smanjenje tlaka usisa, optimizacija tlaka ubrizgavanja, optimizacija trenutka i količine ubrizganog dizelskog goriva, zagrijavanje usisa, poboljšanje miješanja smjese prirodnog plina i zraka te povrat ispušnih plinova natrag u cilindar (EGR). Rad motora uz smanjenje tlaka usisa uzrokuje veće gubitke izmjene radnog medija što utječe na stupanj djelovanja motora. S druge strane, to će povećati korisnost izgaranja, a time možda i stupanj djelovanja motora. Optimizacija tlaka i vremena ubrizgavanja, zajedno s promjenama u količini pilot mlaza dizelskog goriva može utjecati na proces izgaranja na dva načina. Može se poboljšati širenje fronte plamena unutar cilindra, a može se i izazvati tzv. HCCI (*engl. Homogeneous Charge Compression Ignition*) način izgaranja, koji se može ostvariti ubrizgavanjem određene količine pilot mlaza dizelskog goriva za vrijeme usisa. Kod HCCI načina izgaranja, relativno homogena i izrazito osiromašena smjesa komprimira se u stanje gdje se pojavljuje samopazaljenje smjese. Pri visokom opterećenju javljaju se drugačiji problemi. Specifična

potrošnja goriva je manja u odnosu na Dieselov motor, ali zbog manje učinkovitosti izgaranja uzrokovane nemogućnošću napredovanja fronte plamena kroz zonu procjepa, primijećene su veće emisije HC i CO [10], [26], [31], [40]. Neke studije također ukazuju na probleme koji se povezuju sa samozapaljenjem, detonacijom [29] i visokim temperaturama vrha brizgaljke pri visokom opterećenju [10]. Iako je u nekim istraživanjima pokazano da se učinkovitosti slične Dieselovom motoru uz niske emisije čestica i niske emisije NO_X mogu ostvariti i s dvogorivnim načinom izgaranja [40], [41], postoje istraživanja koja ukazuju na smanjenje učinkovitosti u čitavom radnom području i povećanje emisije NO_X pri određenim opterećenjima [31].

Sveobuhvatni zaključak je da određene performanse motora i emisije ispušnih plinova ovise o geometriji prostora izgaranja, udjelu prirodnog plina [26], [41], [43], količini dizelskog goriva [13], karakteristikama brizgaljke [10], tlaku i temperaturi usisa [49], te količini EGR-a [9], [50], [51]. Općenito se može reći da dvogorivni način rada pokazuje neke prednosti s obzirom na NO_X emisije i na krute čestice, uz glavne nedostatke vezane uz HC i CO emisije.

Iako su utjecaji pojedinih parametara pojedinačno istraživani, postoji potreba za generalnim preporukama o izboru radnih parametara u dvogorivnom motoru u ovisnosti o opterećenju. Prema tome, variranjem ulaznih parametara (posebno strategije ubrizgavanja i količine EGR-a) tražit će se različite tehnike izgaranja koje bi mogle rezultirati poboljšanjem performansi i emisija dvogorivnog motora.

Ovo će istraživanje objasniti nepoznanice u spoznajama specifičnog načina izgaranja i doprinijet će razvoju motora s unutarnjim izgaranjem s nižom potrošnjom i emisijom ispušnih plinova, na način da se za pojedine uvjete rada motora daju smjernice za izbor radnih parametara.

Ciljevi i hipoteze istraživanja

Osnovni cilj ovog istraživanja je ispitati mogućnosti postizanja visoke učinkovitosti uz dozvoljenu emisiju štetnih tvari, pri niskom i visokom opterećenju motora koji radi s dvogorivnim načinom izgaranja. Da bi se taj osnovni cilj ostvario potrebno je ostvariti dva preduvjeta: istražiti utjecaj primjene različitih strategija ubrizgavanja kao i HCCI izgaranja na rad dvogorivnog motora te istražiti utjecaj primjene povrata ispušnih plinova (EGR) na rad dvogorivnog motora.

U skladu s ciljevima predloženog istraživanja hipoteze istraživanja su:

- Primjenom prilagodljivog sustava ubrizgavanja dizelskog goriva i prirodnog plina, te upotrebom povrata ispušnih plinova moguće je unutar dvogorivnog motora ostvariti izgaranje difuzijskim plamenom, kombinirano izgaranje difuzijskim i predmješanim turbulentnim plamenom te predmješano kemijski uvjetovano izgaranje homogerne ili slojevite smjese.
- Primjenom odgovarajućeg tipa izgaranja moguće je ostvariti rad dvogorivnog motora s visokom učinkovitosti i niskom emisijom štetnih tvari kako u području visokog, tako i u području niskog opterećenja motora.

Pregled doktorskog rada

Da bi se zadovoljili prethodno postavljeni ciljevi i potvrdile postavljene hipoteze, istraživanje je podijeljeno u 6 glavnih poglavlja:

1) U uvodnom dijelu opisano je područje istraživanja, u kojem je, uz opis konvencionalnih motora s unutarnjim izgaranjem i konvencionalnih goriva, stavljen naglasak na prirodni plin i na njegovu upotrebu u dvogorivnom motoru. Uz opsežan pregled literature, definirani su ciljevi rada i postavljene hipoteze.

2) U drugom dijelu provedene su numeričke 1-D simulacije rada motora koje će se kasnije koristiti za eksperimentalna istraživanja. S obzirom da se za eksperimentalna istraživanja koristi Dieselov motor prilagođen za dvogorivni način rada na način da se plinovito gorivo ubrizgava u usisnu cijev, postoji mogućnost bježanja dijela goriva u ispuh zbog pozitivnog preklapanja ventila. Dieselovi motori zbog boljeg ispiranja cilindara koriste dosta pozitivno preklapanje ventila, što je negativna pojava u slučaju ubrizgavanja goriva u usisnu cijev. Glavni cilj provođenja simulacija bio je utvrđivanje optimalnog vremena ubrizgavanja plinovitog goriva u usisnu cijev kako bi bježanje goriva kroz cilindar u ispuh bilo minimalno. Simulacije su provedene u programskom paketu AVL Boost v2013 koji se koristi za cikličke simulacije kompletnog motornog sustava s naglaskom na strujanje kroz motor i izgaranje u cilindru. Simulacije su provedene na četiri brzine vrtnje (1000, 1500, 2000 i 3000 min^{-1}) i dva različita tlaka na usisu (1 bar i 2,2 bara). Simulirano je 6 različitih trenutaka ubrizgavanja plina (početak ubrizgavanja: 100, 200, 300, 400, 500, 600 °KV nakon GMT) i dva trajanja ubrizgavanja (90° i 180° zakreta koljenastog vratila).

Glavni zaključci istraživanja temeljeni na provedenim simulacijama su:

- bježanje goriva zbog pozitivnog preklapanja ventila najizraženije je na brzini 1000 min^{-1} i iznosi 0,6 % kod usisnog tlaka 1 bar i 2,3 % kod usisnog tlaka 2,2 bara za kontinuirano ubrizgavanje;

- na većim brzinama (2000 i 3000 min^{-1}) bježanje goriva je vrlo malo (zanemarivo);
- optimalno isprekidano ubrizgavanje smanjuje bježanje goriva u ispuh za ~ 50 % u odnosu na kontinuirano ubrizgavnje, dok neadekvatno isprekidano ubrizgavnje može dodatno povećati bježanje u ispuh za 62 % u odnosu na kontinuirano ubrizgavanje;
- optimalno ubrizgavanje povećava učinkovitost motora.

3) U trećem poglavlju opisan je eksperimentalni postav na kojem je provedeno istraživanje. Glavni naglasak stavljen je na preradu motora s Dieselovog na dvogorivni način rada, odnosno na obradu glave motora i zamjenu postojećeg sustava dobave dizelskog goriva s novim, *common rail* sustavom. Prikazan je detaljan opis novo-ugrađenog *common rail* sustava koji uključuje odabir brizgaljke, visokotlačne pumpe i ostalih potrebnih elemenata. Na taj način, uz fleksibilno ubrizgavanje plinovitog goriva u usisnu cijev, ostvaren je potpuno fleksibilan sustav upravljanja s oba korištena goriva. Umjesto prirodnog plina, korišten je metan iz boce. Također, opisana je i mjerna oprema s pripadajućim mjernim nesigurnostima, kao i oprema za upravljanje i kontrolu rada cijelog eksperimentalnog postava. Na kraju, opisana je oprema i način prikupljanja, te obrada izmjerenih podataka.

4) U četvrom poglavlju prikazano je eksperimentalno istraživanje upotrebe prirodnog plina u motoru s vanjskim izvorom paljenja (Ottovom motoru). S obzirom da eksperimentalni postav ima veliku fleksibilnost po pitanju mogućnosti ispitivanja, pa čak i promjenu s Dieselovog načina rada na Ottov način rada, ispitana je mogućnost primjene PP-a u Ottovom načinu rada na tri kompresijska omjera s tri različita faktora pretička zraka. Kako prirodni plin ima predispozicije za korištenje na visokom kompresijskom omjeru, istraživanje je provedeno na kompresijskim omjerima ε = 12, 16 i 18 kako bi se eksperimentalni rezultati mogli usporediti s postojećim Ottovim motorima (uobičajeni kompresijski omjer do ε = 14) i postojećim Dieselovim motorima (kompresijski omjer ε = 16 i više). Osnovni rezultati prikazani su na slici 1., slici 2. i slici 3.

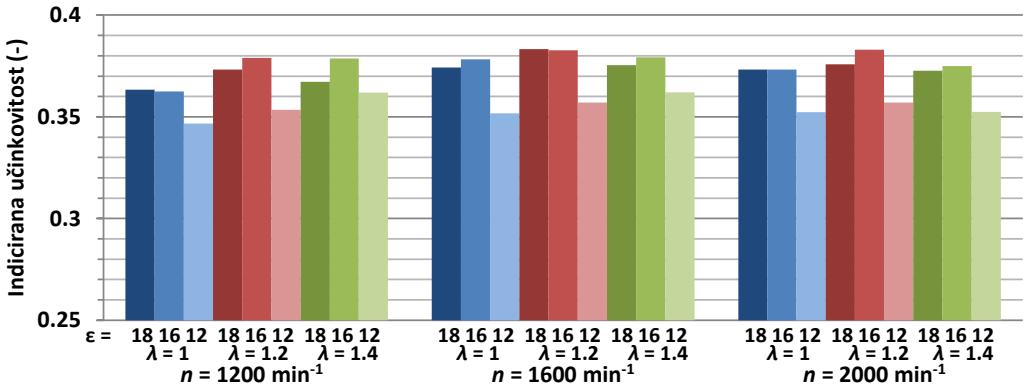

Slika 1. Indicirana učinkovitost - PP u Ottovom načinu rada

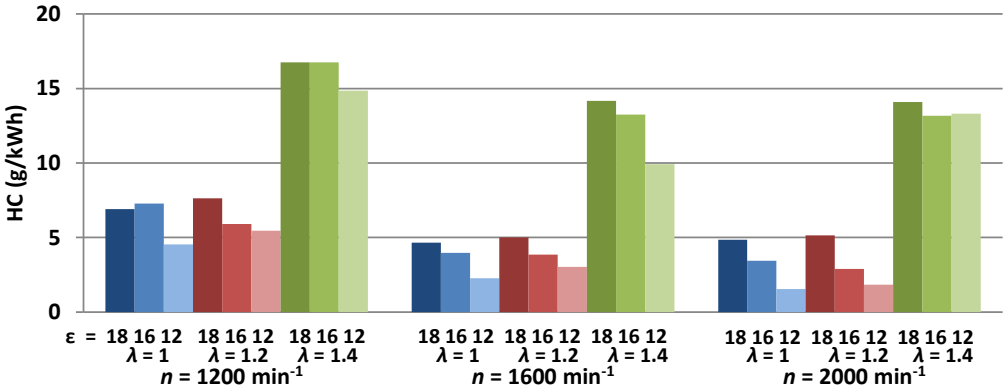

Slika 2. HC emisije – PP u Ottovom načinu rada

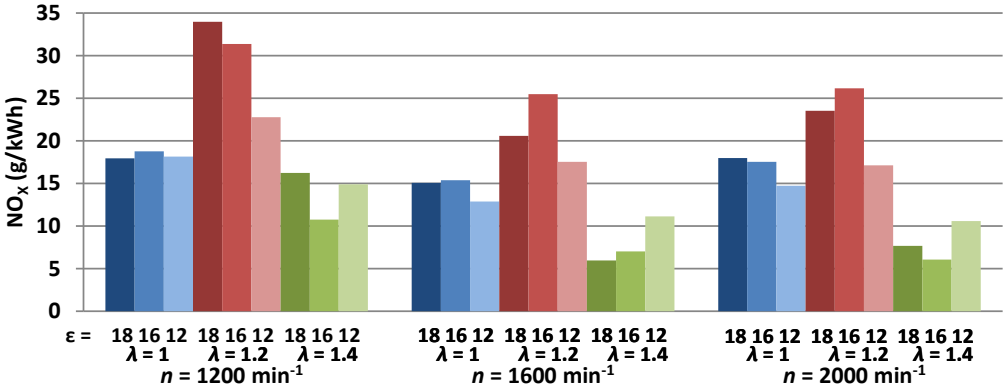

Slika 3. NO_X emisije – PP u Ottovom načinu rada

Provedeno ispitivanje dalo je izniman doprinos u istraživanju korištenja prirodnog plina u Ottovim motorima, jer dosadašnja eksperimentalna istraživanja nisu provođena na tako visokom kompresijskom omjeru. Ispitivanje je provedeno uz tri različita faktora pretička zraka (λ = 1, λ = 1,2 i λ = 1,4), a umjesto PP-a korišten je čisti metan iz boce.

Glavni zaključci prikazanog istraživanja su:

- Učinkovitost Ottovog motora punjenog stlačenim prirodnim plinom značajno ovisi o kompresijskom omjeru. Postoji i utjecaj faktora pretička zraka i brzine vrtnje, ali najznačajni porast u učinkovitosti vidljiv je promjenom kompresijskog omjera s 12 na 16. Daljnje povećanje kompresijskog omjera na 18 rezultira nižom učinkovitošću, zbog većih toplinskih gubitaka.
- HC emisije su na najvišem nivou kod siromašne smjese (λ = 1,4) zbog slabe propagacije plamena kroz prostor izgaranja. Povećanje kompresijskog omjera dodatno povećava HC emisije zbog većeg utjecaja procjepa u ukupnom volumenu prostora izgaranja.
- Emisije NO_X također više ovise o faktoru pretička zraka nego o kompresijskom omjeru, osim kod λ = 1,2 gdje kompresijski omjer ima značajan utjecaj na NO_X. Za

rad motora bez katalizatora, faktor pretička zraka trebao bi biti veći od 1,4. Što nije moguće postići s ovakvim sustavom paljenja.

Iz rezultata se može uočiti da je za upotrebu PP-a u Ottovim motorima pogodniji značajno viši kompresijski omjer od onog koji se uobičajeno koristi u Ottovim motorima. S obzirom da kompresijski omjer 16 prikazuje najbolje rezultate u pogledu učinkovitosti i HC emisija, upravo na tom kompresijskom omjeru je dalje ispitivan dvogorivni način rada.

5) U petom poglavlju prikazano je istraživanje upotrebe prirodnog plina u dvogorivnom motoru. Prvi korak istraživanja bilo je početno mjerenje u kojem su potvrđeni svi nedostaci zabilježeni tijekom pregleda literature, izuzev samozapaljenja i detonacije na visokom opterećenju. Zaključeno je da je to posljedica korištenja čistog metana umjesto prirodnog plina čiji je oktanski broj ipak nešto niži od čistog metana. Drugi razlog je što su ispitivanja provedena kod kompresijskog omjera 16 bez prednabijanja pa vršni tlakovi nisu bili jako visoki.

Da bi se pokušalo utjecati na učinkovitost i emisije ispušnih plinova, prvo je utvrđen utjecaj početka ubrizgavanja dizelskog goriva (U_P) na značajke rada motora. Ispitivanje je provedeno pri tri masena udjela prirodnog plina u ukupnom gorivu (normalni dizelski rad – 0 % PP, dvogorivni rad – 50 % i 90 % PP). Provedenim mjerenjima utvrđeno je da na nižim opterećenjima ne postoji fleksibilnost u varijaciji početka ubrizgavanja dizelskog goriva jer svaka promjena iz optimalne faze s obzirom na maksimalnu učinkovitost znači značajan pad u učinkovitosti i izaziva negativan efekt na emisije ispušnih plinova. Samo na visokom opterećenju i visokoj stopi zamjene dizelskog goriva prirodnim plinom (90 % PP) postoji mogućnost značajno ranijeg ubrizgavanja koje rezultira jednakom učinkovitošću uz smanjenje dušikovih oksida, odnosno postoji mogućnost dvokriterijskog optimiranja (s obzirom na učinkovitost i s obzirom na NO_X). Poboljšanje emisije NO_X na visokom opterećenju prikazano je na slici 4.

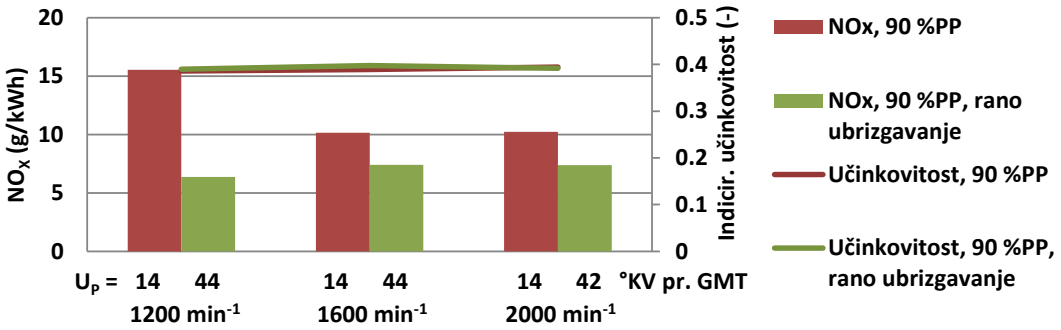

Slika 4. Poboljšanje emisije NO_X primjenom vrlo ranog početka ubrizgavanja U_P

Nakon istraživanja utjecaja početka ubrizgavanja dizelskog goriva, istražen je utjecaj temperature usisa s ciljem poboljšanja izgaranja na niskom opterećenju. Viša temperatura na usisu trebala bi osigurati brže širenje plamena kroz prostor izgaranja i time osigurati bolje iskorištenje goriva. Rezultati utjecaja grijanog usisa na emisije ispušnih plinova kod niskog opterećenja (srednji indicirani tlak p_i = 4 bar), brzine vrtnje n = 1600 min^{-1} i 90 % masenog udjela PP-a prikazani su na slici 5.

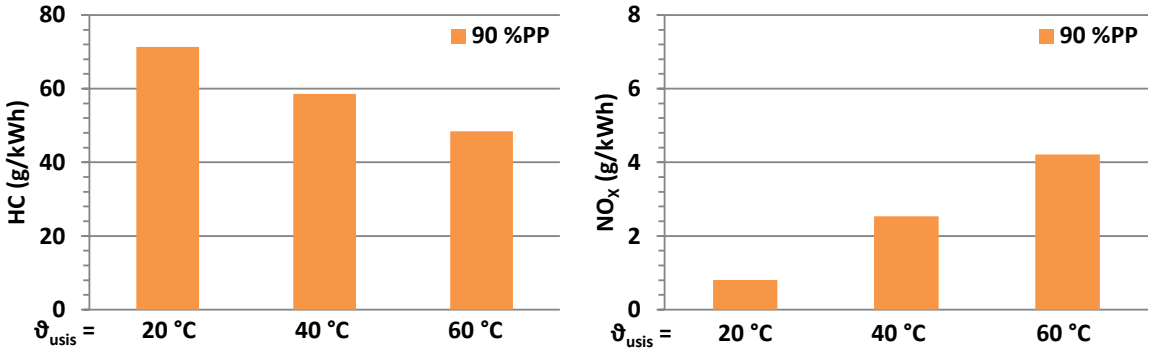

Slika 5. HC i NO_X emisija uz zagrijavanje usisa, p_i = 4 bar

Iz rezultata je zaključeno da grijani usis pomaže boljem iskorištavanju goriva, što je vidljivo iz smanjenja emisije ugljikovodika i ostvarenog porasta u učinkovitosti za 1,5 % kod promjene temperature usisa s 20 °C na 60 °C. Međutim, povišena temperatura pogoduje formaciji dušikovih oksida koji značajno rastu s porastom usisne temperature.

Sljedeći korak u procesu traženja optimalnih radnih parametara bio je vraćanje dijela ispušnih plinova (EGR), što je uobičajeno rješenje za smanjivanje emisije NO_X, na istom opterećenju i istom udjelu PP-a. U ovom dijelu je istražen povrat i hladnih i vrućih ispušnih plinova, a na slici 6. je prikazan njihov utjecaj na emisije HC i NO_X.

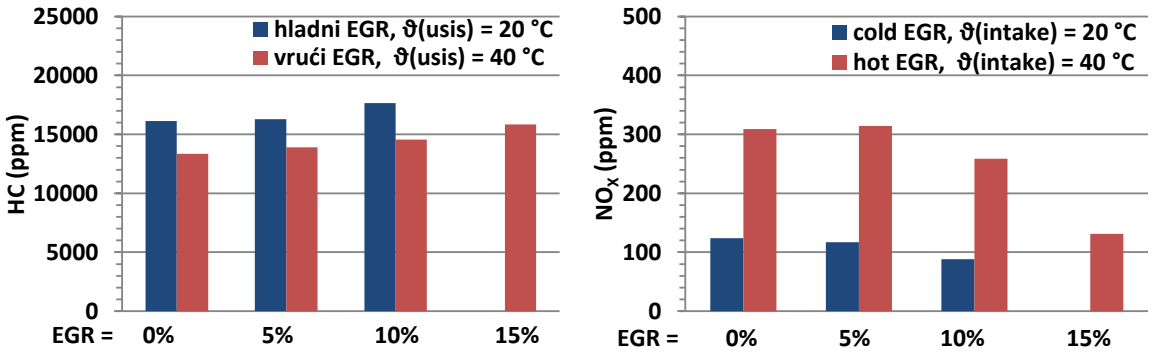

Slika 6. HC i NO_X emisije uz recirkulaciju ispušnih plinova; p_i = 4 bar, 90 % PP

Uz maseni udio plina od 90 % moguće je vratiti samo 10 % hladnih ispušnih plinova, odnosno 15 % vrućih ispušnih plinova. Veća količina EGR-a uzrokuje nestabilan rad i prekid rada motora. Suprotno od očekivanog, pokazalo se da je hladni EGR učinkovitiji od vrućeg, jer je utjecaj temperature značajno veći od utjecaja količine vraćenih plinova. Iz rezultata je

vidljivo da se vrućim EGR-om djelomično pomaže izgaranju i smanjivanju emisije THC, ali se gubi glavna svrha EGR-a, a to je smanjivanje emisije NO_X.

Budući da se ovim strategijama nije uspjelo poboljšati izgaranje u dvogorivnom motoru, završni korak bio je usmjeren prema promjeni vrste izgaranja, odnosno prema ispitivanju HCCI/RCCI (*engl. Homogeneous Charge Compression Ignition, Reactivity Controlled Compression Ignition*) izgaranja. Istraživanje je pokazalo da je uz grijani usis (ϑ_{usis} = 60 °C) i vrlo rano ubrizgavanje ili podijeljeno ubrizgavanje dizelskog goriva moguće značajno smanjiti emisije NO_X, koje čak zadovoljavaju EURO VI regulativu ($NO_X \leq 0.46$ g/kWh) [5], [6], [107] bez naknadne obrade ispušnih plinova uz zadržavanje iste učinkovitosti motora. Na slici 7. su prikazani rezultati za srednji efektivni tlak p_i = 4 bara, brzinu vrtnje n = 1600 min^{-1} i maseni udio plina 50 %. Prva dva stupca prikazuju jedno ubrizgavanje po ciklusu, dok druga dva pokazuju podijeljeno ubrizgavanje u kojem se u prvoj fazi ubrizgava 75 %, a u drugoj fazi 25 % dizelskog goriva (U_P – početak ubrizgavanja).

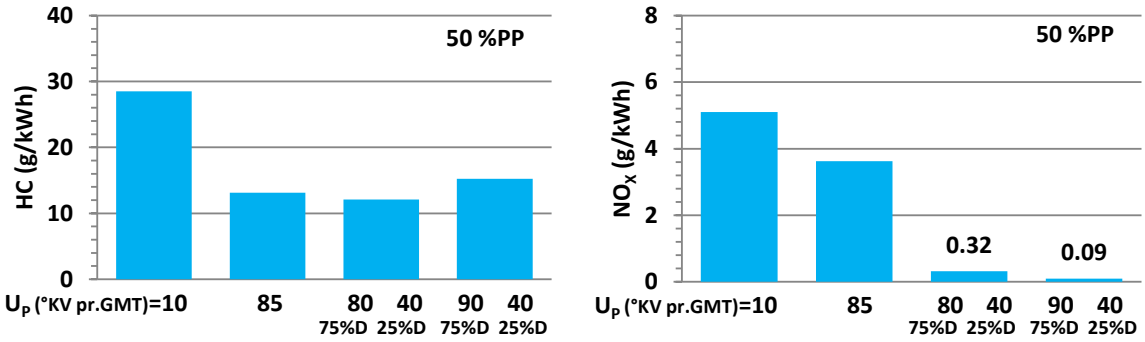

Slika 7. THC i NO_X uz različite strategije ubrizgavanja; p_i = 4 bar, 50 % PP

Istraživanje je provedeno i na većim masenim udjelima prirodnog plina te je utvrđeno da veća količina nije pogodna za niska opterećenja, tj. da ne može zadovoljiti EURO VI regulativu u pogledu NO_X emisija. Ovom metodom ubrizgavanja smanjene su značajno i emisije HC iako one još uvijek zahtijevaju naknadnu obradu. Izmjereni rezultati detaljno su analizirani te je prikazan postupak optimizacije izgaranja, odnosno postupak određivanja potrebne količine goriva u pojedinoj fazi kao i postupak određivanja početka ubrizgavanja. Time je dan značajan doprinos u području istraživanja niskog opterećenja dvogorivnog motora, te određen smjer u kojem bi se trebala provoditi daljnja istraživanja.

Na kraju je istražen i utjecaj hladnog EGR-a na visokom opterećenju, te je pokazano da u tom području EGR ima značajan učinak na smanjenje NO_X emisije. Uz EGR, ranim se ubrizgavanjem dizelskog goriva također može dodatno utjecati na smanjenje NO_X emisije. Ipak, u tom području emisije nisu svedene ispod navedenih granica, ali je postignuto njihovo značajno smanjenje.

6) U zadnjem poglavlju dan je ukupan pregled pojedinačnih zaključaka te je iskazan znanstveni doprinos rada.

Istraživanjem je pokazano da se štetne emisije u dvogorivnom motoru, kao što su HC i NO_X, mogu značajno smanjiti upotrebom odgovarajuće strategije ubrizgavanja dizelskog goriva, te uz primjenu odgovarajućih ostalih radnih parametara. Također je pokazano da se na niskim opterećenjima vrlo učinkovito može koristiti značajan maseni udio prirodnog plina (50 %), što opovrgava zaključke iz prijašnjih istraživanja da bi motor na niskom opterećenju trebao raditi u normalnom Dieselovom načinu rada [26] i da veća količina pilot mlaza, odnosno dizelskog goriva uzrokuje veću emisiju dušikovih oksida [13].

Ukupnim istraživanjem je pokazano da se primjenom prilagodljivog sustava ubrizgavanja dizelskog goriva i prirodnog plina, te upotrebom povrata ispušnih plinova može unutar dvogorivnog motora ostvariti izgaranje difuzijskim plamenom, kombinirano izgaranje difuzijskim i predmješanim turbulentnim plamenom te predmješano kemijski uvjetovano izgaranje homogene ili slojevite smjese.

Provedenim istraživanjem dani su sljedeći znanstveni doprinosi:

- Definiran je utjecaj promjene masenog udjela dizelskog goriva, trenutka početka ubrizgavanja dizelskog goriva, faktora pretička zraka te udjela vraćenih ispušnih plinova na promjene u tipu ostvarenog izgaranja.
- Identificirani su utjecaji tipa ostvarenog izgaranja na značajke rada dvogorivnog motora pri niskom i visokom opterećenju.

Dane su opće smjernice o optimalnim upravljačkim parametrima potrebnim za ostvarenje visoke učinkovitosti uz relativno nisku emisiju štetnih tvari, pri niskom i visokom opterećenju dvogorivnog motora.

Ključne riječi: dvogorivni motor, dvogorivno izgaranje, kompresijsko paljenje, stlačeni prirodni plin, metan, alternativno gorivo, dizelsko gorivo, HCCI proces izgaranja, parametri izgaranja

List of Figures

List of Tables

Nomenclature

Symbol	Unit	Description
Latin letters		
A	m^2	Surface area
c_v	J/(kgK)	Specific heat capacity at constant volume
D_{cyl}	m	Cylinder Bore
H	m	Engine stroke
h_w	$W/(m^2K)$	Woschni heat transfer coefficient
i	-	Transmission ratio
m_{air}	kg	Air mass
$m_{air,\ stoic}$	kg/kg	Stoichiometric air mass
m_{cyl}	kg	In-cylinder mass
m_{diesel}	kg	Diesel fuel mass
m_{ref}	kg	In-cylinder air mass at standard conditions
n	min^{-1}	Engine speed
n_c		Number of revolutions per power stroke
p	Pa	Pressure
p_0	Pa	Standard pressure
p_{cyl}	Pa	In-cylinder pressure
p_{fuel}	Pa	Fuel pressure
p_{intake}	Pa	Intake pressure
$p_{motored}$	Pa	Motored pressure
Q	J	Heat

Symbol	Unit	Description
Q_{wall}	J	Heat transferred to the cylinder walls
$Q_{wall,head}$	J	Heat losses through the cylinder head
$Q_{wall,piston}$	J	Heat losses through the piston
$Q_{wall,liner}$	J	Heat losses through cylinder liner
$q_{m,air}$	kg/s	Air mass flow
$q_{m,diesel}$	kg/s	Diesel fuel mass flow
$q_{v,cycle}$	mm^3/cycle	Diesel fuel volumetric flow
$q_{v,diesel}$	ml/min	Diesel fuel volumetric flow
R_{air}	J/(kgK)	Specific gas constant of air
R_{cyl}	J/(kgK)	In-cylinder gas mixture constant
T	K	Temperature
T_0	K	Standard temperature (293,15 K)
T_{cyl}	K	In-cylinder temperature
T_{EM}	Nm	Torque on electric motor driveshaft
$T_{fuel\ pump}$	Nm	Torque on high-pressure fuel pump driveshaft
V_{cyl}	m^3	In-cylinder volume
V_H	dm^3	Cylinder volume (Engine displacement)
x_{piston}	m	Current piston position measured from TDC
Z	%	Mass participation rate

Greek letters

Λ	-	Air delivery ratio
γ	-	Residual gas content
ε	-	Compression ratio
η_V	-	Volumetric efficiency

Symbol	Unit	Description
λ	-	Excess Air Ratio
λ_{CNG}	-	Premixed Excess Air Ratio (refers to the CNG)
λ_{tot}	-	Total Excess Air Ratio (refers to the total fuel: diesel + CNG)
ρ_{air}	kg/m^3	Air density
ρ_{diesel}	kg/m^3	Diesel fuel density
φ	-	Air equivalence ratio
ϑ	°C	Temperature
ϑ_{intake}	°C	Intake temperature

Abbreviations

Mark	Description
AC	Alternating Current
AFR	Air to Fuel Ratio
AFR_{diesel}	Air to Fuel Ratio for diesel fuel
ATDC	After Top Dead Center
BSFC	Brake Specific Fuel Consumption
BTDC	Before Top Dead Center
C	Cylinder
CA	Crank Angle
CA5	Crank Angle at which 5% of energy has been released
CA10	Crank Angle at which 10% of energy has been released
CA50	Crank Angle at which 50% of energy has been released
CA90	Crank Angle at which 90% of energy has been released
CI	Compression Ignition

Mark	Description
CD	Combustion duration
CO	Carbon Monoxide
CO_2	Carbon Dioxide
CoV(IMEP)	Coefficient of Variation of Indicated Mean Effective Pressure
CR	Compression Ratio
CVS	Crankcase Ventilation System
DPF	Diesel Particulate Filter
EGR	Exhaust Gas Recirculation
EU	European Union
FID	Flame Ionization Detection
F.S.	Full Scale
FTDC	Firing Top Dead Centre
GTL	Gas to Liquid
H_2	Hydrogen
H_2O	Water
HC	Hydrocarbons
HCCI	Homogeneous Charge Compression Ignition
He	Helium
HPDI	High Pressure Direct Injection
HPV	High Pressure Valve
IC	Internal Combustion
ID	Injection Duration
IVC	Intake Valve Closure
IMEP	Indicated Mean Effective Pressure
J	Junction

Mark	Description
LHV_{diesel}	Lower Heating Value – diesel fuel
LNG	Liquefied Natural Gas
LTC	Low Temperature Combustion
LTHR	Low Temperature Heat Release
MBT	Maximum Brake Torque
MP*x*	Measuring point *x*
MTBE	Methyl Tertiary-butyl Ether
N_2	Nitrogen
NDO	Normal Diesel Operation
NG	Natural Gas
NGV	Natural Gas Vehicle
NH_3	Ammonia
NI	National Instruments
NO_X	Nitrogen Oxides
NSRC	NO_X storage and reduction catalyst
O_2	Oxygen
PFI	Port Fuel Injector
PI	Positive Ignition
PID	Proportional–Integral–Derivative
PL	Plenum
PM	Particulate Matter
PWM	Pulse-width Modulation
R	Restrictor
RCCI	Reactivity Controlled Compression Ignition
RoHR	Rate of Heat Release

Mark	Description
RON	Research Octane Number
SB	System Boundary
SCM	Software Calibration Manager
SCR	Selective Catalytic Reduction
SI	Spark Ignition
SOC	Start of Combustion
SOI	Start of Injection
ST	Spark Timing
TDC	Top Dead Center
TEL	Tetraethyl Lead
THC	Total Hydrocarbons
TWC	Three-Way Catalyst
WHSC	World Harmonised Stationary Cycle
WHTC	World Harmonised Transient Cycle
WOT	Wide Open Throttle

1. Introduction

The continuous growth of industry and human population increases world energy consumption all the time. The increase in energy consumption can also be expected in the future, because of the expected growth of human population (2 billion in the next 25 years) [1]. Given that the internal combustion (IC) engines will still be used in future decades and keeping in mind that most of the oil reserves are located in political instability areas, there is a need for safe and sustainable energy sources [2].

As it is well known, transport sector is in the past few years identified as one of the most significant polluters and its negative environmental influence attracts a lot of attention [3]. In 2012, transport sector was responsible for approximately 23 % of total greenhouse gas emissions. These emissions have an impact on climate changes and global warming [4]. The main greenhouse gas from IC engines is carbon dioxide (CO_2). Besides greenhouse gas emission, the IC engines produce specific emissions (harmful emissions) such as carbon monoxide (CO), unburned hydrocarbons (HC), nitrous oxides (NO_X), soot and other chemical compounds which are the product of incomplete combustion or high in-cylinder temperatures. High concentrations of these emissions can be harmful to human health, which is a serious issue for governments and manufacturers around the world. Reduction of exhaust gas emissions from IC engines requires a lots of effort in the automotive industry and in order to fulfill this objective, world governments are issuing regulations which restrict allowed exhaust gas emissions from IC engines in motor vehicles [5], [6]. These regulations are forcing manufacturers to improve the existing combustion processes and exhaust gas after treatment systems, or to develop the new ones, which will result in reduced fuel consumption and exhaust gas emissions compared to conventional spark ignition (SI) and/or compression ignition (CI) engines [7]. On the other side, the same regulations lead to the use of alternative, environmentally more acceptable fuels [8]. In this context, natural gas (NG) is recognized as the alternative fuel which can be used in IC engines (both spark ignition and compression ignition) with a number of benefits [2]. Although natural gas is also a fossil fuel, because of its chemical composition it produces significantly less CO_2 compared to the gasoline or diesel fuel [9]. It can completely replace the gasoline in spark ignition engine, while in compression ignition engines due to the high octane number and high resistance to auto ignition, it can be used in so-called dual-fuel combustion mode with addition of pilot diesel fuel which represent

high energy source for initiation of combustion [10]. This technique has a great potential for decreasing harmful exhaust emissions while maintaining the performance on the level of conventional fuels used in IC engines. Besides mentioned advantages, there are still some disadvantages which will be experimentally researched with the goal of finding explanations on these phenomena.

1.1. Conventional fuels in internal combustion engines

Conventional fuels used in IC engines are derived from fossil fuels (coil and petroleum) which are formed by natural resources such as anaerobic decompositions of buried dead organisms. Natural gas is also a fossil fuel but it is often selected as an alternative fuel because of its properties.

Liquid fuels are one of the major energy sources in transport sector. They are mainly obtained from the crude oil, but they can also be obtained from biomass, coal tar, sand and oil shale, etc. Typical crude oil is a mixture which contains alkanes, alkenes, aromatics and cycloalkanes of organic compounds containing C, H, O, N and S elements [11].

Most of the motor vehicles are fuelled by the gasoline and diesel (Petroleum derived product), whose properties are constantly changing through years, depending on the development of injection and combustion technologies, performance requirements, environmental regulations, etc. The main properties of automotive fuels are: combustion quality, high heat of combustion, high volumetric energy content, low temperature performance, high temperature performance, oxidation stability, deposit formation control, material compatibility and flow characteristics [11].

1.1.1 Motor Gasoline

Gasoline is a reference fuel used in spark ignition IC engines which consists mostly of organic compounds obtained by the fractional distillation of petroleum, enhanced with a variety of additives. Gasoline is hydrocarbon fuel which contains normal paraffins, isoparaffins, olefins, aromatics and to a smaller extent cycloparaffins. The main requirement on gasoline is its auto-ignition resistance which is characterised by the octane number [12]. The most common type of octane rating worldwide is the Research Octane Number (RON), which is determined by running the fuel in a test engine with a variable compression ratio under controlled conditions and comparing the results with those for mixtures of iso-octane and n-heptane. Typical research octane number of motor gasoline is equal to RON = 92 … 98. The usual way of increasing the octane number is the use of additives (octane boosters) such

as methyl tertiary-butyl ether (MTBE), and ferrocene, while tetraethyl lead (TEL) is prohibited due to the adverse effect on three-way catalytic converters and general tendency to decrease the harmful emissions of lead compounds on the environment. Adding the aromatic alcohols, ethanol, and methanol to the gasoline also increase the ON of gasoline and give additional benefit to the environment. They are cleaner fuels and cause very little pollution when they burn. Gasoline has hydrogen to carbon molar ratio that varies from 1.7 to 2.0 and is typically characterized by the molecular formula C_8H_{16} [11]. Other specifications of gasoline are shown in Table 1.

Table 1. Gasoline properties [11], [12]

Characteristics	Value [unit]
Name (in EU)	Eurosuper 95, Eurosuper 98
Density	720 to 760 kg/m^3
Thermal expansion coeff.	$900 \cdot 10^{-6}$ K^{-1}
Boiling range	35 – 315 °C
Viscosity (at 20 °C)	$0.5 \cdot 10^{-6}$ m^2/s
Vapour pressure (at 20 °C)	50 to 90 kPa
Lower heating value	42.9 MJ/kg
Air to fuel ratio	14.5

1.1.2 Diesel fuels

Diesel fuel is a liquid fuel used in diesel engines and is originally obtained by crude-oil distillation. Also, there are some alternatives such as biodiesel (from vegetable oils) and synthetic diesel (usually produced from gaseous fuel from coal reforming or biomass, also named gas to liquid fuel - GTL), which are increasingly being developed. In all the cases, nowadays diesel must be free of sulphur [11].

The main characteristic of a diesel fuel is the ignition quality which is expressed by the cetane number. The ignition quality represents the ease of auto-ignition of diesel spray injected in the hot compressed air inside the cylinder. Most commonly used cetane improving additives are nitrates and peroxides, e.g. isopropyl nitrate, cycle-hexyl nitrates, ethyl-hexyl nitrate and di-tertiary-butyl peroxide [11]. These compounds decompose readily at high compression temperatures and produce free radicals that promote pre-combustion reactions in the fuel-air mixture and thereby reduce ignition delay. Another important characteristic of a

diesel fuel is its lubricity, which ensures lubrication of the pumping and injection elements. Other significant properties of diesel fuel are given in Table 2.

Table 2. Diesel fuel properties [12]

Characteristics	Value [unit]
Type	Type A – road vehicles
Density	780 to 860 kg/m^3
Thermal expansion coeff.	$800 \cdot 10^{-6}$ K^{-1}
Viscosity (at 40 °C)	$3 \cdot 10^{-6}$ m^2/s
Vapour pressure (at 38 °C)	1 to 10 kPa
Lower heating value	43 MJ/kg
Cetane number	45 (40 to 55)
Molecular formulas	$C_{11}H_{21}$, $C_{12}H_{23}$, $C_{12}H_{26}$, $C_{13}H_{26}$, $C_{14}H_{30}$

1.2. Natural gas as alternative fuel

Natural gas is a fossil fuel, mostly composed of methane (> 85%), which is recognized as a potential substitute for conventional fuels [2], [10]. It is noticed that the combustion of natural gas is "cleaner" than other conventional fuels and gives potential for decreasing CO_2 emission up to 25% because of the high hydrogen to carbon ratio [9], [10]. In comparison with conventional liquid fuels (diesel and gasoline) methane has higher octane number (120+), higher lower heating value (J/kg), higher stoichiometric air to fuel ratio (AFR) and significantly lower density and molar mass [13]. Although it has higher lower heating value, because of the higher stoichiometric air to fuel ratio the lower heating value of the mixture is approximately equal to the conventional liquid fuels. In ICEs natural gas can be used in both spark ignited (SI) and compression ignited (CI) engine. Natural gas can be stored in the form of compressed natural gas (CNG) or liquefied natural gas (LNG). Table 3 shows the chemical composition of the NG.

On the vehicles, the natural gas is stored into the high-pressure cylinders, which results in weight penalty of the vehicles; especially in heavy-duty vehicle where it may increase weight of the vehicle by 600 to 1000 kg to provide an acceptable range of operation [11]. Low weight cylinders made of composite material are available and can reduce the cylinder weight by more than half, but these composite material cylinders may be 3 or 4 times more expensive than conventional steel cylinders. Besides the increased weight and lost space on the vehicle, the main disadvantage of using natural gas is a lack of refuelling grid.

Table 3. Composition and properties of NG [14]

Component	mole %
Methane	93.9 (87.0 to 97.0)
Ethane	4.2 (1.5 to 9.0)
Propane	0.3 (0.1 to 1.5)
iso - Butane	0.03 (0.01 to 0.03)
normal - Butane	0.03 (0.01 to 0.03)
iso - Pentane	0.01 (trace to 0.04)
normal - Pentane	0.01 (trace to 0.04)
Hexanes plus	0.01 (trace to 0.06)
Nitrogen	1 (0.2 to 5.5)
Carbon Dioxide	0.5 (0.05 to 1.0)
Oxygen	0.01 (trace to 0.1)
Hydrogen	trace (trace to 0.2)
Water	max 8 mg/m^3
LHV	47.1 MJ/kg
Density	0.777 kg/m^3
Ignition point	564 °C
Octane number	>120

1.3. Internal combustion engines

An IC engine is a heat engine where the combustion of a fuel occurs with an oxidizer (usually air) in a combustion chamber resulting in a produced mechanical work. In an IC engine, the expansion of the high-temperature and high-pressure gases produced by combustion apply pressure to some engine component, depending on the type of the engine, usually to the pistons, turbine blades or rotor. Produced force moves the component over a distance and thereby transforms the chemical energy of the fuel into the useful mechanical energy (work).

The term *Internal Combustion Engine* usually refers to four-stroke or two-stroke piston engines and Wankel rotary engines. These engines are the most common power source for land and water vehicles. The focus of this work is on the four-stroke piston engines fuelled by gasoline, diesel fuel or/and natural gas.

As mentioned above, one of the directions of development with the aim of satisfying the regulations related to the exhaust gas emissions from IC engines can be optimization and improvement of current combustion processes in conventional spark ignition (SI) or

compression ignition (CI) engines. Due to the significant differences in combustion processes between the SI and CI engines, exhaust gas emissions are also different.

1.3.1 Spark ignition engine

A spark-ignition engine is an IC engine, which is generally fuelled by gasoline, where the combustion process of the air-fuel mixture is ignited by a spark generated at the spark plug. Usual applications of the spark ignition engines are passenger cars, motorcycles, small trucks, aircrafts, outboard and small inboard marine units, moderate-sized stationary pumps, lighting plants, machine tools, and power tools.

Spark ignition engines fuelled by gasoline, except direct injection gasoline engines, usually operates with stoichiometric mixture in the entire range of load due to the ignition source and combustion mode. They reach a lower thermal efficiency compared to the CI engines due to the operation at lower compression ratio. In gasoline engines, a mixture of fuel and air is compressed during the compression stroke and the compression ratios are limited by Annotation of PhD Thesis the auto-ignition (fuel property) or engine knock. For CI engines, only air is compressed during the compression stroke eliminating the fuel's auto-ignition or pre-ignition. Therefore, CI engines can operate at higher compression ratios and reach higher thermal efficiency. Although gasoline engines produce significant amounts of CO, HC and NO_X emissions, stoichiometric mixture ($\lambda = 1 \pm 2\%$) enables efficient operation of a three-way catalytic converter, which reduces the NO_X emissions and oxidizes CO emission and unburned hydrocarbons (HC). This after treatment system very efficiently converts harmful exhaust gas emissions into CO_2 and H_2O [15]. On the other side, a direct injection gasoline engines operate with non-homogeneous mixture. The mixture around the spark plug is stoichiometric or rich, while in the other regions the mixture is lean. These engines reach higher efficiency and lower fuel consumption, which means lower CO_2 emission, but emit higher HC and NO_X emissions. Produced NO_X emissions cannot be reduced by standard three-way catalyst (TWC reaches high efficiency with the condition that the mixture of fuel and air is around stoichiometry: $\lambda = 1$), but could be reduced using the newly developed NO_X storage and reduction catalyst (NSRC) [16].

Besides gasoline, the SI engine can be run on liquefied petroleum gas (LPG), methanol, ethanol, bioethanol, natural gas, hydrogen, etc. For the use of the alternative fuel, existing engines can be converted to operate on both the original fuel and the alternative fuel or the new engine can be designed to operate on alternative fuel which then results in better performance [17].

Natural gas, as a promising alternative fuel, can completely replace gasoline in the spark ignition engine. Because of the higher octane rating, it can be used at higher compression ratios, which theoretically means higher thermal efficiency. On the other side, higher compression ratio increases the in-cylinder temperature that leads to the higher NO_X emissions. In order to avoid increased temperature and to keep the NO_X emission at the acceptable level, the engine should operate either with stoichiometric mixture, either with very lean mixture [10], [18]. With stoichiometric mixture the lower engine efficiency is obtained, while the operation with very lean mixture could lead to misfires and also lower engine efficiency [3]. Additionally, in comparison with conventional fuels, methane displaces more air due to the lower molecular mass, which results in lower volumetric efficiency and lower power output.

Mentioned disadvantages prevent SI engines used in motor vehicles and fuelled with natural gas to achieve the engine efficiency similar to compression ignition engines [19]. Also since the lack of refuelling grid might require engine to run in bi-fuel mode, the different optimal compression ratio for gasoline and NG means that the engine can only be optimised for gasoline and therefore will run with lower than optimal efficiency, if fuelled only by natural gas [3]. Variable compression ratio can be an option, but this requirement means more complex engine design.

1.3.2 Compression ignition engine

Compression ignition diesel fuelled engines have been a major source of power for heavy-duty transportation and off-road applications. They are also becoming increasingly popular in light duty vehicles because of the combination of features required by consumers, such as high torque at low speed, great durability and reliability and lower fuel consumption compared to gasoline SI engines.

In CI engines, fuel is often injected into the engine cylinder near the end of the compression stroke. The liquid fuel is usually injected at high velocity as one or more jets through small orifices or nozzles in the injector tip. The atomized fuel absorbs heat from the surrounding heated compressed air, vaporizes, and mixes with the surrounding high-temperature high-pressure air. As the piston continues to move closer to top dead center (TDC), the mixture temperature reaches the fuel's ignition temperature. After the ignition delay period, ignition of some premixed fuel and air occurs. This ignition is marked by a sharp cylinder pressure increase as combustion of the fuel-air mixture takes place. Increased pressure resulting from the premixed combustion compresses and heats the unburned portion

of the charge and increases the evaporation rate of the remaining fuel. Atomization, vaporization, fuel vapour-air mixing, and combustion continue until all the injected fuel has combusted.

Diesel fuelled IC engine emits very low CO emission and HC emissions, but significantly higher NO_X emissions and particulate matter (PM). Because of the lean mixture, the three-way catalyst cannot efficiently reduce NO_X emissions, therefore the reduction of NO_X emissions depends on the improvement of the in-cylinder combustion process or on the use of advanced exhaust gas after treatment systems, which are unavoidable for satisfying the latest, very strict, regulations related to exhaust gas emissions from IC engines (e.g. Euro VI).

The formation of NO_X in the cylinder may be significantly reduced by the optimization of the combustion chamber and intake port geometry, and of the diesel fuel injection strategy that encompasses the injection pressure and multiple injections per cycle. These strategies and optimizations allow reduction of the local in-cylinder temperatures as well as fuel-rich zones that are the source of NO_X emission. Cooled exhaust gas recirculation (EGR) is also confirmed and widely used method for decreasing the in-cylinder temperatures and NO_X emissions accordingly.

The above mentioned advanced exhaust gas after treatment systems for the reduction of NO_X emissions are SCR catalysts (Selective Catalytic Reduction) and absorption catalysts. Absorption catalyst accumulates NO_X compounds during the engine operation in lean burn mode. When the catalyst is full and the absorption is not possible anymore, the engine shortly operates with a rich mixture resulting in higher CO and HC emissions which are used as reactants for the reduction of absorbed NO_X [15].

The SCR catalyst uses reactant (urea) which is injected into the exhaust pipe in front of the catalyst and causes the chemical reactions in the catalyst that reduces NO_X to N_2 and H_2O. This after treatment system among all commercially available after treatment technologies, has the highest potential of use for the NO_X reduction of diesel fuelled CI engines [20]-[22]. The main disadvantage of SCR technology is the need for urea solution, which impose the responsibility of engine operators as well as the need for infrastructure for deliver it.

Second major harmful product from diesel engine is soot, which has a negative effect on both human health and the environment. Different mechanisms of soot formation correspond to the different phases of diesel fuel combustion. Soot can be formatted in fuel rich zones, from the fuel injected into the flame, from the fuel injected into the burnt gases, etc. [23]. The formation of soot can also be reduced by the optimization of the in-cylinder combustion processes or by the use of diesel particulate filter (DPF) which removes the soot from the

exhaust gases. Diesel particulate filter accumulates soot in its porous walls. When the filter is filled, a certain amount of diesel fuel is injected late, during the expansion stroke, which increases the temperature of the exhaust gases and results with reactions that lead to combustion of the absorbed soot [24]. This combustion of the soot cleans the DPF and enables another cycle of soot accumulation.

Although diesel fuelled CI engines achieve higher efficiency compared to the gasoline SI engines, the harmful effect of the exhaust gas emissions is forcing manufacturers to develop new combustion techniques that use cleaner, alternative fuels.

1.3.3 Dual-fuel internal combustion engines

As described above, spark ignition engines fuelled by natural gas, especially gasoline engines converted to run on natural gas have some disadvantages that limit their application. On the other hand, compression ignition engines due to the higher compression ratio, which leads to the higher engine efficiency, represent a better solution for natural gas application. Since NG has a high auto-ignition temperature, it cannot completely replace diesel fuel in a compression ignition engine, because it will not ignite [9]. Therefore, NG is utilized in CI engines in a so-called dual-fuel combustion process. In the dual-fuel combustion process, NG is the main source of energy ignited by a certain amount of highly reactive fuel. In diesel dual-fuel engines, diesel fuel is used as a highly reactive fuel that initiates combustion process. The relative amount of natural gas in the total fuel contained in the cylinder is usually defined as a diesel substitution ratio [10] or as a natural gas mass participation rate [25], [26]. Diesel substitution ratio (E) is based on the energy level and shows the ratio between energy supplied by NG over the total energy supplied by NG and diesel fuel:

$$E = \frac{\mathrm{LHV_{NG}} \cdot \dot{m}_{\mathrm{NG}}}{\mathrm{LHV_{NG}} \cdot \dot{m}_{\mathrm{NG}} + \mathrm{LHV_{D}} \cdot \dot{m}_{\mathrm{D}}} \cdot 100 \ \ [\%\mathrm{NG}] \tag{1}$$

while the natural gas mass participation rate (Z) is defined as:

$$Z = \frac{\dot{m}_{\mathrm{NG}}}{\dot{m}_{\mathrm{NG}} + \dot{m}_{\mathrm{D}}} \cdot 100 \ \ [\%\mathrm{NG}] \tag{2}$$

where $\dot{m}_{\mathrm{D}}$ represents mass flow of diesel fuel in kg/h, $\dot{m}_{\mathrm{NG}}$ represents mass flow of natural gas in kg/h, $\mathrm{LHV_D}$ represents lower heating value of diesel fuel in MJ/kg and $\mathrm{LHV_{NG}}$ represents lower heating value of natural gas in MJ/kg. The mass participation rate is usually used in relevant experimental research [25] - [29], and will also be used in presented research.

In general, depending on the mixture preparation and combustion process, there are three main engine concepts of dual-fuel operation [30]:

- High pressure direct injection (HPDI) dual-fuel engine,
- Conventional dual-fuel engine,
- Low Temperature Combustion dual-fuel (LTC DF) engine.

The HPDI engine is a concept that uses a specially designed fuel injector which allows injecting both fuels into the cylinder under high pressure as shown on Figure 1. This type of dual-fuel operation results in a mixing-controlled combustion or diffusion flame and offers significant reduction in NO_X and PM but with a compromise in power output, CO and HC emissions as well as specific fuel consumption compared to the conventional dual-fuel engine [31]. However, this concept requires engine design specifically for dual-fuel combustion and cannot be realized in existing diesel engines, which represents a disadvantage in some applications, such as upgrading the old engines.

The LTC DF engine is a concept where both fuels are injected into the intake pipe or one fuel is injected into the intake pipe while other is injected into the cylinder, but very early so that it has enough time to mix with in-cylinder charge. The premixed mixture is then ignited at the end of compression stroke when the ignition temperature of the mixture is reached and the combustion and rate of heat release is controlled by the chemical reaction rates. Depending on the stratification level the combustion can be classified into the homogeneous charge compression ignition (HCCI) for fully premixed, or reactivity controlled compression ignition (RCCI) for partially stratified mixtures. Although this type of combustion provides good efficiency and low NO_X emissions, the combustion control over the intake temperature and chemical kinetics of the fuel/air mixture is very challenging [32].

The conventional dual-fuel engine is a concept that is suitable for upgrading the existing diesel engines. Natural gas is injected into the intake pipe, which ensures very good CNG / air mixing through intake and compression stroke, while the diesel fuel is injected at the end of compression stroke directly into the cylinder for initiation of combustion. The original diesel fuel supply system can be used with the addition of control modules and natural gas fuel supply system. The main benefit of a conventional dual-fuel engine is the simple and short change from dual-fuel operation to normal diesel operation (NDO), which allows simultaneous use of both fuels or the use of only diesel fuel when natural gas is not available. The engine design of a conventional dual-fuel engine is shown on Figure 1.

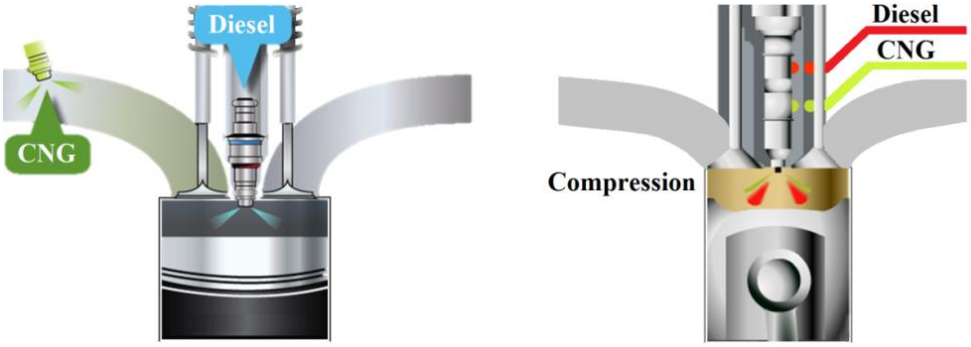

Figure 1. Conventional dual-fuel, HPDI dual-fuel; reproduced from [33]

Combustion process in conventional dual-fuel engine has both CI engine and SI engine characteristics, which means that it is a blend of mixing-controlled combustion process and flame propagation. During the injection of diesel fuel into the combustion chamber, the mixing process of diesel with air/NG mixture depends on the global fluid motion and in-cylinder turbulence which result in a mixing-controlled combustion process. Flame propagation occurs in areas where fuel, air and residual gases are premixed and the flame is somehow initiated. The combustion process of dual-fuel engine is usually divided into three main phases:

- Combustion of the diesel pilot,
- Combustion of natural gas in the premixed diesel fuel region,
- Flame propagation through the air/fuel/residual gas mixture.

Previous research of dual-fuel combustion shows that the initial combustion rate depends on the amount of pilot fuel, while the addition of NG increases the ignition delay of pilot fuel [31]. This is a result of several effects which include: lower temperature and pressure at the end of compression due to the decreased specific heats ratio of air/NG mixture compared to the pure air, the chemical influence of NG on the ignition of diesel fuel, and decreased volumetric efficiency compared to the normal diesel operation. These effects in combination with a reduced diesel fuel quantity require an optimization of operating parameters of direct injection such as injection timing and injection pressure.

In comparison to the spark ignition engine where the combustion starts from the single ignition source (spark plug), in the dual-fuel combustion mode the flame starts from multiple ignition sources depending on the number of nozzle holes of the diesel fuel injector. Depending on the load and diesel fuel quantity in the mixture, the diesel pilot fuel areas are increasing or decreasing resulting in a combustion process closer to CI engines or closer to SI engines.

From the mentioned characteristics of the combustion process in the conventional dual-fuel engine one can conclude that the operating parameters of direct fuel injection have significant influence on the combustion, as well as on the produced power and exhaust gas emissions.

1.4. State of the art

It is well known that the first IC engine was a gas fuelled engine, which was developed just 20 years after the development of the steam engine. This engine utilized coal gas combustion instead of steam. With the beginning of the cheap production of petroleum products after Second World War in regions such as Middle East, the use of IC engines begins to grow rapidly. As a by-product of oil extraction, oil rigs produced natural gas, which was mixed with the intake air and burned in diesel engines. This was the first example of a dual-fuel engine [34]. Since then, many different types of dual-fuel engines have been developed, which were designed either as diesel ignited gas engines, or mixed combustion engines that use natural gas together with another fuel [34].

The first Natural Gas Vehicle (NGV) is patented in the US in the late 1800's, while adoption of natural gas as a primary fuel source in Europe begun shortly after the Second World War [35]. The number of NGV worldwide is constantly increasing and now exceeds 25 million (25.15 mil. in March 2018) [36]. There are three types of NGVs: (1) dedicated, which run only on NG, (2) Bi-fuel, which switch between gasoline and NG, and (3) Dual-fuel, which run on diesel and NG simultaneously, or on 100% diesel. In the last couple of years dual-fuel technology was applied in light, medium and heavy duty commercial vehicles [37].

Although the number of NGVs is increasing steadily, the research of the application of natural gas in compression ignition engines in dual-fuel combustion mode shows that in addition to some advantages of this mode, compared to the compression ignition engine that runs with diesel fuel, there are some disadvantages.

Many of the authors that performed experimental investigations showed that the dual-fuel combustion is a promising technique for the decrease of the emissions of nitrous oxides (NO_X) and soot, while maintaining high engine efficiency [13], [26], [31] ,[38]-[40]. The main mentioned disadvantages are increased CO and HC emissions as well as the reduction in efficiency at low loads [26], [31], [38], [40], [41]. *Konnigson F.* in [10] and *Gharehgani et al.* in [42] also noted the tendency towards knock and preignition at high loads.

Most of the research was carried out by a simple substitution of the diesel fuel by natural gas, where diesel engine was converted into the port injection dual-fuel engine. This is

often performed without optimization of the operating parameters for each substitution ratio or engine load. *Lounici et al.* in [26] set the start of injection of diesel fuel at 13 °CA BTDC and used 10% of the full load diesel fuel quantity as a pilot fuel quantity, while the increase of power was performed by the addition of the natural gas. The results follow previously mentioned general trends in emissions and efficiency, but leave a lot of space for the optimization of the entire combustion process. The similar conversion process was performed by *Mustafi et al.* in [38] where the injection timing was set to 28 °CA BTDC. Besides the results related to emissions (increased HC and decreased NO_X and PM compared to the NDO), the authors showed the increased ignition delay and shorter combustion duration in dual-fuel mode compared to NDO.

On the other hand, many studies presented below showed that the engine performance and exhaust gas emissions depend on the combustion chamber geometry and on the characteristic of the nozzle as well as diesel substitution ratio, diesel pilot fuel quantity, injection pressure, injection timing, intake pressure, intake temperature and the amount of EGR.

Daishy et al. in [43] as well as authors in [26] and [41] presented the influence of diesel substitution ratio on the dual-fuel combustion. As mentioned above, the increased ignition delay in dual-fuel combustion mode, which increases with the addition of NG, results in lower in-cylinder temperature at TDC, which can lead to incomplete combustion and the decrease of engine efficiency. From the emissions point of view, the HC and CO emissions generally increase as the diesel substitution ratio increases, with exception at high loads, where the decreased excess air ratio provides better flame propagation through the combustion chamber resulting in lower HC emissions [41]. Also, *Lounici et al.* in [26] showed that better flame propagation at high loads increases thermal efficiency. NO_X emission decreases as the diesel substitution ratio increases due to the lower local in-cylinder temperatures. However, this trend may be changed at high loads if the injection timing is changed, which results in increased temperature and higher engine efficiency. As described, the trends of performance and emission characteristics are not only the function of diesel substitution ratio. Besides the above mentioned effects, it is worth to note that the increase of NG in the total injected fuel decreases soot emissions significantly.

Zhang et al. in [44] as well as *Yang et al.* in [45] investigated the effects of diesel pilot fuel injection pressure. As injection pressure increases, injection velocity also increases which means more injected fuel before the moment of ignition. This effect increases the temperature and reduces HC emissions due to the faster flame propagation through the premixed charge.

On the other hand, higher in-cylinder temperature supports NO_X formation. As shown in [30], the increase in injection pressure from 250 bars to 500 bars, increases the in-cylinder temperature and indicated efficiency accordingly, but further increase of injection pressure to 750 bars decreases the efficiency. Decreased efficiency at 750 bars is a result of early combustion phasing and higher influence of heat losses to the cylinder walls. The above mentioned publications and results lead to the conclusion that the injection pressure should also be optimized for dual-fuel operation in order to find optimal injection setup.

The influence of injection timing is researched by *Abd Alla et al.* in [46]. They compared three different Start of Injection (SOI) points: SOI = 25, SOI = 27.5 and SOI = 30 °CA BTDC at various loads. Although the experiment is performed in a small range of SOI values, results indicate general behaviour of the engine in dependence of injection timing. Advanced SOI leads to the higher in-cylinder temperature at TDC and higher in-cylinder pressure accordingly, which means higher indicated efficiency, but at the same time higher NO_X emissions. Also, the higher temperature improves combustion efficiency and reduces CO and HC emissions. At medium and high loads, the engine shows tendency to knock with advanced injection timing.

Shu et al. in [47] also performed an experimental study of the effects of injection timing on thermodynamic and emission characteristics of natural gas-diesel dual-fuel engine. They compared combustion characteristics for pilot injections between 6 °CA BTDC and 16 °CA BTDC. The results showed that brake thermal efficiency first increases and then decreases with advancing the injection timing, with maximum value at 12 °CA BTDC. Drop in efficiency is caused by the increase of thermal losses with advancing the injection over 12 °CA BTDC. Advancing the SOI increases the in-cylinder temperature and increases the period in which the temperature is larger than 1800 K, which largely promotes NO_X emissions. Hydrocarbon emissions decrease with the advance of the combustion phasing, but they are not changed drastically. Therefore, it can be concluded that the combustion phasing has significant influence on combustion process and exhaust gas emissions. Delay of the combustion phasing significantly decreases NO_X emissions, with a small penalty in indicated efficiency and HC emissions.

The effect of diesel pilot fuel quantity is experimentally investigated by *Abd Alla et al.* in [13]. Authors showed that the increase of diesel pilot fuel quantity improves engine efficiency, but this could lead to the knock at high loads. The higher quantity of pilot fuel also raises NO_X emissions that are result of increased maximum temperatures of the charge. *Selim*

et al. in [48] reached similar conclusions, where it was confirmed that the increase of pilot fuel quantity lead to the increase in efficiency and torque.

The effect of charge conditions on dual-fuel performance is investigated by *Ghareghani et al*. in [49] and as expected, the increase in boost level increases dual-fuel engine power output. Authors also noticed higher tendency to knock combustion as intake pressure increases.

Papagiannakis et al. researched in [50] the influence of inlet air preheating on dual-fuel combustion. They concluded that the inlet air preheating leads to the improved engine efficiency at high load, but higher combustion efficiency also increases the maximum cylinder pressure, which could be harmful to engine, with respect to the mechanical strength. Negative impact of dual-fuel combustion on CO emission can also be reduced with inlet air preheating (CO emission can be reduced up to 40% at high load). The higher intake temperature also reduces the soot emissions. The negative influence of the increased intake temperature is related to the increase of NO_X emissions. Also, intake air preheating enhances flame propagation at low loads which is a positive influence, but at the high loads the preheated air increases the risk of knock occurrence [30].

The influence of EGR on dual-fuel combustion was also investigated by *Papagiannakis et al*. [50]. It was shown that increased in-cylinder pressure caused by inlet air preheating could be reduced by a slight simultaneous increase of EGR percentage. Further benefit of using EGR is related to the reduction of NO_X emissions, but EGR negatively affects both CO and soot emissions. The final conclusion regarding the EGR was that in combination with increased intake air temperature EGR could be a promising solution for improving efficiency and reduction of CO emission. The same topic was investigated by *Serrano et al*. in [9] where hot EGR was used at low load. Results showed that the increased intake temperature promotes flame propagation and improves efficiency. Cold EGR on the other hand is a better solution at high loads for reducing the in-cylinder temperatures and knock occurrence as well as reducing NO_X emissions, but at the expense of engine efficiency caused by reduced in-cylinder temperatures [51].

Based on the literature review, it can be concluded that dual-fuel combustion shows some benefits related to the NO_X and soot emissions while maintaining the engine efficiency similar to normal diesel operation, but there are still some disadvantages at low loads (increased HC and CO emissions, reduced efficiency) and at high loads (preignition and knock occurrence). Although the influence of operating parameters is separately discussed in previous investigations, there is a need for general recommendations with respect to the

selection of operating parameters in dual-fuel engine in dependence of operating conditions. Also, varying operating parameters could result in different combustion modes which have a potential for improvement of dual-fuel engine performance and emissions.

The literature review showed above represents the motivation for research of dual-fuel operating parameters and possible combustion modes presented in this thesis. This research will increase the general knowledge related to the dual-fuel combustion processes and will give guidelines for further development of dual-fuel engines, which includes recommendations for the selection of operating parameters in dependence of operating conditions, especially for conditions at low and high engine load.

1.5. Objective and hypotheses of research

The main objective of this work was to investigate the possibilities of achieving high overall engine efficiency, while maintaining the harmful exhaust gases emissions below the prescribed limits, at low and high loads of engine operating in dual-fuel combustion mode. In order to achieve the above defined objective, two minor objectives were defined:

- Explore the influence of several fuel injection strategies and HCCI combustion mode on dual-fuel engine operation,
- Explore the influence of EGR on dual-fuel engine operation.

Considering the above stated objectives, the hypotheses of the research are:

- By using the fully flexible fuel injection systems for diesel fuel and natural gas, and EGR strategy, it is possible to achieve diffusion flame combustion, premixed flame propagation, and premixed chemically controlled combustion of homogeneous or stratified mixture in dual-fuel engine.
- By using the appropriate mode of combustion, it is possible to achieve high efficiency and low harmful exhaust gases emissions in dual-fuel engine operation both at low and high engine loads.

1.6. Structure and content of work

The thesis is divided into the six main chapters, which includes the above given introduction. The second chapter presents the preparation of the conversion process of experimental engine, from normal diesel operation to dual-fuel, which includes the numerical analysis of the fuel slip through the engine cylinder due to the valve overlap. Results of the analysis give recommendations for NG injection strategies. In the third chapter a complete experimental setup together with the modification of the existing diesel engine and conversion to dual-fuel combustion is explained. Fourth chapter shows experimental research of using NG in spark ignition engine at three different compression ratios (CR = 12, CR = 16 and CR = 18), on the same engine geometry that will be used for dual-fuel operation. These results will provide a benchmark results related to the performance and emissions of spark ignition natural gas fuelled engine, especially at high compression ratios, which were not investigated comprehensively so far. In the fifth chapter the experimental results of the dual-fuel engine operation performed for the purposes of this work are presented and discussed together with some individual conclusions from particular tests. The last chapter summarizes all main conclusions and recommendations related to the dual-fuel combustion process.

2. Numerical Investigation of Fuel Slip

The conversion from conventional diesel engine to dual-fuel engine operation requires the addition of gas supply system to the intake pipe and the modification of the engine control unit. The main disadvantages of dual-fuel combustion, compared to the normal diesel operation, are a decrease in engine efficiency and significant increase of the HC and CO emissions. Significant increase of HC emission is shown in [13] and [48], while increase of CO emission is confirmed in [25]. The hydrocarbon emissions are a result of unburned methane, which is considered as greenhouse gas, like carbon dioxide. One of the reasons for increased concentration of HC emissions is the valve overlap, which leads to fuel slip (port-injected fuel) into the exhaust. In order to achieve better cylinder scavenging, the conventional diesel engine is designed with positive valve overlap. This design is suitable for engines that feature a direct fuel injection system, where the fuel is usually injected after the intake and exhaust valves are closed. Due to this valve overlap, once the gas fuel supply system is added to the intake pipe, some of the gaseous fuel flows through the cylinder into the exhaust pipe. This phenomenon occurs at all ranges of engine loads and speeds, especially in charged engines because of the higher pressure difference between the intake and exhaust ports. The necessity of optimization of the injection strategy in dual-fuel operation in terms of both energetic and environmental behaviour was confirmed by the authors in [52]. Also, the authors in [53] showed that Start of Injection point has a significant influence on the dual-fuel combustion process.

In order to prepare the process of conversion of existing diesel engine, which is a part of the experimental setup used in this work, into the dual-fuel engine, the numerical simulations of the engine were performed. The main objective of these numerical simulations was to find the best injection strategy of gaseous fuel into the intake pipe, which will lead to the smallest amount of fuel slipping into the exhaust pipe due to the valve overlap. All simulations were performed with the cycle simulation tool AVL Boost™ v2013, which is a 1D/0D software designed for cyclic simulations of the entire engine systems with the emphasis on flows through the engine, on combustion in the cylinder and on the overall engine performance.

2.1. Description of simulation model and test cases

The numerical simulation model is based on the existing Hatz diesel engine 1D81 and on the whole experimental setup that was built at the Laboratory of IC engines and motor vehicles at the Faculty of Mechanical Engineering and Naval Architecture. The simulation model includes the complete geometry of the experimental setup with entire intake and exhaust system and all additional devices, as shown in Figure 2.

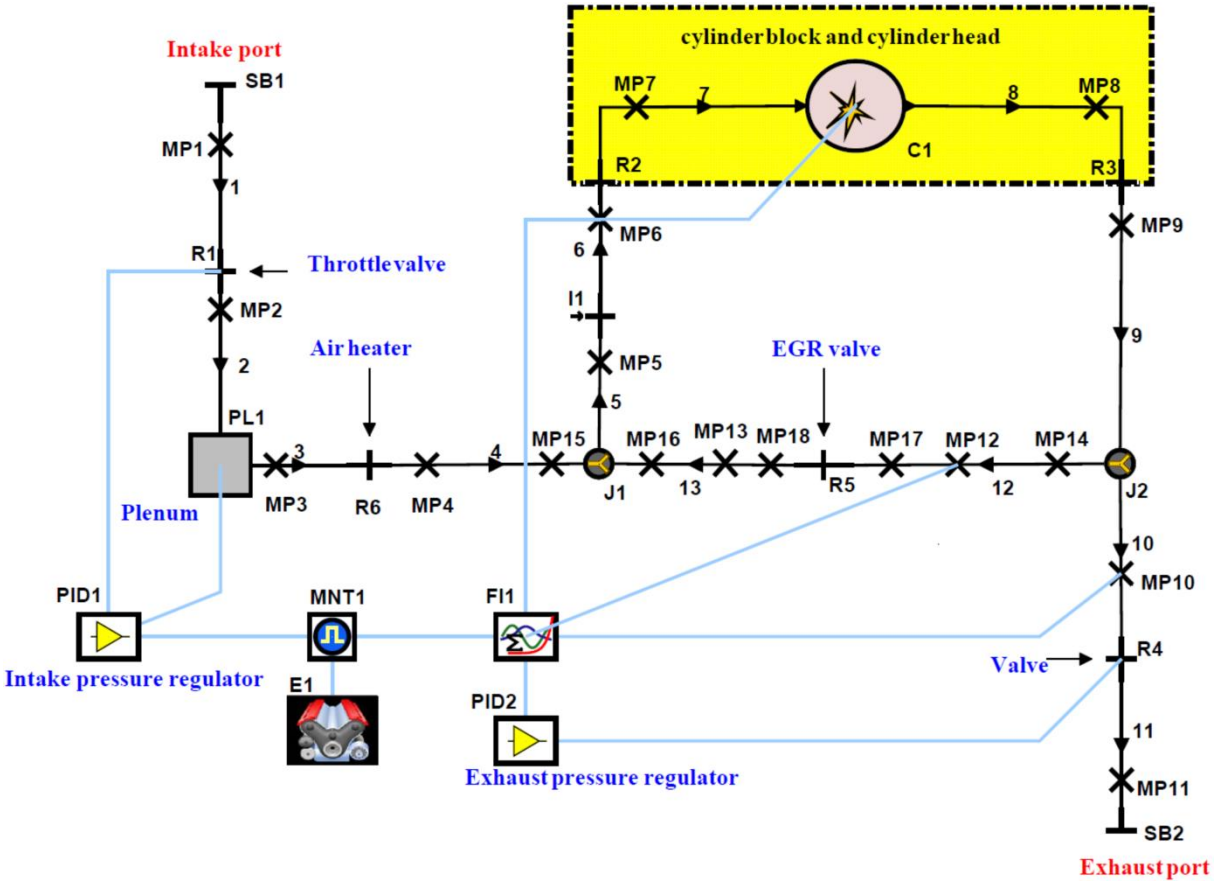

Figure 2. Engine model created in AVL Boost™ v2013

The numerical model consists of: intake line (from System Boundary 1 – SB1 to Cylinder – C1), exhaust line (from Cylinder to System Boundary 2 – SB2) and Exhaust Gas Recirculation line (from Junction 2 - J2 to Junction 1 - J1). The intake line consists of throttle valve or restricto – R1, plenum – PL1, air heater (only flow resistance of the air heater is modelled with single restriction element), fuel injector and junction with the EGR line. The exhaust line consists of valve for pressure regulation and a junction with the EGR line. In order to be able to perform the appropriate fuel slip analysis, the lift curves of the experimental engine were measured and imported in the numerical model (Figure 3).

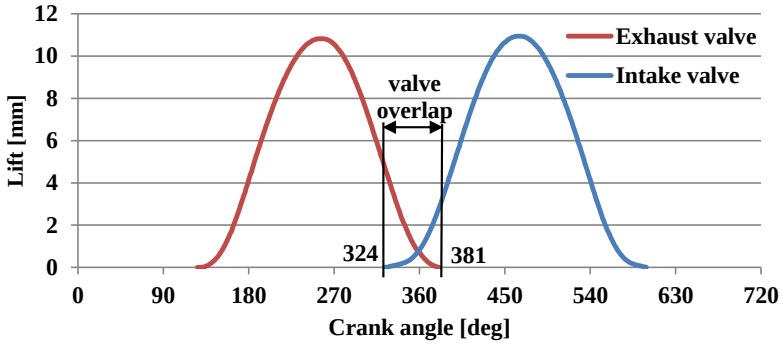

Figure 3. Intake and exhaust valve lift curves

The proportional–integral–derivative (PID) controllers are placed for fine adjustment of the operating parameters. In order to appropriately monitor the entire process, lots of measuring points were placed in the simulation model. The Vibe function with constant parameters in all the cases was used to define the rate of heat release. Used parameters are: Start of Combustion (SOC) = -20 °CA ATDC, Combustion duration (CD) = 60 °CA, shape parameter m = 2 and parameter a = 6.9, according to the AVL Boost™ Users guide [54]. The mixture of methane and diesel fuel with 95% of the methane mole fraction was applied as a fuel.

The analysis of the fuel slip from the cylinder is made by monitoring the amount of fuel (kg/cycle) in the intake (measuring point 7) and in the exhaust pipe (measuring point 8). In the first step, the effect of continuous port fuel injection on the gaseous fuel slip to the exhaust pipe due to the valve overlap was analysed. Table 4 shows the test cases that were simulated with continuous fuel injection.

Table 4. Test cases with continuous fuel injection

Case Name	n [rpm]	p_{intake} [bar]	$p_{exhaust}$ [bar]	λ *(excess air ratio)*	EGR [%]
1.1	1000	1	1.018	1.5	0
1.2	1500		1.018		
1.3	2000		1.025		
1.4	3000		1.031		
2.1	1000	2.2	1.03	1.5	0
2.2	1500		1.03		
2.3	2000		1.05		
2.4	3000		1.07		

Once the calculation with continuous injection strategy was made, the intermittent port injection strategy was applied and the influence of different injection timings (different SOI timings and different injection durations) on gaseous fuel slip to the exhaust was analysed. In the numerical model, the SOI is defined as a relative value to the Firing Top Dead Center

(FTDC) which is set to 0° CA. The simulated test cases that applied intermittent injection strategy are given in Table 5.

Table 5. Test cases with intermittent fuel injection

Case Name	n [rpm]	p_{intake} [bar]	$p_{exhaust}$ [bar]	λ (*excess air ratio*)	EGR [%]	Injection duration [°CA]	SOI [° CA] relative to FTDC
3.1	1000	1	1.018	1.5	0	90, 180	0, 100, 200, 300, 400, 500
3.2	1500		1.018				
3.3	2000		1.025				
3.4	3000		1.031				
4.1	1000	2.2	1.03	1.5	0	90, 180	0, 100, 200, 300, 400, 500
4.2	1500		1.03				
4.3	2000		1.05				
4.4	3000		1.07				

The first set of results was obtained with injection duration (ID) of 180 °CA (Figure 4), while the second set was made with the injection duration of 90 °CA (Figure 5). The cases with shorter injection duration assume greater mass flow during injection. The final set of simulations was performed with finer resolution in order to optimize the SOI point. The criteria for determining the optimal SOI point was the lowest fuel concentration in the exhaust pipe (measuring point 8).

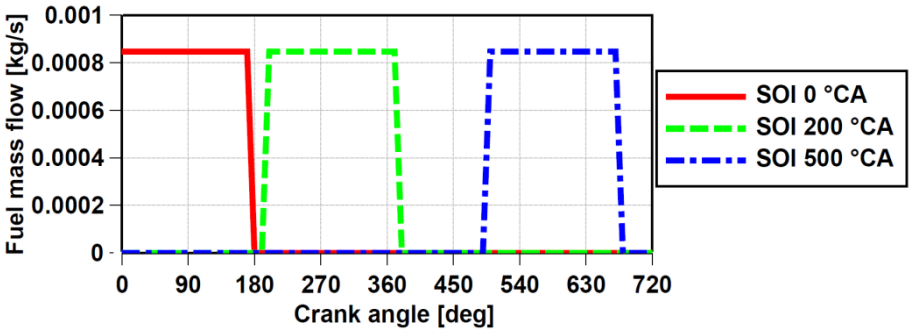

Figure 4. Injection profiles with ID = 180 °CA

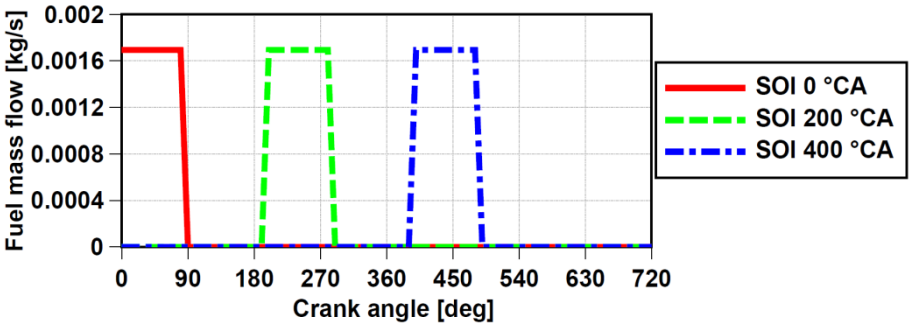

Figure 5. Injection profiles with ID = 90 °CA

2.2. Results and discussions

It was mentioned that the measure for monitoring the fuel slip is the mass of fuel in the exhaust port (MP8). Instead of using the absolute value of mass concentration that changes as the excess air ratio changes, the relative value of fuel slip was calculated by dividing the exhaust fuel concentration by the intake fuel concentration:

$$\text{Fuel slip} = \frac{\text{Exhaust fuel concentration (MP8)}}{\text{Intake fuel concentration (MP7)}} \times 100\ [\%] \tag{3}$$

Figure 6 shows the fuel slip dependence on engine speed and intake pressure for continuous injection. Continuous line shows the results for the average value of intake pressure of 1 bar while the dashed line shows results for the intake pressure of 2.2 bars. It is important to keep in mind that the simulations were performed only at four different speeds. Therefore the straight lines between them are not representative.

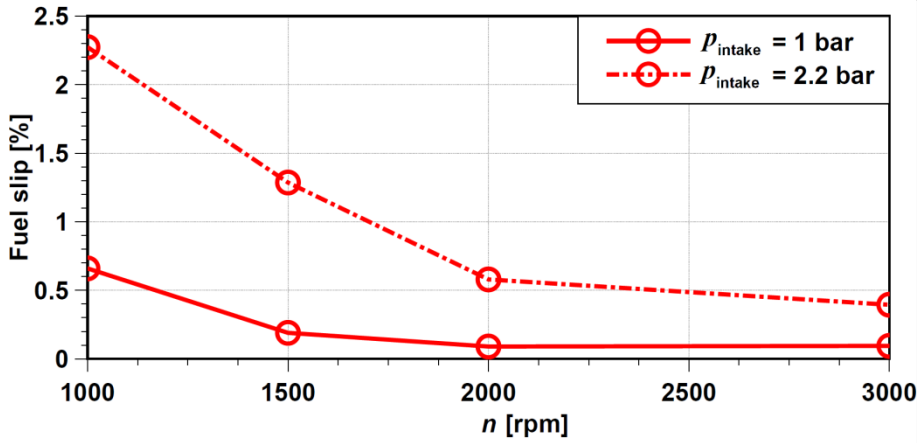

Figure 6. Fuel slip through exhaust valve for continuous injection

It can be observed that at lower engine speed the fuel slip is more pronounced, while at the high engine speed it is much lower. As can be seen in Figure 6, at 1000 rpm fuel slip is 0.6% at naturally aspirated condition and 2.3% at charged condition. The higher intake pressure leads to a higher fuel slip level, which is to be expected due to the higher air/fuel flow through the cylinder during the valve overlap.

The results of the initial simulations with intermittent injection strategy, for different SOI values, and with ID = 180 °CA and p_{intake} = 1 bar are shown in Figure 7. On the same figure the corresponding result of the case with the continuous injection is also shown.

The results show that cases with SOI = 0, 100 and 200 °CA have very similar results and that the fuel slip in these cases is the lowest. The cases with SOI = 300 and 400 °CA have even worse results than the case with continuous injection. The difference between results of

different injection timings is the highest at 1000 rpm, while at higher engine speeds the differences are much smaller and in some cases can be neglected.

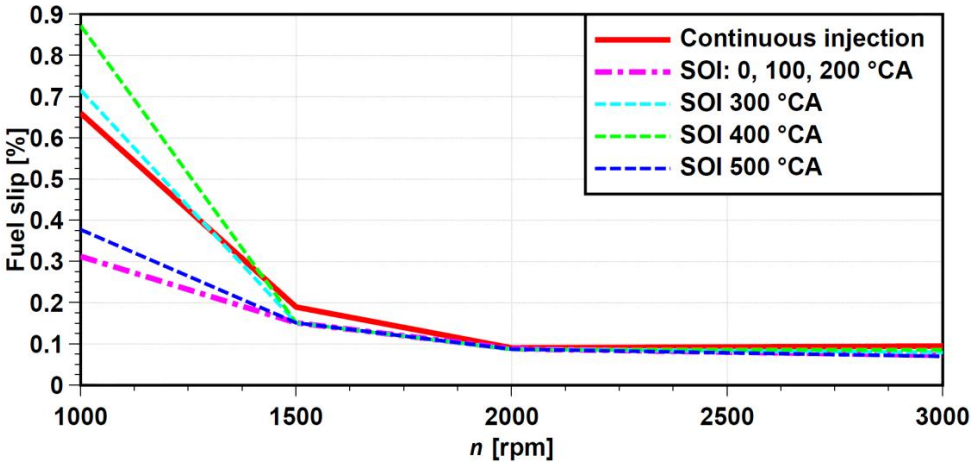

Figure 7. Fuel slip at p_{intake} = 1 bar for different start of injection timings (ID = 180 °CA)

The results of different injection timings but now with shorter ID (ID = 90 °CA) are shown in Figure 8. With a shorter ID the result of the case with SOI = 300 °CA becomes similar to the result of the cases with SOI = 0, 100 and 200 °CA, which are almost the same as with ID = 180 °CA, while at the case with SOI = 400 °CA the fuel slip increases, compared to ID = 180 °CA and is much higher than the cases with SOI = 0, 100, 200 and 300 °CA.

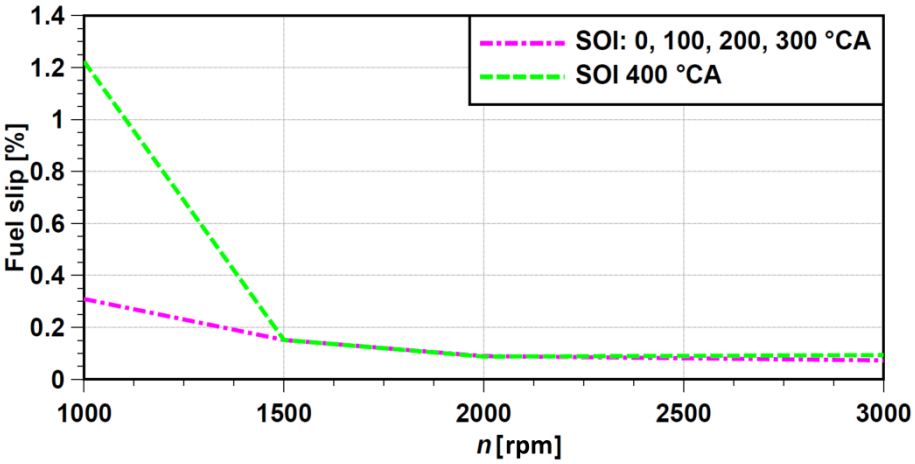

Figure 8. Fuel slip at p_{intake} = 1 bar for different start of injection timings (ID = 90 °CA)

Similar behaviour is obtained in charged conditions with p_{intake} = 2.2 bars with the difference in obtained values. Figure 9 shows the result for ID = 180 °CA and the same trend as in the case with ambient conditions can be noticed. The cases with SOI 0, 100 and 200 °CA are almost the same and show the lowest fuel slip. The significant difference at higher intake pressure compared to lower pressure is that the influence of SOI is also significant at higher engine speeds. When the ID is lower (ID = 90 °CA) the case with SOI = 300 °CA again becomes equal to the cases with SOI = 0, 100 and 200 °CA, as it was noticed at ambient

intake pressure conditions. This leads to the conclusion that maybe SOI is not the most important parameter for minimizing fuel slip and that the End of Injection (EOI) might have more influence on total fuel slip.

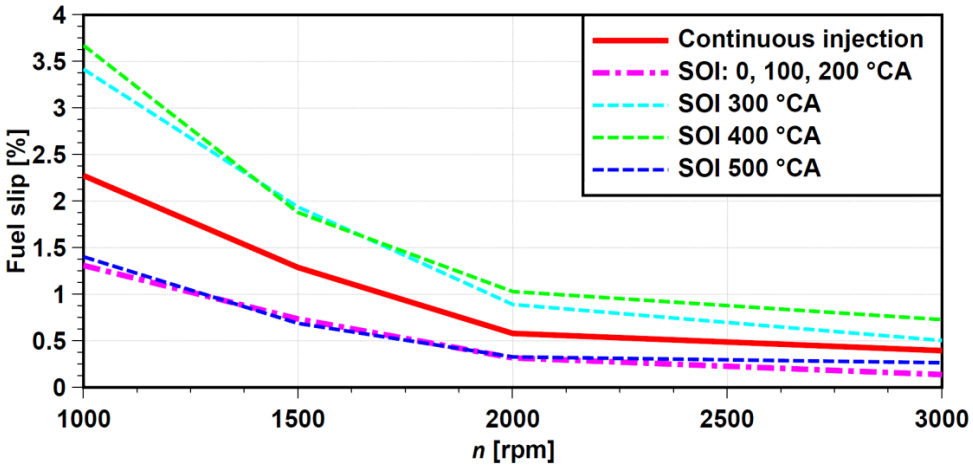

Figure 9. Fuel slip at p_{intake} = 2.2 bar for different SOI (ID = 180 °CA)

The test case with SOI = 300 °CA and ID = 90 °CA has the EOI at 390 °CA, which is similar to the case that has SOI at 200 °CA and ID = 180 °CA. A detailed analysis of results lead to the conclusion that the EOI timing should not be later than some critical point after which fuel slip starts to increase. By refining the results shown in Figure 8 with smaller SOI steps between SOI = 300 °CA and SOI = 360 °CA (Figure 10), it can be noticed that the SOI = 320 °CA is the latest SOI timing with ID of 90 °CA that has the same low fuel slip. All later injections (SOI = 340 °CA or later) result in increasing of the fuel slip to exhaust pipe. This means that the critical point for EOI is around 410 °CA.

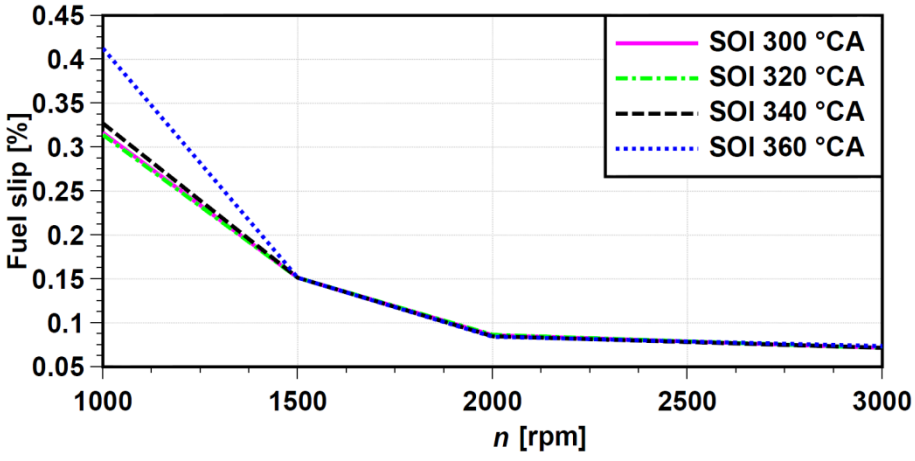

Figure 10. Fuel slip for SOI 300 °CA to 360 °CA (p_{intake} = 1 bar, ID = 90 °CA)

The refined test was also performed with ID = 180 °CA (Figure 11) and the results of this test confirm that the value of critical point for EOI is around 410 °CA. The result with SOI = 240 °CA (black line) is just slightly higher than for SOI = 200 or 220 °CA, and further

increase of SOI timing results in further increase of the fuel slip. This means that the increase of fuel slip starts once EOI becomes larger than 400° CA.

Finally, the results show that the appropriate injection timing at engine speed n = 1000 rpm can result in the reduction of the fuel slip up to 43% compared to the case with continuous injection, while inappropriate injection timing can result with the increase of fuel slip up to 62% in charged conditions.

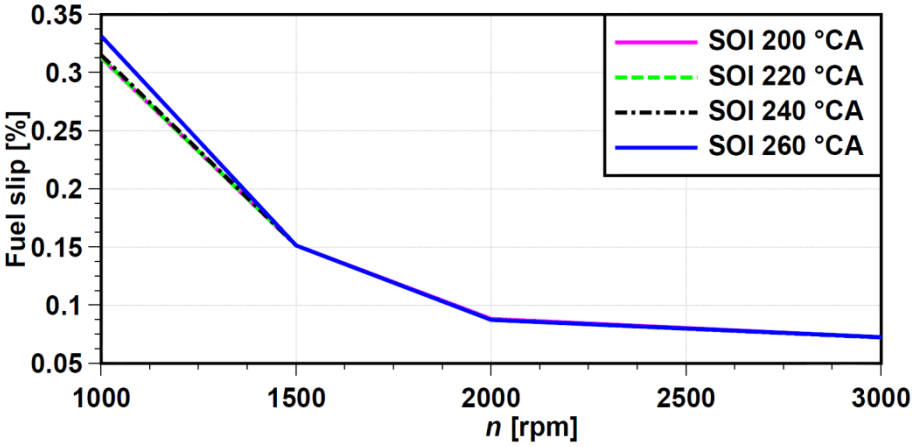

Figure 11. Fuel slip for SOI 200 °CA to 260 °CA (ID = 180 °CA)

The results of the simulation also reveal the cause of the obtained fuel slip into the exhaust pipe. The major source of the fuel slip into the exhaust pipe is the fuel that is retained in the intake pipe, close to the intake valve, after the intake valve closes. This fuel waits for the intake process of the next cycle, and during the valve overlap part of the fresh mixture slips into the exhaust.

Figure 12 shows the fuel concentrations close to the intake valve during one operating cycle for several injection timings. It can be seen that even though the cases with SOI = 0, 100 and 200 °CA have different injection profiles the fuel concentration at the intake valve changes much later (around 400 °CA). This is caused by the fact that only then the flow through the intake system brings the fuel from the injection point, which is located 100 mm upstream of the intake valve. If the injection is too late (SOI = 300 or 400 °CA) all the injected fuel does not come into the cylinder and therefore the concentration after the intake valve closure is higher (intake valve closure IVC = 600 °CA). Larger concentration of the fuel located upstream the intake valve results with higher fuel slip to the exhaust during the valve overlap. In the cases with early injection all the injected fuel flows into the cylinder (fuel concentration around 540 °CA is almost 0) but at the end of intake stroke the backflow of charge from cylinder to the intake pipe, caused by late intake valve closing, causes the small increase of the fuel concentration in front of the intake valve.

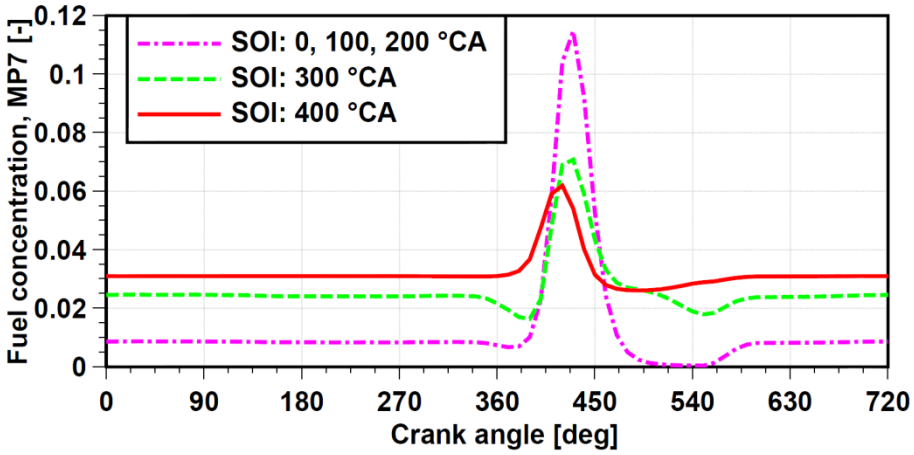

Figure 12. Fuel concentration in intake pipe vs. CA (p_{intake} = 1 bar, ID = 180 °CA, n = 1000 rpm)

The analysis of the results showed that the injection timing has an influence on the fuel slip from the cylinder due to the valve overlap. The most important parameter for determining the optimum injection timing is the EOI. The results for different injection timings obtained in this research are valid only for the simulated experimental engine and for the intake system geometry (location of fuel injector on intake pipe) that was defined in this research.

2.3. Conclusions

In this chapter, the effects of the port injection timing on the fuel slip into the exhaust pipe of conventional dual-fuel engine due to the valve overlap is numerically investigated. The main question in this study was whether the fuel slip from the cylinder can be reduced by the appropriate injection timing strategy.

The main conclusions of the presented study are:

- The fuel slip from cylinder due to valve overlap is highest at low engine speed (1000 rpm) – 0.6% of the injected fuel slips in the exhaust in the case of naturally aspirated engine and 2.3% at charged conditions;
- At higher engine speeds (2000 rpm, 3000 rpm) the fuel slip becomes very low;
- Decrease of fuel slip can be achieved through the optimization of the injection timing. Appropriate intermittent injection timing can reduce fuel slip up to 43% compared to the continuous injection at defined excess air ratio, while the inappropriate intermittent injection timing can result in an increase of the fuel slip up to 62% in charged conditions; For this engine the port fuel injection strategy should inject all the fuel no later than 400 °CA (40 °ATDC during intake stroke).

3. Experimental Setup

All experimental measurements are performed on the experimental setup located in the Laboratory of IC engines and motor vehicles at the Faculty of Mechanical Engineering and Naval Architecture. The testing room is equipped with the experimental engine, engine dynamometer, intake and exhaust lines and all relevant equipment for engine management and data acquisition. The experimental single cylinder engine, connected to the alternating current (AC) motor (engine dynamometer), is shown in Figure 13, left.

Figure 13. Left: Experimental engine; right: fuel tanks and exhaust gas analyser

The tanks for liquid and gaseous fuels are located in a separate room (Figure 13, right), while the management and monitoring of the engine operation is performed from the control room shown in Figure 14.

Figure 14. Control room

3.1. Structure of experimental setup

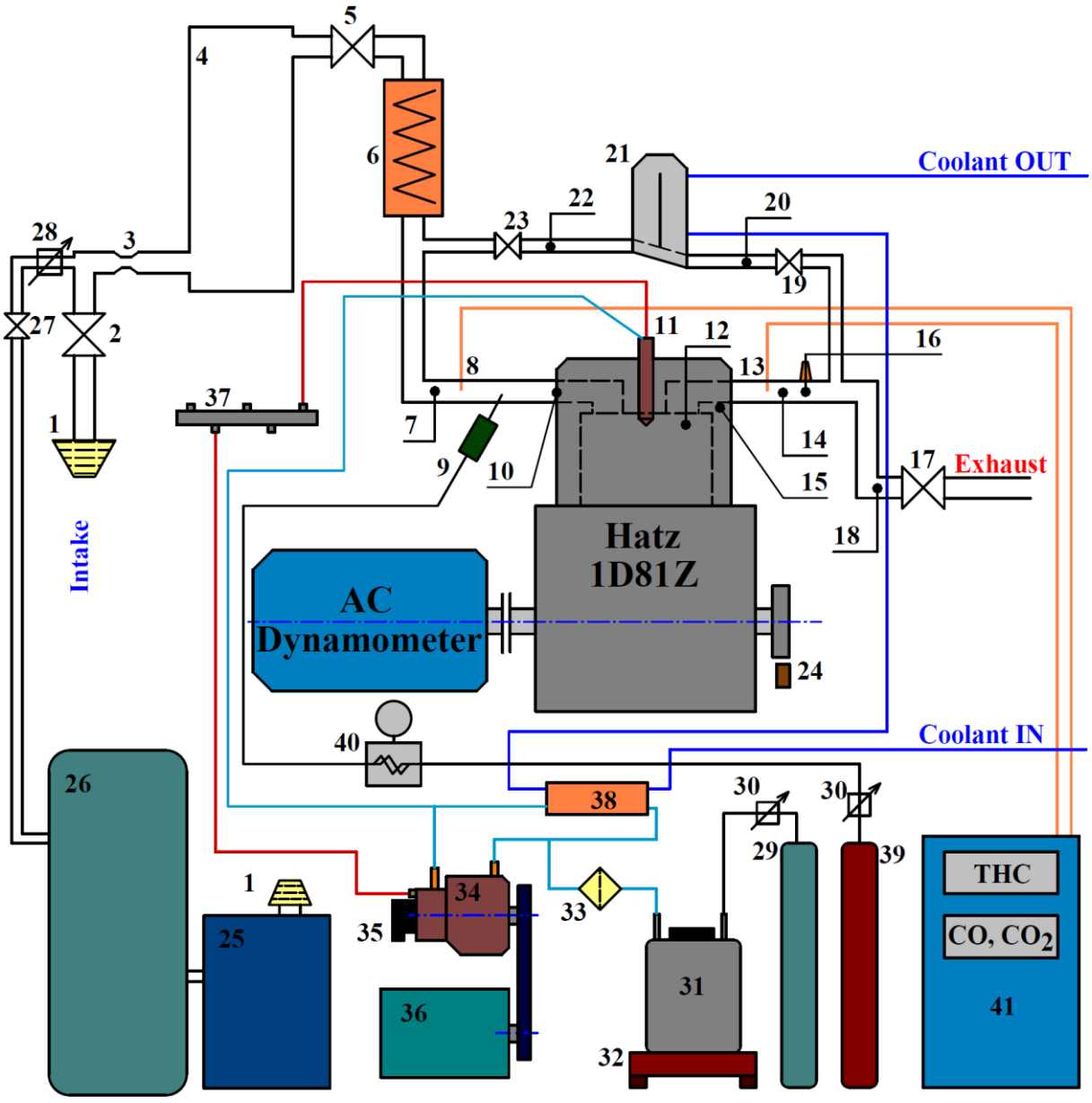

1 Air filter
2 Shut off valve
3 Air flow meter
4 Plenum
5 Throttle
6 Air heater
7 Intake temperature sensor
8 Intake gas sampling
9 Gaseous fuel injector
10 Intake pressure sensor
11 Piezo fuel injector
12 High pressure sensor
13 Exhaust gas sampling
14 Exhaust temperature sensor
15 Engine head temp. sensor
16 Lambda, NO_X sensor
17 Exh. pressure regulation valve
18 Temperature sensor
19 Shut off valve
20 EGR IN Temperature sensor
21 EGR valve and EGR cooler
22 EGR OUT temperature sensor
23 Shut off valve
24 Crank angle decoder
25 Air compressor
26 Air pressure vessel
27 Shut off valve
28 Pressure regulator
29 Compressed Nitrogen (N_2)
30 Two stage pressure regulator
31 Liquid fuel tank
32 Weight scale
33 Fuel filter
34 High pressure pump
35 High pressure valve
36 Electric motor
37 Fuel accumulator (Rail)
38 Fuel cooler
39 Compressed Methane (CH_4)
40 Coriolis flow meter
41 Gas analyser

Figure 15. Schematic diagram of experimental setup

Figure 15 shows all mechanical components of the experimental setup used in the research. As it can be seen, the base of the setup is a single cylinder diesel engine Hatz 1D81Z [55] which is connected to the AC engine dynamometer.

The intake line (components 1 - 10) is equipped with the air filter, the mass flow meter, the settling tank for smoothing of the flow, the throttle, the air heater, the intake temperature sensor, the injector for gaseous fuel, the sampling point for measurement of CO_2 and the intake pressure sensor in front of the intake valve. Charging of the engine can be achieved by closing the shut off valve 2 and opening the shut off valve 27, which opens the line 25 – 28 on which the following components are located: air compressor, air pressure vessel and pressure regulator which allows maintaining the desired intake pressure.

The exhaust line (13 - 17) contains the exhaust gas temperature sensor, the sampling point for measurement of THC, CO and CO_2 emissions, the sensor for oxygen concentration and NO_X emission and the control valve which enables the control of the desired pressure in the exhaust line.

The exhaust gas recirculation line (19 - 23) is equipped with two shut off valves, one at each side of the EGR valve, which are used to open or close the EGR line, exhaust gas cooler and temperature sensors before and after the cooler. The EGR control valve is located in front of the cooler and is designed so that it allows exhaust gas flow through or in bypass of the cooler. Thus, the hot or cold exhaust gas could be returned to the intake side.

The gaseous fuel (methane) from the pressure cylinder is used to supply the port fuel injector, while flow is controlled by appropriate opening of the fuel injector. The methane mass flow is measured by a Coriolis flow meter Endress+Hauser Promass A100 and the usual pressure of the gaseous fuel in front of the fuel injector was about 4 barg.

Diesel fuel is stored in the closed tank pressurised by nitrogen from the pressure cylinder and the pressure in the container is controlled by a pressure regulator. By using pressurized tank with low pressure (p_{fuel} = 4 barg), diesel fuel is supplied through the fuel filter to the high pressure fuel pump, which increases the fuel pressure up to 1350 bars. The desired fuel pressure is maintained by the solenoid valve embedded in the high pressure fuel pump. Highly pressurised fuel flows through the high pressure pipeline towards the fuel accumulator (*rail*) and finally to the piezo fuel injector. The diesel fuel supply system is separated from the engine and the power for propulsion of the high pressure fuel pump is taken from the separate electric motor (Figure 15).

The fuel return lines from the injector and high pressure fuel pump are mutually connected and flows through the cooler towards the intake side of the high pressure pump.

Also, as it can be seen in Figure 15, the return line is not connected to the fuel tank as usually in the diesel common rail systems. Although, the fuel return to the tank would provide better cooling effect of the fuel, it would also cause mixing of the liquid fuel and vibrations within the fuel tank which would, considering the fuel flow measurement is performed by the measurement of the weight of the fuel tank by a highly precise scale, present a source of error in measurement, i.e. a large noise in the measurement signal. With the presented scheme of connection, the mixing is avoided and the weight scale shows always stable value which allows precise measurement of the fuel consumption.

3.2. Experimental engine

As mentioned above, the experimental setup is built by using Hatz 1D81Z engine as a basis. This IC engine was chosen because of the robust and simple design, which makes it suitable for exploring different fuels and different operating conditions. Figure 16 shows the engine and its components in the original version.

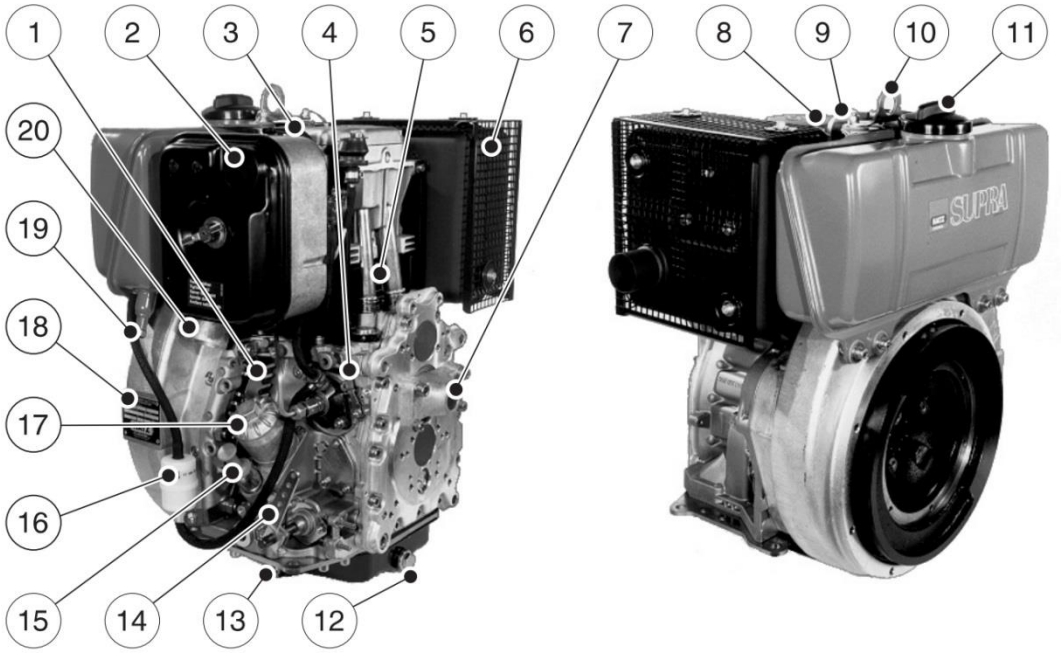

1 Cooling air inlet
2 Dry-type air cleaner
3 Decompression lever
4 Stop lever
5 Cooling air outlet
6 Silencer (muffler)
7 Guide sleeve for starting handle
8 Cylinder head cover
9 Cold-start oil metering device
10 Suspension lug
11 Tank filler cap
12 Oil drain plug, governor housing
13 Oil drain plug, governor side
14 Speed control lever
15 Oil filler pipe and dipstick
16 Fuel filter
17 Oil filter
18 Type plate
19 Tank drain plug
20 Combustion air intake

Figure 16. Hatz 1D81Z engine [56]

The engine is mounted in to the test cell without many additional original parts such as dry-type air cleaner, silencer, fuel tank, fuel filter, tank drain plug, etc., i.e. only the main engine parts are kept. The parts that were taken off are replaced with other components that were installed onto the experimental setup, as shown in Figure 15.

The main technical data and technical characteristics of the experimental engine are given in Table 6 and Figure 17.

Table 6. Technical data [56]

Type		**1D81**
Engine model		**Z**: non-encapsulated, add. system of balancing
Mode of operation		air-cooled four-stroke diesel engine
Combustion method		Direct-fuel injection
Number of cylinders		1
Number of strokes		4-stroke
Bore / stroke	mm	100 /85
Connecting rod length	mm	127
Compression ratio		20.5
Displacement	cm^3	667
Engine oil content: without filter with filter	dm^3	1.8 1.9
Consumption of lubrication oil after running-in period		approx. 1 % of fuel consumption at full load
Engine oil pressure Oil temperature 100 ± 20 °C	min.	0.6 bar at n = 850 rpm
Direction of rotation looking at the flywheel		counterclockwise
Valve clearance at 10 - 30 °C Inlet Exhaust	mm	 0.10 0.20
Max. angle from vertical in any direction (continuous operation)	max.	25°
Weight (incl. fuel tank, air-cleaner, exhaust silencer and electric starter)	kg	107
Power	kW	5 to 10.3
Torque	Nm	36.3 at 2000 rpm

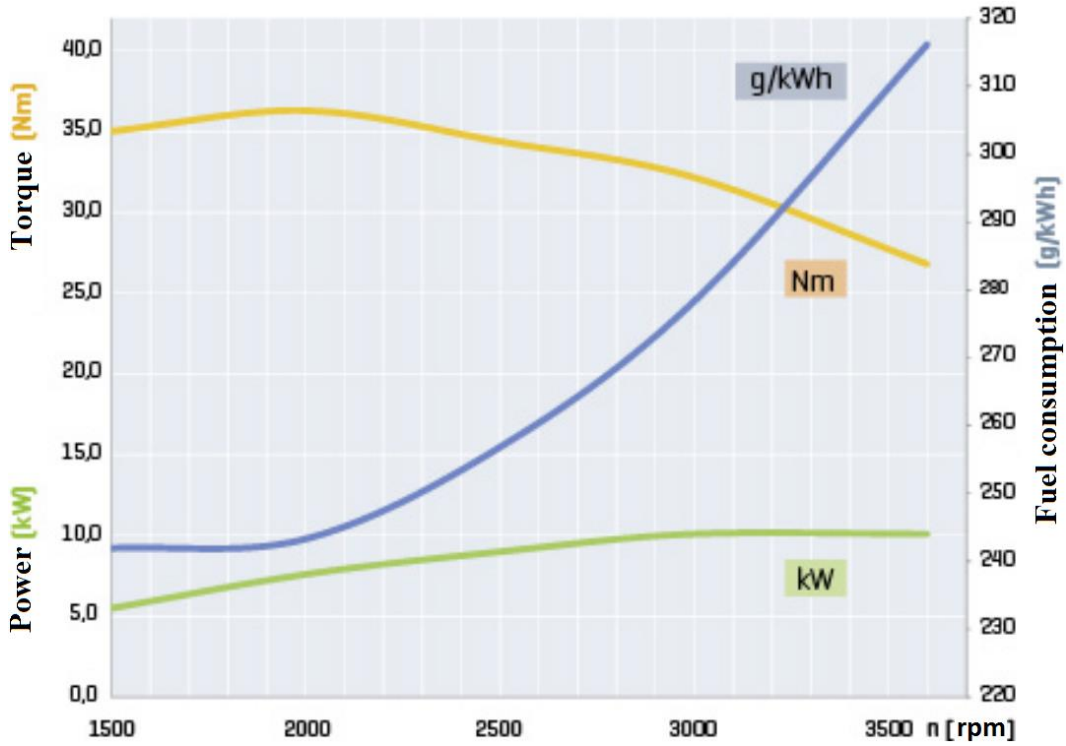

Figure 17. Performance curves of the original Hatz 1D81Z engine [55]

As shown in the Figure 17, the engine is designed for a range of speeds from 1500 to 3500 rpm. The maximum torque is achieved at 2000 rpm, while the maximum power is obtained from 3000 rpm.

3.2.1 Piston

The top of the original piston has a typical design of the compression ignition engine with the direct fuel injection.

As known, the in cylinder air motion in CI engines is usually characterized by a swirl motion, squish flow and turbulence [57], which have a significant influence on the combustion. The swirl motion is generated in the intake port and when introduced into the cylinder, the swirl–squish interaction produces a complex turbulent flow structures at the end of compression, which is much more intense in re-entrant combustion chamber [58], [59].

This re-entrant combustion chamber is located in the piston bowl, below the fuel injector as it can be seen in Figure 18. The largest influence of this combustion chamber on the swirl and turbulence is observed around top dead centre (TDC) when most of the air is compressed into the smaller diameter of the combustion chamber, in which by the conservation of the angular momentum and by the reduction of the radius of rotation, the speed of rotation increases [57]. This intense air motion breaks down the fuel jets [60] and has significant influence on fuel-air mixing, combustion and emission formation [61].

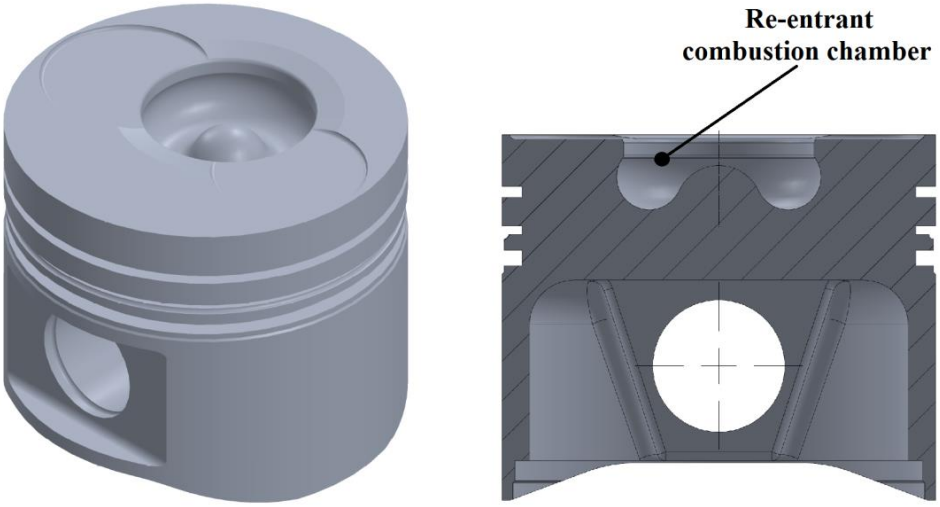

Figure 18. The design of original piston from Hatz 1D81Z engine

The piston diameter equals 99.9 mm and as can be seen in Figure 18 at the positions of the intake and exhaust valve it has valve pockets. The cylindrical side is equipped with three piston rings, two compression rings and one oil ring.

Piston modification

The previous review of literature and the numerical research of knock occurrence in the experimental engine showed that the original compression ratio of 20.5 could be too high for the operation in dual-fuel combustion mode. Therefore it was decided that the original compression ratio will be lowered to CR = 16. The reduction of the compression ratio can be achieved in two ways: by using a thicker cylinder head gasket or by lowering the piston top height. Figure 19 shows the influence of the cylinder head gasket thickness on the compression ratio for two different pistons. One is the original piston, and the second is the piston whose top is machined and lowered by 0.7 mm.

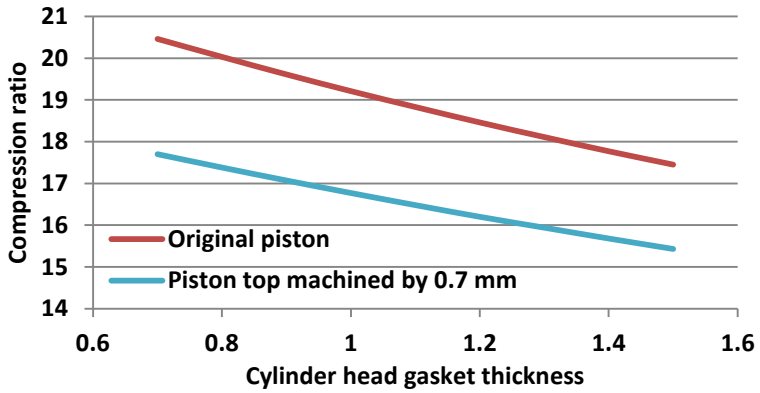

Figure 19. Compression ratio vs. cylinder head gasket thickness

The relations shown in Figure 19 are calculated from the measured volume of the cylinder bowl, volume of valve pockets and known data from technical engine specifications. Considering that the thickest available cylinder head gasket for Hatz 1D81Z has a thickness of 1.3 mm [62], which is not enough to lower the compression ratio to 16, it was decided that the piston height has to be lowered. Therefore, the piston height was lowered by 0.7 mm (Figure 20), which is sufficient to achieve the compression ratio 16 if a gasket with a thickness of 1.3 mm is used.

Figure 20. Left: original piston; right: after machining (-0.7 mm)

Machining process changed the valve pocket depth from 1 mm to 0.3 mm while the cylinder bowl volume, which is located below the machining surface, has not changed.

3.2.2 Modification of engine head

As mentioned before in the introduction, the change of engine operation from diesel to dual-fuel with the fully adjustable fuel injection system requires the installation of electrically controlled injector into the cylinder head. On the other hand, in order to enable spark ignition combustion mode a simple mechanical redesign of the second engine head allowed mounting of the spark plug in place where the original fuel injector was placed. Regardless of the combustion process, the pressure sensors for measurement of the intake pressure and of the in-cylinder pressure were installed in the cylinder head. All mentioned design modifications and requirements caused the need for machining of the cylinder head.

Intake pressure sensor installation

The intake pressure sensor is mounted in front of the intake valve instead of the port for the blow-by gases from the crankcase. In the hole for the blow-by pipe connection, the thread

for mounting of the pressure sensor was made (Figure 21), while the blow-by pipe is left open to the air. In this way the sensor measures the pressure changes just in front of the intake valve. This change slightly modified the crankcase ventilation system (CVS) from closed to the opened. Blow-by gases, consisting of the combustion products and of the oil vapours, are no longer returned to the intake port.

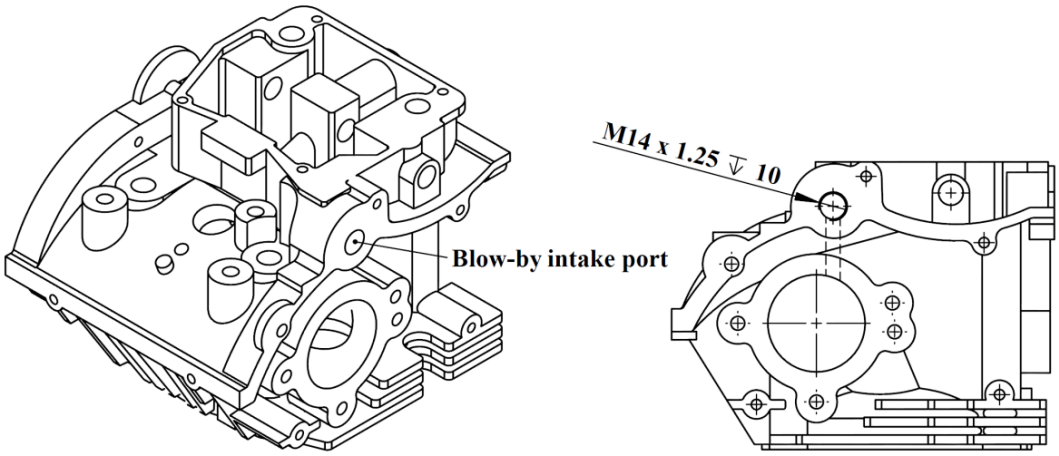

Figure 21. Machining for mounting the intake pressure sensor

For measuring the intake pressure the AVL low pressure indicating sensor LP11DA is used. It consists of the piezoresistive sensor for precise measurement of static and dynamic pressure variations. The sensor is equipped with an integrated amplifier and is installed into the cooling adapter which ensures that the temperature of the sensor does not exceed 232 °C, which is the limit of its operation [63]. The installed sensor in the cooling adapter is shown in Figure 22. Detailed specifications of sensor are given in Table 7.

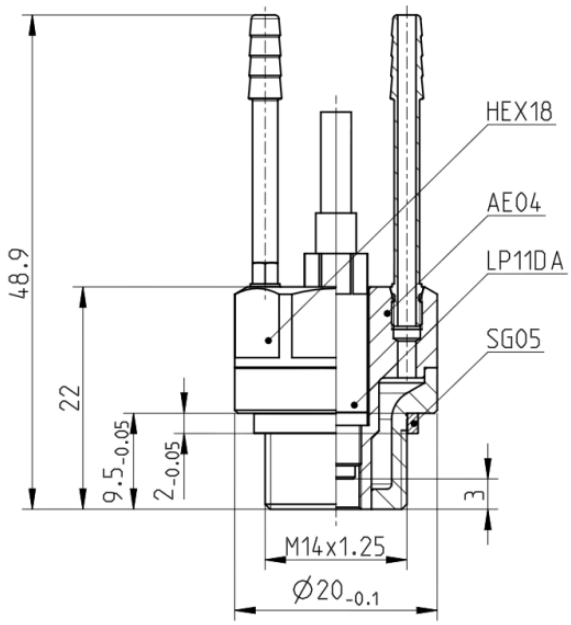

Figure 22. LP11DA pressure sensor in cooling adapter [63]

Table 7. Specifications of LP11DA pressure sensor [63]

Specifications	
Measuring range	0…10 bars
Thread diameter	M5 x 0.5
Sensitivity	930 mV/bar
Overload	20 bars
Linearity	< 0.1 %
Operating temperature	-55 … 232 °C
Compensated temp. range	-20 … 200 °C
Frequency response	50 kHz
Weight	15 g
Amplifier output	0.2 … 9.5 V (± 150 mV)
Power supply (DC)	24 V

High pressure sensor installation

The AVL GH14DK high pressure sensor is used for measurement of the in-cylinder pressure. It is an accurate and robust sensor designed for supercharged engines with very high specific output. It has double shell design, thermally optimized piezoelectric elements and improved membrane material. These features make the sensor durable and suitable for e.g. knock analysis [63].

Figure 23 shows deep borehole for the installation of the high pressure sensor. The hole is drilled and machined with specially designed AVL tools.

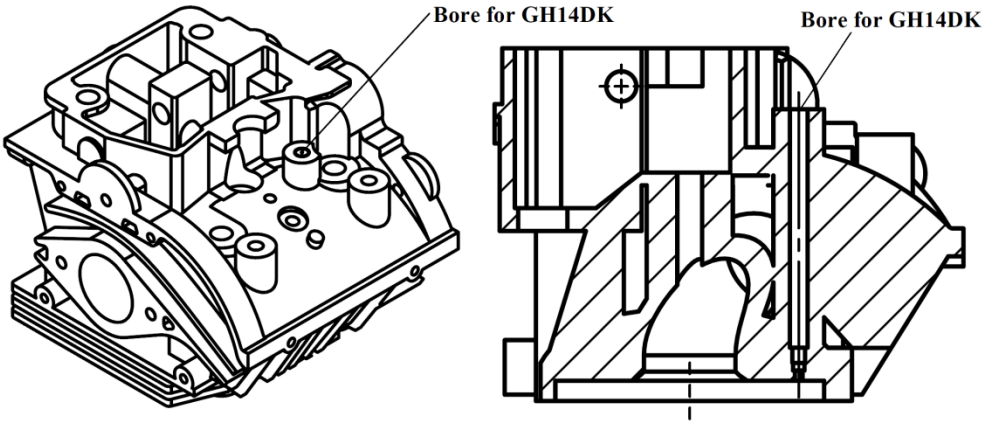

Figure 23. Design of the housing for mounting of the high pressure sensor

Detail view of the housing for the high pressure sensor is shown in Figure 24. Also, the position of the hole that connects the sensor with the combustion chamber is shown on the right side of the Figure 24. The main specifications of sensor are shown in Table 8.

Table 8. Specifications of GH14DK pressure sensor [63]

Specifications	
Measuring range	0…300 bars
Sensitivity	19 pC/bar
Overload	350 bars
Linearity	≤ ± 0.3 %
Operating temperature	-40 … 400 °C
Compensated temp. range	-20 … 200 °C
Natural frequency	170 kHz
Lifetime	≥ 10^8 load cycles
Thermal sensitivity changes	≤ ± 2 % (20 … 400 °C)
Cyclic temperature drift	≤ ± 0.7 bar

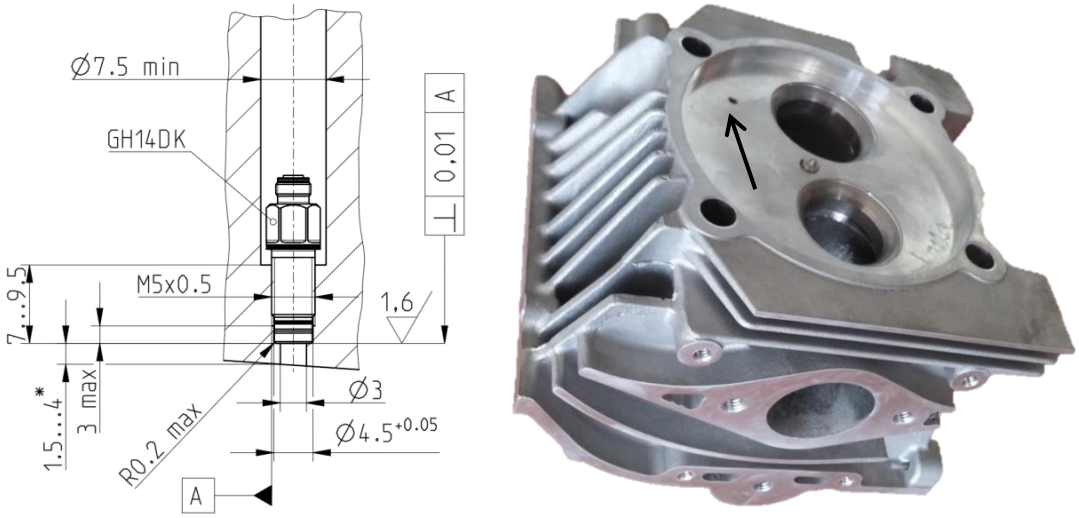

Figure 24. Left: AVL GH14DK installation [63]; right: location of high pressure sensor

Fuel injector installation

The change of the original fuel supply system with the new one (common rail system) required the installation of the new (piezo) fuel injector in the cylinder head. Considering that the selected fuel injector did not fit into the existing borehole, the cylinder head was redesigned for its installation. Figure 25 shows the original cylinder head on the left side and the redesigned borehole for piezo injector at the right side.

Because of the different geometry of the piezo injector compared to the original injector, the original borehole was fully filled with the material and the new borehole was made. As shown on Figure 26, the angle of the borehole, which defines the angle of the injector, is decreased from 20° to 10°, relative to the longitudinal axis of the cylinder. The change of angle was made because the new injector is designed for fully vertical installation

(parallel with the cylinder). Considering that the injector cannot be installed in the vertical position because of the limitations of the cylinder head design, 10° angle was selected as the smallest feasible angle.

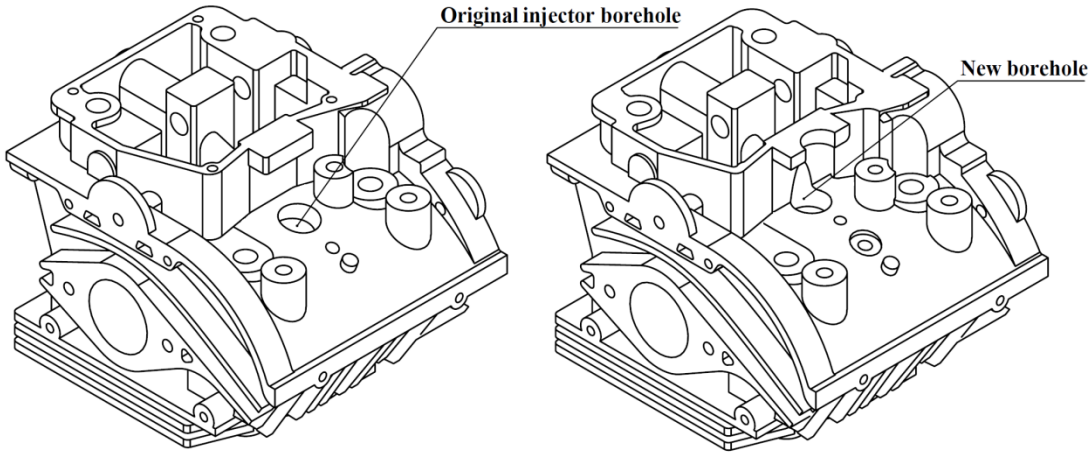

Figure 25. Redesign of cylinder head – new borehole for fuel injector

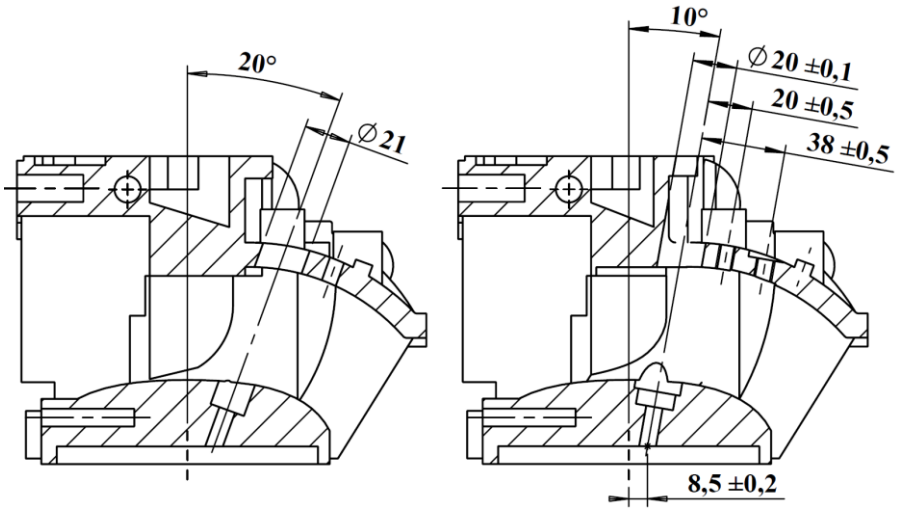

Figure 26. Angle of injector installation

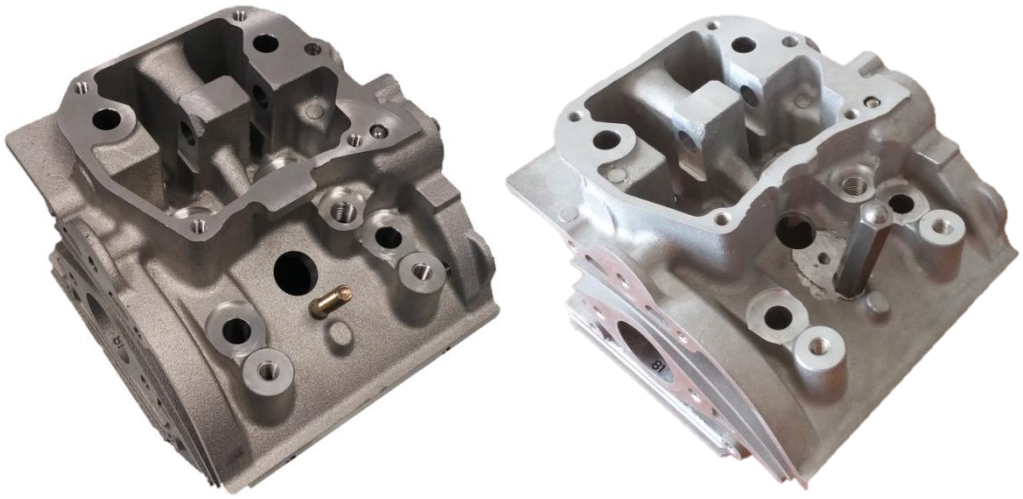

Figure 27. Cylinder head; left: before machining; right: after machining

The Figure 27 shows the cylinder head before and after the redesign process. Besides the new borehole, the elements for mounting of the fuel injector were also adjusted as shown on Figure 28.

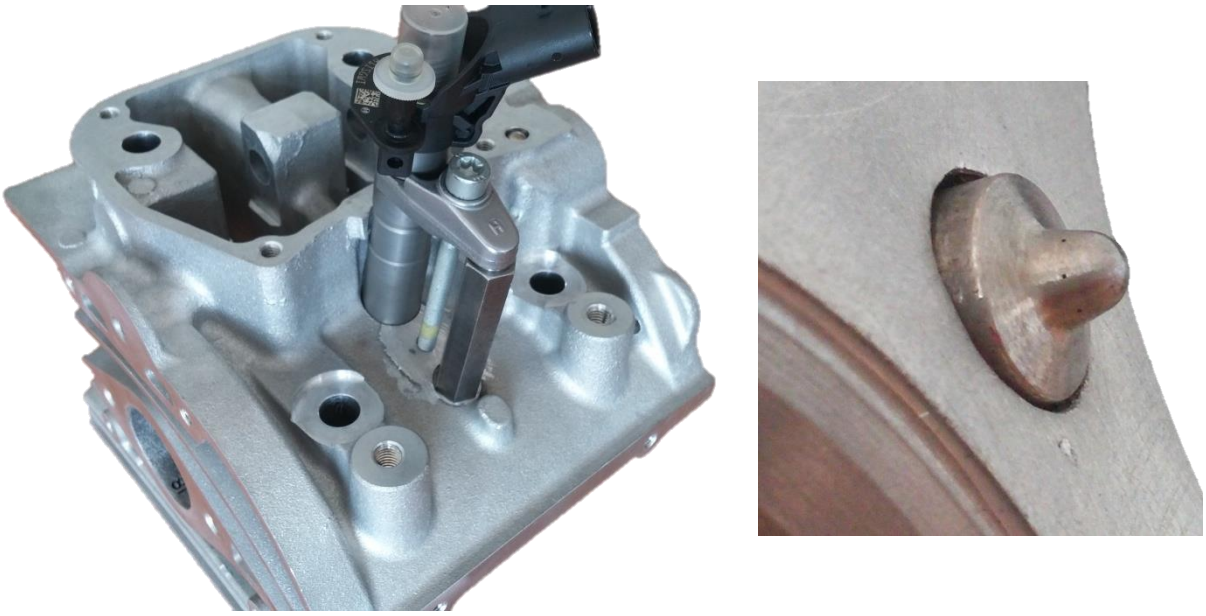

Figure 28. Cylinder head and fuel injector assembly (left - outside view; right – view from the in-cylinder side)

Although fuel injector is not mounted vertically, the angle of 10° ensures the fuel injection into the cylinder without direct spray on the cylinder head surface. The spray angle between nozzle holes is 152° which means that although the fuel is not injected symmetrically into the combustion chamber all the centers of the spray are within the combustion chamber (Figure 29). For the relative comparisons of normal diesel combustion process with the dual-fuel combustion process (performed in this research), the adjustable fuel injection system with high flexibility is more important than the fully optimized combustion chamber design.

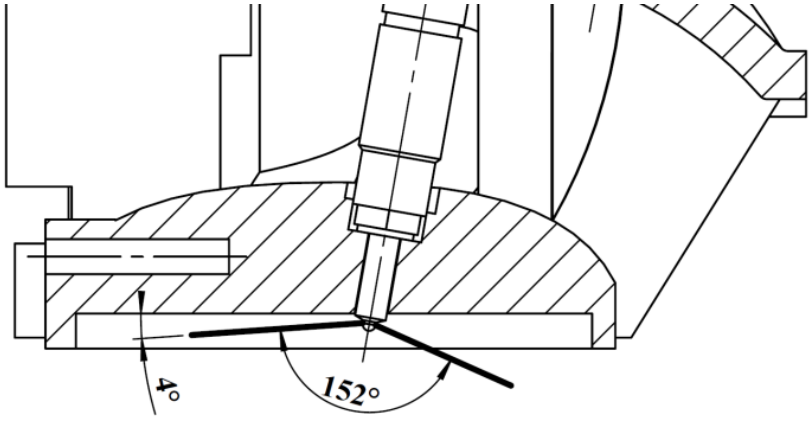

Figure 29. Fuel injection

3.2.3 Implementation of the fuel supply system

For the research of the influence of operating parameters on the dual-fuel combustion, the original mechanical fuel supply system for diesel fuel was replaced with the new, fully adjustable fuel supply system.

The original high pressure fuel supply system is a mechanical assembly set designed for normal diesel operation in the range of engine speed from 1500 to 4000 rpm, without any possibility of changing the injection pressure, injection timing or injection duration (the fuel injector is mechanically adjusted to open at 400 bars at all engine speeds). Therefore, the original high pressure fuel pump, high pressure pipeline and the fuel injector are completely removed from experimental engine. Figure 30 shows the removed original high pressure fuel supply system.

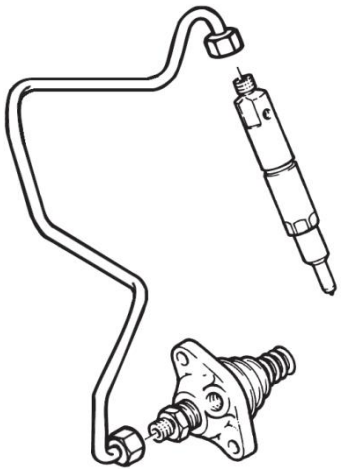

Figure 30. Original high pressure fuel supply system, reproduced from [64]

Instead of the removed fuel supply system, the common rail fuel supply system is embedded into the experimental setup, as shown and described above at the beginning of this chapter in Figure 15. Figure 31 shows the scheme of the whole diesel fuel supply system.

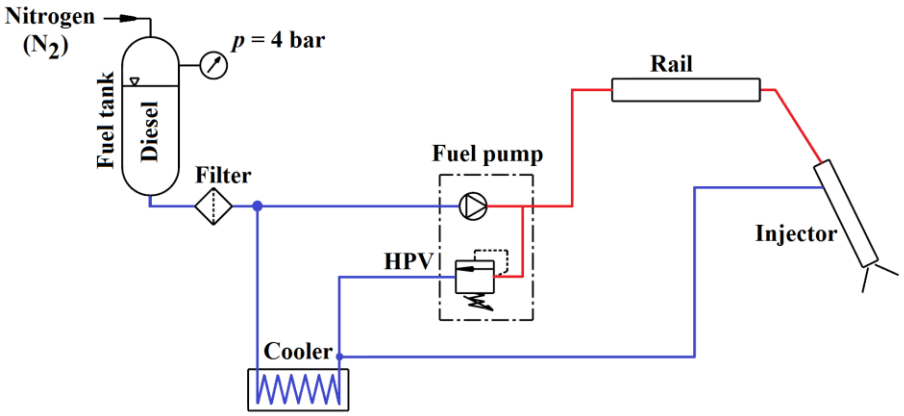

Figure 31. Diesel fuel injection system (red – high pressure; blue – low pressure)

The main components of the new high pressure fuel supply system are: piezo fuel injector, high pressure fuel pump, fuel accumulator and high pressure pipelines.

Piezo fuel injector

The main component of the new fuel supply system is the fuel injector which is controlled by a piezo actuator. This technology provides very short switching times, resulting in precise control of injection phases and injection quantities. Due to the fully flexible control of the fuel injection, it is possible to split the fuel quantity per cycle on smaller amounts which are separately injected through several phases. The example of multiple injection phases in normal diesel operation is shown in Figure 32. This injection strategy primarily ensures a reduction in NO_X emissions, together with a well optimized efficiency and quieter engine operation [65]. The advanced low temperature combustion (LTC) has the main influence on the reduction of NO_X and PM (soot) due to the lower charge temperature and the sufficiently long time available for mixing [66].

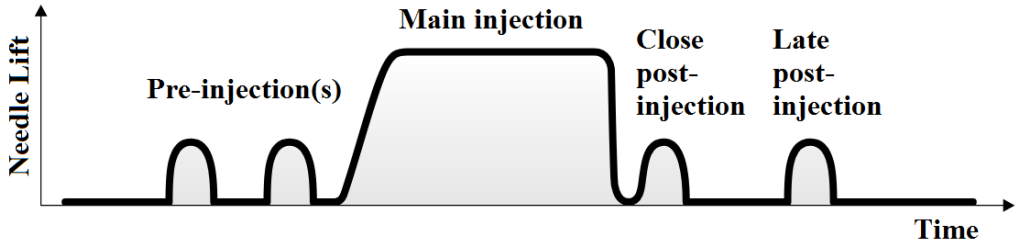

Figure 32. Multiple injections per cycle [67]

Figure 33 shows the main components of the Bosch CRI 3.0 piezo fuel injector which was used in this work. The working principle is based on the piezoelectric effect that enables the transformation of mechanical load into an electrical signal and vice versa. When an electrical current is applied to piezoelectric ceramic, its length instantly changes shape. This change in length is used to generate mechanical force. A piezo injector uses this effect to activate an injection valve's opening and closing mechanism.

The rapidly switching CRI3 piezo injector allows up to 10 short injection intervals within one operating cycle. The control is performed via a piezo actuator made of several hundred layers of a piezo ceramic material. The ceramic expands by a few thousandths of a millimeter as soon as voltage is applied, setting the jet needle in motion. This coupling of actuator and nozzle needle enables the very short reaction times and very small preinjection quantities.

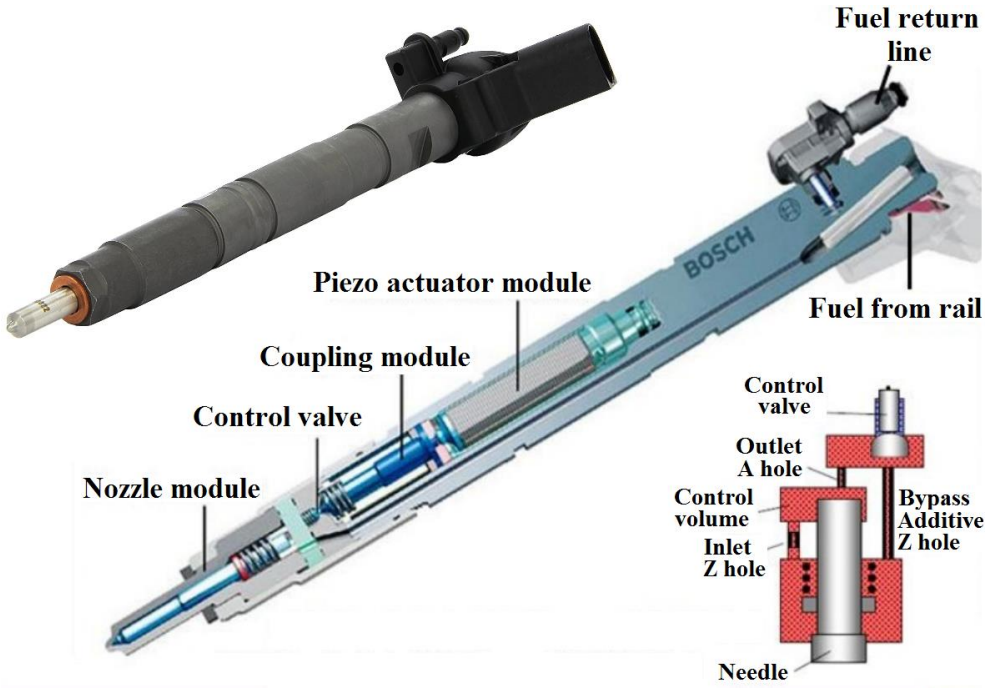

Figure 33. Bosch CRI3 fuel injector (B0 445 115 078), reproduced from [68]

The selection of the injector for the experimental setup was based on the fuel flow and the fuel pressure. Input parameters for the calculation of required fuel quantity are given in Table 9.

Table 9. Input parameters for maximum diesel fuel flow calculation

Parameter	Value	Unit
V_H	0.667	dm^3
CR	max = 20.5	-
n	3000	rpm
T_0	298	K
m_{ref}	0.00078	kg
$\rho_{air\ (T=298\ K)}$	1.1839	kg/m^3
λ	1.00	-
AFR_{diesel}	14.5	kg_{air}/kg_{fuel}
ρ_{diesel}	832	kg/m^3
LHV_{diesel}	43	MJ/kg_{fuel}

In the calculation of the required fuel flow, the following equations are used [60].

Volume flow of diesel fuel is calculated as:

$$q_{v,diesel} = \frac{q_{m,diesel}}{\rho_{diesel}} \quad (4)$$

where are:

$q_{v,\,diesel}$ [m^3/s] – volumetric flow of diesel fuel,

$q_{m,\,diesel}$ [kg/s] – mass flow of diesel fuel,

ρ_{diesel} [kg/m^3] – density of diesel fuel.

The mass flow of diesel fuel is calculated from the fuel mass per cycle m_{diesel} (kg/s) and engine speed n (rpm):

$$q_{m,\mathrm{diesel}} = m_{\mathrm{diesel}} \cdot \frac{n}{60 \cdot n_c} \tag{5}$$

where n_c represents number of revolutions per one cycle (for a 4-stroke engine $n_c = 2$).

The fuel mass per cycle is expressed from:

$$m_{\mathrm{diesel}} = \frac{m_{\mathrm{air}}}{AFR_{\mathrm{diesel}} \cdot \lambda} \tag{6}$$

m_{air} [kg/cycle] – air mass per cycle,

AFR_{diesel} [kg_{air}/kg_{fuel}] – air to fuel ratio for diesel fuel,

λ [-] – excess air ratio.

The air mass per cycle is given by the referent in-cylinder air mass (m_{ref}) and air delivery ratio (Λ) of engine:

$$m_{\mathrm{air}} = m_{\mathrm{ref}} \cdot \Lambda \tag{7}$$

from which follows air delivery ratio:

$$\Lambda = \frac{m_{\mathrm{air}}}{m_{\mathrm{ref}}} \tag{8}$$

which according to [60], after combining equations and introducing the amount of residual gases results in:

$$\Lambda \approx \frac{1}{1+\gamma} \cdot \frac{\mathrm{CR}}{\mathrm{CR}-1} \cdot \frac{T_0}{T_{\mathrm{intake}}} \cdot \frac{p_{\mathrm{intake}}}{p_0} \tag{9}$$

$\gamma = 0.04$ – assumed residual gases content,

CR – Compression ratio.

The calculated fuel quantities in dependence of the intake pressure (p_{intake}), by using input parameters from Table 9, are given in Table 10.

Table 10. Required fuel flows through the fuel injector

p_{intake} [bar]	Λ -	m_{air} [kg]	m_{diesel} [kg]	$q_{m,air}$ [kg/s]	$q_{m,diesel}$ [kg/s]	$q_{v,diesel}$ [ml/min]	$q_{v,cycle}$ [mm^3/cycle]
1.0	0.92	0.0007157	0.0000494	0.01789	0.001234	89	59
1.5	1.38	0.0010736	0.0000740	0.02684	0.001851	133	89
2.0	1.84	0.0014314	0.0000987	0.03579	0.002468	178	118
2.5	2.29	0.0017893	0.0001234	0.04473	0.003085	222	148

According to the calculated values of the fuel flow and according to the fact that the desired injection pressure was minimum 1350 bars, Bosch piezo injector (part number: B0 445 115 078) designed for 3.0 TDI engine from VW group was chosen. This engine contains 6 cylinders with a total volume of 3000 cm^3 and produces maximum output power of 175 kW, which means 29 kW per cylinder (cylinder volume equals to 0.5 dm^3). Injector contains 7 holes symmetrically placed around the top of the injector and is designed for vertical installation. The angle between holes is 152° as shown previously in Figure 26. The supported operating injection pressure is up to 1800 bars.

Since the characteristics of the fuel injector (fuel flow in dependence of injection duration and of fuel pressure) are not widely available in the literature and were not given by the manufacturer, they were measured and recorded on the fuel injector testing device at the company Purić d.o.o. [69]. The results of these tests are shown in Table 11, Figure 34 and Figure 35.

Table 11. Fuel quantity, mm^3/cycle [69]

		Injection duration [μs]								
		100	150	200	250	300	800	1300	1800	2300
Fuel pressure	300 bar	0	0.1	0.5	0.9	1.5	15.1	35.1	56.3	75.9
	800 bar	0	1	2.4	4.3	7.3	47.5	90	119.9	142.2
	1300 bar	0	1.9	4.3	7.7	13.2	71.9	119.6	150	177.8
	1800 bar	0	2.6	5.3	11.6	18.2	90.8	137	172.8	206

From the results in Figures 34 and 35, and Tables 9, 10 and 11 one can conclude that the fuel injector meets the required fuel flow quantities (mm^3/cycle). For the highest required fuel flow of 148 mm^3/cycle (Table 10), the estimated injection duration with the highest pressure is around 1500 μs. Since the results shown in Table 10 are calculated at 3000 rpm the

injection duration of 1500 μs would span over the 27° CA which is acceptable. From the Figure 35, where the characteristic of fuel injector for very short injection durations is shown, it can be seen that for triggering of the injection duration shorter than 100 μs there is no flow independently of the injection pressure.

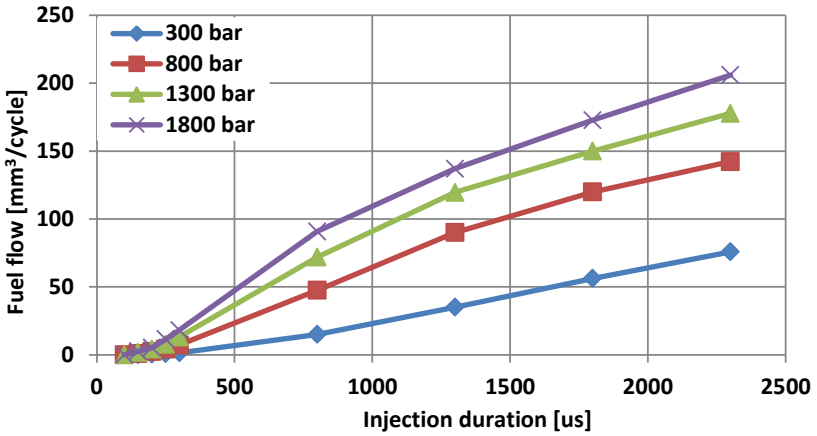

Figure 34. Characteristic of fuel injector

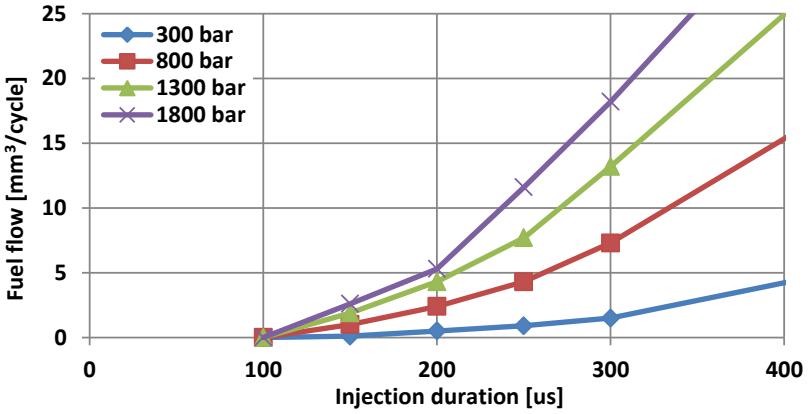

Figure 35. Characteristic of the fuel injector at small injector openings

High pressure fuel pump

The high pressure fuel pump is the interface between the low pressure and the high-pressure stages which is responsible for providing adequate high-pressure fuel under all operating conditions. This also includes the provision of extra fuel as needed for rapid build-up of pressure in the rail. The high pressure pump continuously generates the system pressure as needed in the high pressure accumulator. This means that, in contrast to the conventional systems, the fuel does not have to be specially compressed for each individual injection process.

According to the desired pressure of 1350 bars and required fuel flow quantities (Table 11) Bosch high pressure fuel pump CR/CP1S3/L70/10-1S (part number 0 986 437 015) was

chosen. Figure 36 shows schematic of the longitudinal section of the selected fuel pump, while Table 12 shows the main characteristics.

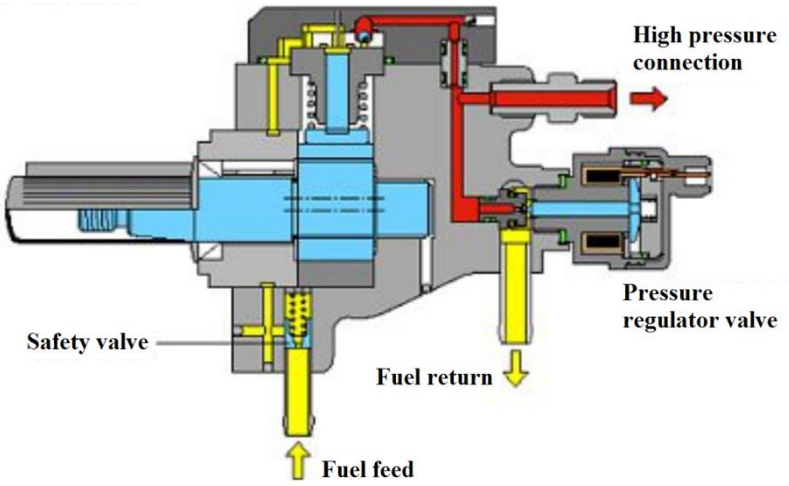

Figure 36. High-pressure fuel pump Bosch CP1 [70]

Table 12. Characteristics of high-pressure fuel pump [71], [72]

Parameter	Value	Unit
Max. pressure	1350	bar
Operating volume (V_P)	700	mm^3
Direction of rotation	left	-
Power torque	16	Nm
Inlet pressure	2.5 - 4	bar

Inside the high-pressure pump, the fuel is compressed with three radially arranged pump pistons which are positioned at an angle of 120° to each other. Since three delivery strokes take place for every revolution, only low peak drive torques are generated so that the stress on the pump drive remains uniform [71].

This high-pressure fuel pump requires pre-supply fuel pump which pumps fuel from the tank to the inlet of the high-pressure pump. The pre-supply fuel pump should be able to ensure the inlet pressure of at least 1.5 bars which opens the safety valve in the fuel inlet. Forced fuel flows through the safety valve and into the high-pressure pump's lubrication and cooling circuit. The driveshaft with its eccentric cams moves three pump plungers up and down in accordance with the shape of the cam. The pre-supply pump forces fuel through the high-pressure pump's inlet valve into the pumping-element chamber whose pump piston is moving downwards. The inlet valve closes when the piston pump passes bottom dead center, and fuel can be compressed beyond the delivery pressure. The increasing pressure opens the outlet valve as soon as the rail pressure is reached, and the compressed fuel enters the high-pressure circuit [71].

Since the high pressure pump is designed for a large delivery (fuel flow), the excessive high-pressure fuel is delivered during idle and part-load operation. This excess fuel is returned to the tank via the pressure-control valve which is installed directly on the high pressure pump. This electronically controlled pressure-control valve enables the stable control of the rail pressure which can be changed during engine operation.

In order to monitor and record the fuel consumption during operation, the experimental setup uses Ohaus Explorer weight scale [73] with accuracy of 0.1 g, which hosts the fuel tank. The recirculation of fuel through the fuel tank in such a system is not suitable because it causes fuel mixing and vibrations of the tank. These vibrations would cause unstable and imprecise weight measurement, i.e. they would cause strong noise in the measurement signal. Therefore, the fuel return line is connected to the inlet of the high-pressure fuel pump as previously shown in Figures 15 and 31. Also, instead of the pre-supply fuel pump, the gas (N_2) from the pressure cylinder is used to pressurize the fuel into the high-pressure fuel pump. This system of fuel supply pressurizes both the inlet and return ports of the high-pressure pump which are mutually connected by the high-pressure fuel pump. This means that the safety valve is pressured on both sides with the same pressure and cannot be moved to open the high pressure channel. Therefore, the safety valve was replaced with a new one that did not comprise a spring and is fixed in the housing. That design allows the fuel flow in high-pressure line as well as in the lubrication and cooling circuit.

The high pressure pump is installed on the experimental setup independently of the engine and its drive. It is mounted in a separate housing and driven by the electric motor by means of a toothed belt as shown in Figure 37.

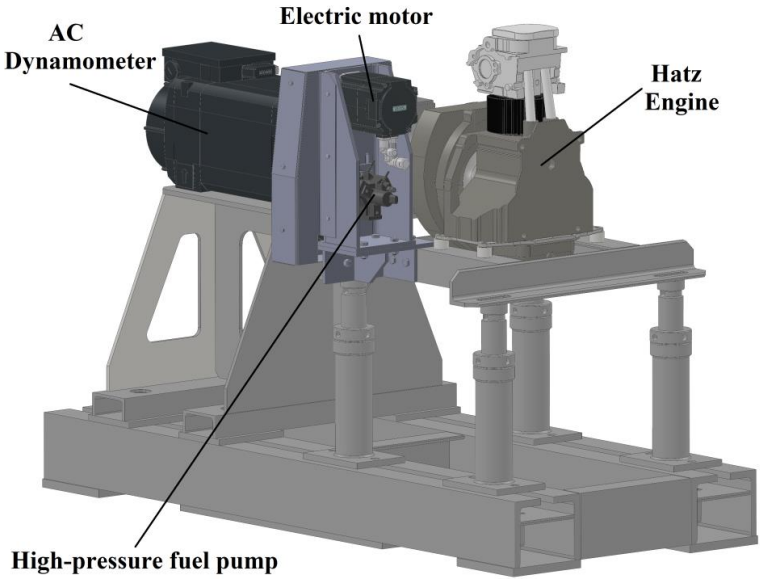

Figure 37. Installation of the high pressure pump on experimental setup

The torque for the high-pressure pump driven is equal to 16 Nm, while the delivery rate depends on the rotational pump speed. Required rotational pump speed for the fuel flow shown in Table 10 can be calculated from the equation [74]:

$$n_{\text{pump}} = \frac{q_{\text{v,diesel}}}{V_{\text{p}}} = \frac{222\,000\ (\text{mm}^3/\text{min})}{700\ (\text{mm}^3)} = 317\ \text{rpm} \tag{10}$$

For driving the high-pressure fuel pump, the Siemens 1FL6064-1AC61-0AA1 electric motor (Figure 38) was chosen whose basic data is shown in Table 13.

Table 13. Engineering data, Siemens 1FL6064-1AC61-0AA1 [75]

Parameter	Value	Unit
Rated speed	2000	rpm
Rated torque (100 K)	7.16	Nm
Rated current	4.6	A
Rated power	1.5	kW
Maximum torque	21.5	Nm
Static torque	8	Nm

Figure 38. Siemens 1FL6064-1AC61-0AA1 [75]

As shown in Table 13, the rated torque (7.16 Nm) is lower than requested (16 Nm). Therefore, for satisfying the requested torque with respect to the minimum high-pressure pump rotational speed, toothed belt pulleys with transmission ratio of i = 3.6 were chosen. Drivetrain of the high-pressure fuel pump is shown in Figure 39. Selected transmission ensures maximum torque of:

$$T_{\text{fuel pump}} = i \cdot T_{\text{EM}} = 3.6 \cdot 7.16 \text{ Nm} = 25.8 \text{ Nm} \quad (11)$$

$T_{\text{fuel pump}}$ [Nm] - torque on high-pressure fuel pump driveshaft,

T_{EM} [Nm] - torque on electric motor driveshaft.

The maximum high-pressure fuel pump speed is then equal to:

$$n_{\text{fuel pump}} = \frac{n_{\text{EM}}}{i} = \frac{2000}{3.6} = 555 \text{ rpm} \quad (12)$$

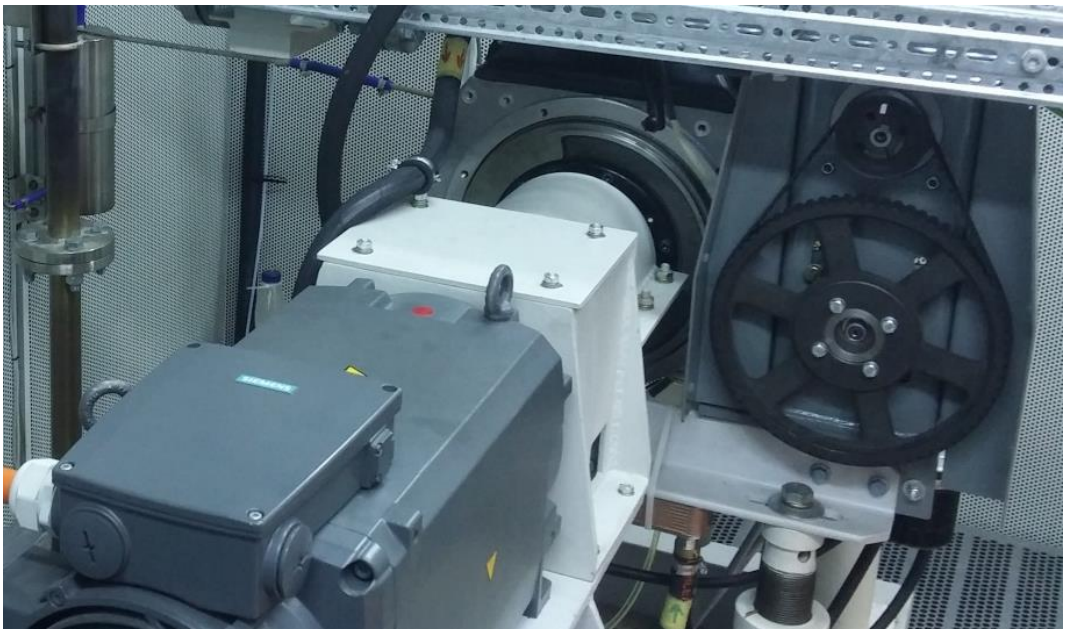

Figure 39. Drivetrain of the high-pressure fuel pump

As shown, the high-pressure fuel pump driven by electric motor provides desired fuel pressure and fuel flow necessary for normal diesel CI operation of the experimental engine. More details regarding the calculation of the high-pressure fuel pump drivetrain system (regarding the selection of the toothed belt and pulleys) can be found in [76].

High-pressure fuel accumulator (rail)

The high pressure accumulator stores the fuel at high pressure and provides the fuel under the high pressure to the injector. At the same time pressure oscillations which are generated due to the intermittent high-pressure pump delivery and the injection of the fuel are damped by the rail volume.

This high-pressure accumulator is on the engines common to all cylinders, hence it is named “common rail”. Even when the large quantities of fuel are extracted, the inner pressure of the common rail maintains almost constant. This ensures that the injection pressure remains constant during the period when the injector is opened.

The fuel pressure accumulator used on the experimental setup is originally made for VW/Audi group, for V6 TDI engine which contains two equal pressure accumulators mutually connected. Each fuel pressure accumulator is connected to the three fuel injectors.

Since the experimental engine is a single cylinder engine, the outputs on the rail intended for other cylinders are blocked. Figure 40 shows the fuel accumulator mounted to the experimental setup.

Figure 40. High-pressure fuel accumulator (rail)

The high-pressure pipelines that are used for connecting the high-pressure fuel pump with the fuel accumulator and the fuel accumulator with the fuel injector are designed for fuel pressures up to 2000 bars. They are provided by the company Maschinenfabrik Guido GmbH [77].

High-pressure sensor

The Bosch high-pressure sensor (part number 0 281 002 706) designed for operating pressure of up to 1800 bars is mounted on the fuel accumulator (rail) [78]. The sensor accuracy in range 35 - 1800 bars equals to 1.5% F.S. [79].

3.2.4 Port fuel injection

The schematic of the port fuel injection system is shown in Figure 41. Pressure cylinder with methane is equipped with a pressure regulator which delivers gaseous fuel to the port fuel injector at constant pressure of 4 barg. The flow smoothing tank is mounted on the pipeline which decreases the flow oscillation caused by the intermittent operation of the fuel injector. For the measurement of the fuel mass flow the Coriolis Proline Promass A100 flow meter is used. It provides highly accurate measurement of small quantities of liquid and gases (max. measured error for mass flow of gas fuel equals to ±0.5%). A detailed specification of flow meter can be found in [80].

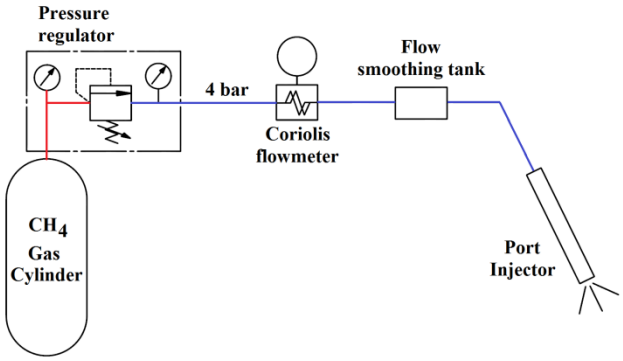

Figure 41. Schematic of the port fuel injection system

For injection of the gaseous fuel into the intake pipe the Hana H2001 injector is used. It is mounted to the intake pipe approx. 80 mm in front of the intake valve. The main specifications of the injector are given in Table 14 while other specifications can be found in [81].

Table 14. Fuel injector Hana H2001 specifications

Parameter	Value	Unit
Voltage (DC)	12	V
Pick Current	6.4	A
Hold Current	2	A
Resistance	1.9	Ω
Max. pressure	4	bar
Flow	130 - 175	l/min
Opening time	2	ms
Closing time	1.2	ms
Fuel	LPG/CNG/LNG	
Temperature range	-40 up to 125	°C

3.3. Modification of experimental setup for SI operation

One of performed research on the previously described experimental engine was the experimental investigation of the influence of compression ratio on performance and emissions of natural gas fuelled spark ignition (SI) engine. This research was performed as the benchmark for further dual-fuel operation. Through the research, three different compression ratios were used with the aim of finding the differences in achieved performance and exhaust gas emissions. One of the compression ratios used was similar to the compression ratio of gasoline engines (CR = 12), while the other two compression ratios were similar to the compression ratio of diesel engines (CR = 16 and CR = 18). Performed research also showed which compression ratio between CR = 16 and CR = 18 is more suitable for operation with

natural gas and this compression ratio was further used in dual-fuel operation. For the mentioned research, experimental engine was converted from CI engine to SI engine operation. The new cylinder head was used and instead of the original diesel fuel injector, the spark plug was mounted into the cylinder head. Figure 42 depicts simplified scheme of experimental setup.

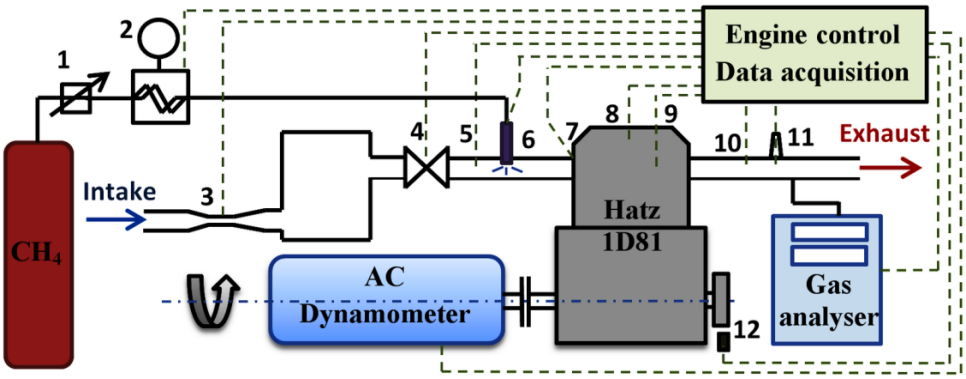

Figure 42. Experimental setup for SI engine operation

The change from original compression ratio (20.5) to compression ratio of 18 and 16 is obtained by addition of a thicker cylinder head gaskets and by changing the height of the piston (the piston height is 0.7 mm lower compared to the original height), while the compression ratio of 12 is achieved by another piston, whose height is reduced for 3 mm compared to the original piston. Instead of natural gas, pure methane (99.95 % vol.) from the pressure cylinder is used as a fuel.

3.4. AC Engine Dynamometer

The engine dynamometer is a device that allows engine testing in operating points that are defined by engine speed and engine torque. The dynamometer on the used experimental setup is based on the Siemens asynchronous motor 1PH8137-1DG00-1BA1 [82] that can operate in two different modes: loading mode (IC engine is braked by AC motor) or motoring mode (the AC motor drives the IC engine). In motoring mode, the motor uses electrical energy from the network and pushes the engine, while in the loading mode it converts the mechanical work from the IC engine output shaft to the electrical energy and returns it to the network. Therefore, engine dynamometer is used to start the engine and to get to the desired engine speed, after which it switches to the load mode once the IC engine starts to produce work. Main characteristics of the motor are shown in Figure 43.

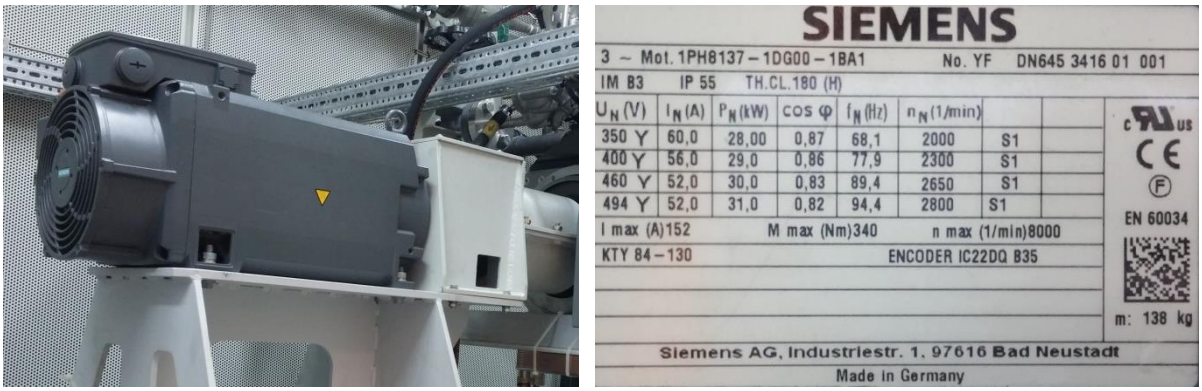

Figure 43. Engine dynamometer; nameplate on dynamometer

In addition to the main operating modes, the control of the engine dynamometer can be performed in two different methods. The first method sets engine speed as a constant (n/alpha) while the second sets the engine torque (T/alpha) as a fixed value. The operator has the ability to manually manage the dynamometer via the panel screen in the control room or via LabVIEW application (remote control). Touch screen of the manual control is shown in Figure 44 while the LabVIEW application will be explained below in the chapter Control system.

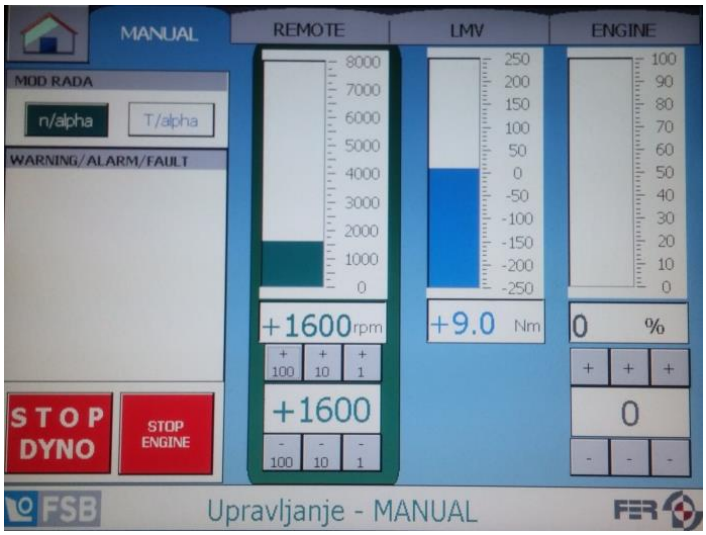

Figure 44. Touch screen for the manual control of the dyno, located in the control room

3.5. Measurement of the exhaust emissions

For the measurement of THC, CO_2 and CO emissions the standard methods for measurement of specific gases were used. A non-dispersive infra-red analyser was used for measurement of CO and CO_2 emission, while the flame ionisation detector (FID) analyser was used for measurement of THC emission. Both analysers come from the manufacturer Environment S.A and are embedded into the same analyser cabinet as shown in Figure 45.

Figure 45. Analysers for THC; CO and CO_2 emission; reproduced from [83]

The analyser Graphite 52M utilizes the most sensitive and widely used FID technology which ensures high accuracy (Table 15), sensitivity and stability of the measurement of THC emission. The main features of the analyser are heated detector up to 191 °C which allows measurement of high concentration of HC, fast response time and suitability for wet and corrosive sample measurements. It is driven by the fuel mixture of H_2 and He [83].

Table 15. Specifications of the THC, CO and CO_2 analysers [83], [84]

Device	Range	Accuracy
Graphite 52M	0 - 20,000 ppm	< 1% of the displayed value between 15% and 100% of the F.S.
MIR 2M	- CO: 500 to 50,000 ppm - CO_2: 100 to 250,000ppm	Zero drift: <1% full scale (F.S.) / 24 h Span drift: <1% F.S. / 24 h Linearity: <1% of reading from 20 to 100% F.S

The main features of the multi-gas infra-red analyser model MIR 2M which uses non dispersive infra-red gas correlation filter principle (IR GFC) for measurement of CO and CO_2 emissions are short response time, high precision with very small span and zero drift, and simultaneous 2-channel monitoring [84]. The first channel was used for measurement of CO and CO_2 emissions in the exhaust pipe, while the second channel was used for the measurement of CO_2 emission in the intake pipe. The sample of exhaust gas flows through the dryer before it comes into the analyser because the used measurement method (IR GFC) requires dry exhaust gases. Recalculation of dry exhaust gas emissions on wet exhaust gas emissions is carried out using the method which will be explained later in Post-processing chapter.

The NO_X, Lambda and O_2 are measured by a ceramic sensor that is mounted in the exhaust stream of the engine. The ceramic sensor is a part of the measurement device NO_X 5210 which is shown on Figure 46.

Figure 46. NO_X 5210 and ceramic sensor for NO_X, lambda and O_2

The NO_X 5210 can be used for all fuel types (H:C, O:C, N:C, and H_2) and its specifications are given in Table 16.

Table 16 NO_X 5210 – Specifications [85]

Parameter	Specification
Ranges	NO_X 0 to 5000 ppm λ 0.4 to 25 AFR 6 to 364 φ 0.04 to 2.5 O_2 0 to 25%
Accuracies	NO_X (Type T) ± 5 ppm(0 to 200 ppm), ± 20 ppm(200 to 1000 ppm), ± 2.0% (elsewhere) λ ± 0.008 (at 1 λ), ± 0.016 (at 0.8 to 1.2 λ), ± 0.018 (elsewhere) AFR ± 0.15 (at 14.6 AFR), ± 0.4 (at 12 to 18 AFR), ± 1.0 (elsewhere) %O_2 ± 0.4 (0 to 2% O_2), ± 0.8 (elsewhere)
Response Time	Less than 1 s. Less than 150 ms (λ, AFR, φ, O_2)

3.6. Control system and data acquisition

For the management of the engine and for control of the other equipment of the experimental setup, the National Instruments (NI) equipment was used. NI Crio-9074 with modules NI 9401, NI 9474, NI 9870 and NI 9474 [86] was used for generating the signals necessary for engine management while the NI cDAQ-9188 with modules NI 9215, NI 9263, NI 9472, NI 9421, NI 9203, NI 9213, and NI 9862 [86] was used for acquisition of data from

various sensors. Figures 47 and 48 shows the NI equipment used for engine management and data acquisition.

Figure 47. NI Crio-9074

Figure 48. NI cDAQ-9188

For the detection of the position of the crankshaft and of the piston, which is necessary for controlling the injection timing and/or spark timing, two Hall sensors, one with trigger wheel and the other with wheel with magnets, are mounted on the camshaft and crankshaft respectively. Figure 49 shows Hall sensors mounted on the engine. The Hall sensor mounted on the crankshaft and triggered by the wheel with magnets (Figure 49 left) is used for the definition of the crank angle within single revolution of the crankshaft, while the other sensor triggered by the trigger wheel mounted on the camshaft (Figure 49 right) is used for determination of the part of the cycle (power strokes or gas exchange).

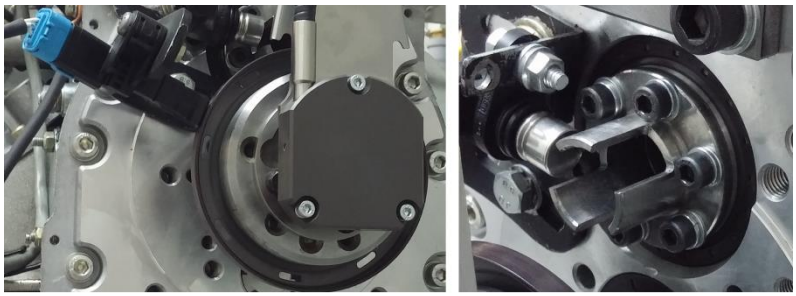

Figure 49. Left: Hall sensor on the crankshaft; Right: Hall sensor on the camshaft

The operation of described devices and actuators as well as the acquisition of data from the described sensors is provided by the in-house developed code within the National

Instruments LabVIEW software. It is a systems engineering software for the applications that require test, measurement, and control with rapid access to hardware and data insights [87]. Figures 50, 51 and 52 show the main windows of the applications created in LabVIEW which are used for the control and monitoring of the experimental setup.

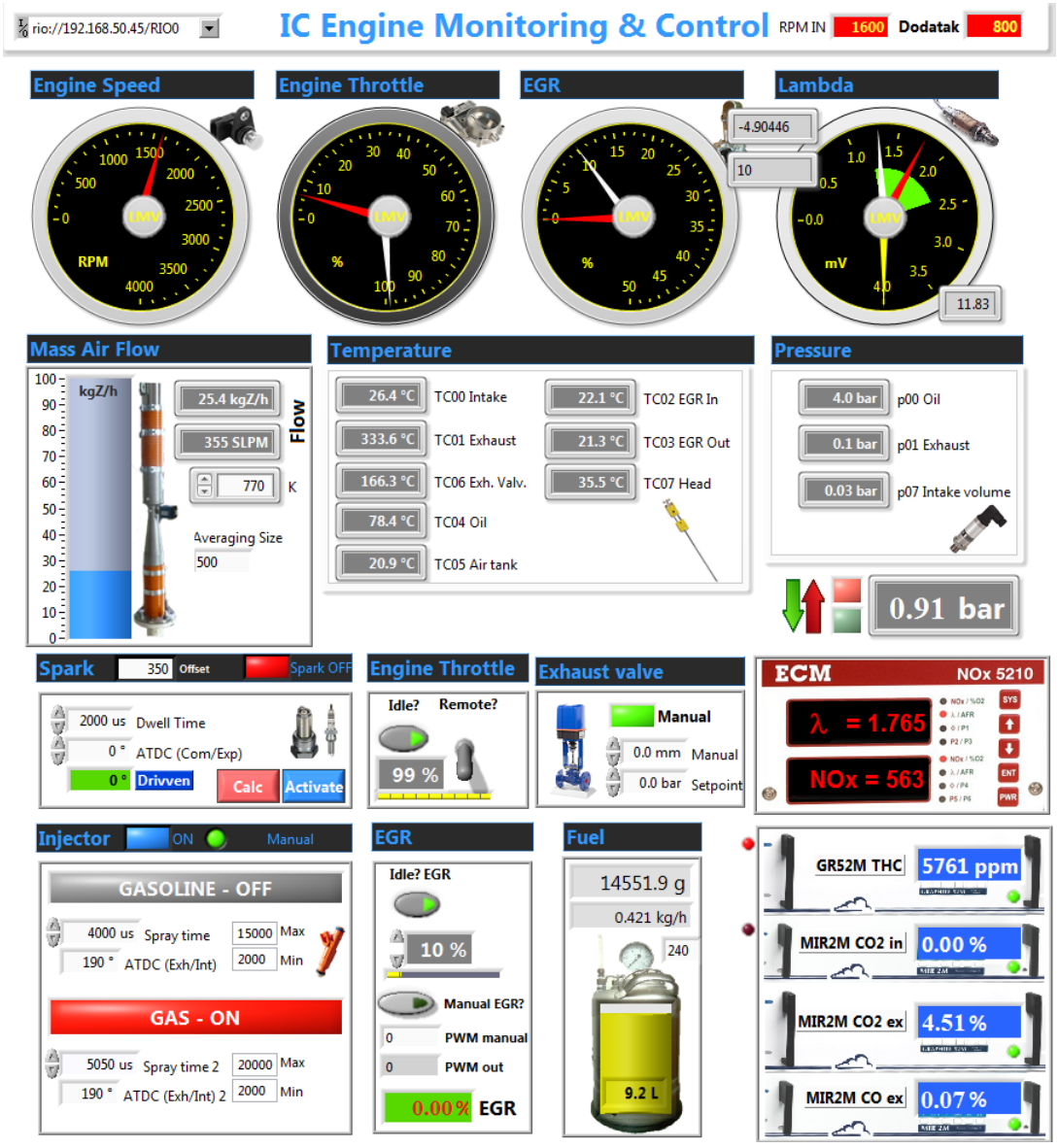

Figure 50. LabVIEW application for engine monitoring and control

As shown in Figure 50, the application for monitoring and control of the engine provides a lot of information such as: engine speed, throttle position, EGR valve position, lambda value, air mass flow, temperatures, pressures, exhaust emissions, consumption of the liquid fuel calculated from the change of fuel mass on the weight scale, amount of EGR; and allows control of some parameters such as: intake pressure, spark timing, throttle position, exhaust valve opening, fuel injection in the intake pipe and EGR valve position. As mentioned above, the engine dynamometer is also controlled and monitored via LabVIEW,

with a separate application as shown in Figure 51, as well as a gas fuel flow meter and a fuel pump drive electric motor.

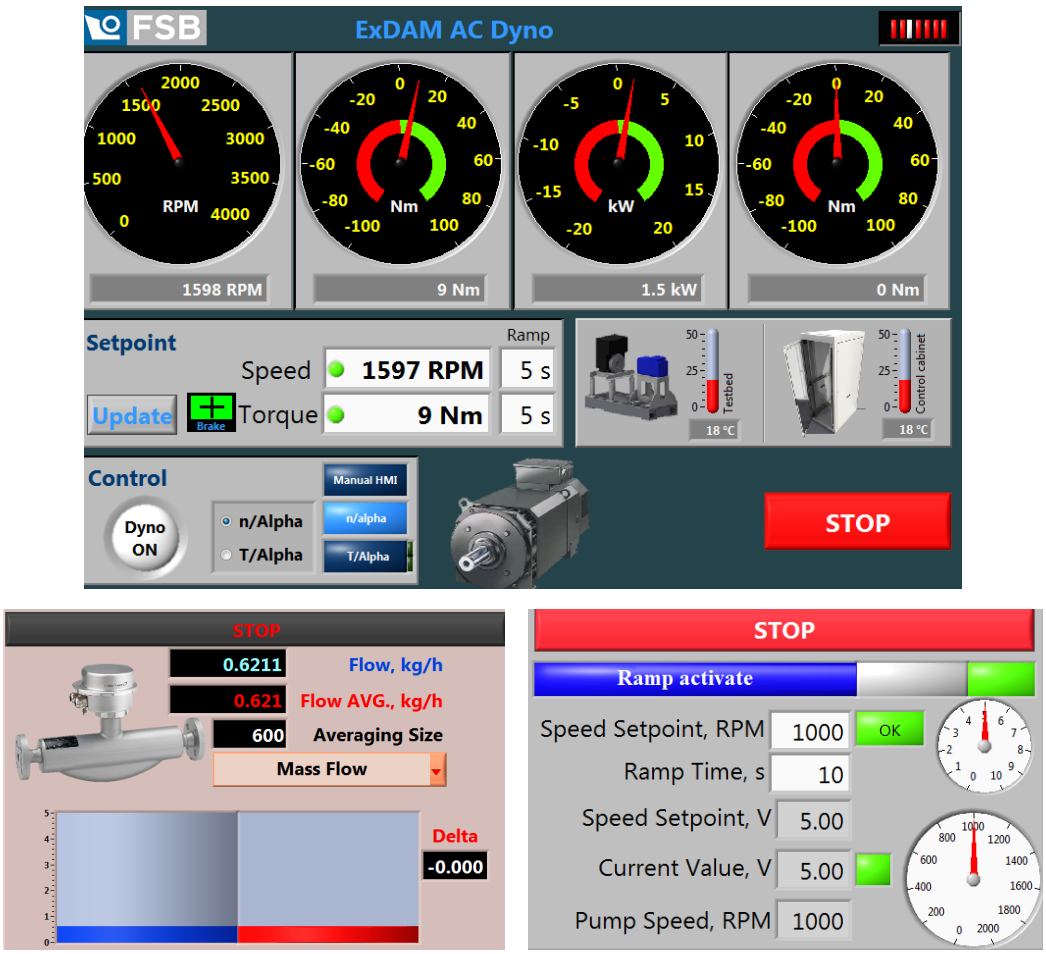

Figure 51. LabVIEW applications (dynamometer, coriolis flow meter, fuel pump)

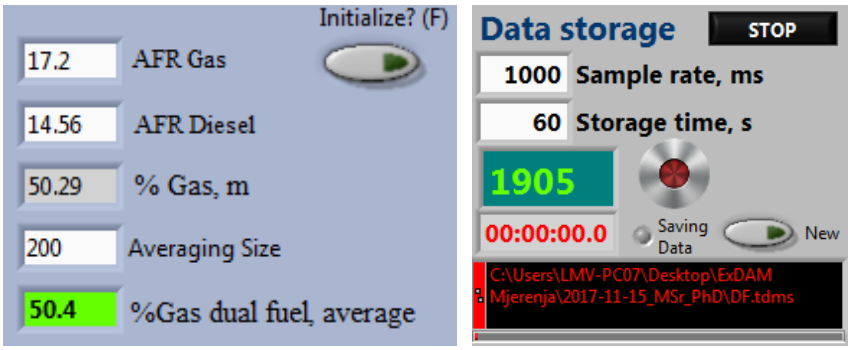

Figure 52. LabVIEW applications (dual-fuel, data storage)

For the monitoring of the dual-fuel operation the separate application that calculates the mass ratio of natural gas in the total fuel flow from the measured diesel mass flow and natural gas mass flow was created as shown in Figure 52 left. Also, the data acquisition setup in terms of sample rate and the total sample run time can be altered by the user during operation, Figure 52 right.

Engine operating parameters, which are recorded over the selected time frame, are stored in Microsoft Excel file usually called Summary File. Summary file includes operating parameters such as: engine speed, intake temperature, exhaust temperature, temperatures in EGR line, oil temperature, ambient temperature, oil pressure, pressure in intake and exhaust pipe, air mass flow, spark timing, injection timing, lambda, throttle position, engine head temperature, mass fuel flow – coriolis flow meter, calculated mass fuel flow from weight scale, calculated gas mass fuel ratio in dual-fuel mode, NO_X emissions, THC emission, CO and CO_2 emission.

The above described National Instruments equipment is used for the control and communication with all devices, actuators and sensors installed on the experimental setup, except the direct injection system which is controlled by the other National instruments modules specifically designed for that purpose.

For the control of direct injection, the NI Direct Injector Driver System [88] is used, shown in Figure 53. The system is based on NI cRIO 9066 and contains input module NI 9411, driver module for direct injector NI 9751, analog input module NI 9201 and port fuel injector (PFI) module NI 9758.

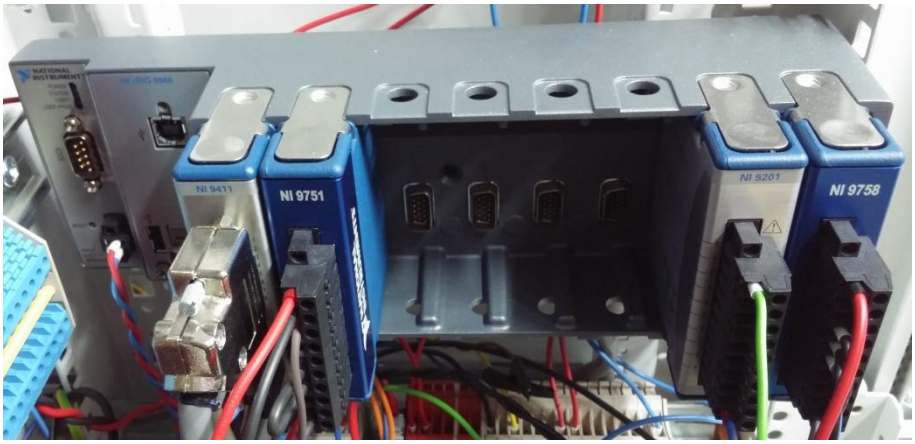

Figure 53. NI Direct Injector Driver System

System synchronizes the injector channels with crankshaft and camshaft position sensors. Direct injection driver module NI 9751 provides the power electronics necessary to drive high-power piezoelectric direct injectors. Piezo injector is connected to the module according to the wiring diagram shown in Figure 54. Driving piezo injectors requires in-series inductance on the high side wire (INJ+ wire) and short-circuiting of channel 3. Short-circuiting of channel 3 is required to discharge the piezo actuator.

The DI Driver System supports a common rail pressure control feature with NI 9758 PFI Driver and NI 9201 analog input module. The fuel rail has a pressure sensor connected to

the end, providing analog pressure feedback to the NI 9201 analog input module for rail pressure PID control. The rail pressure PID control function generates a pulse-width modulation (PWM) duty cycle send to the high pressure valve (HPV) and used to maintain a specified rail pressure set point. The HPV is a proportional solenoid valve controlled with a low side driver channel via PWM operation. This solenoid valve requires up to 3A continuous current operation. Therefore it is important to utilize the LS channel locking feature which locks LS3 with LS4 via the PFI and LS Driver Setup window. The locked pair of channels can be used to operate the HPV with up to 3A continuous current. Figure 55 shows a wiring diagram for a HPV with locked LS3 and LS4 pair.

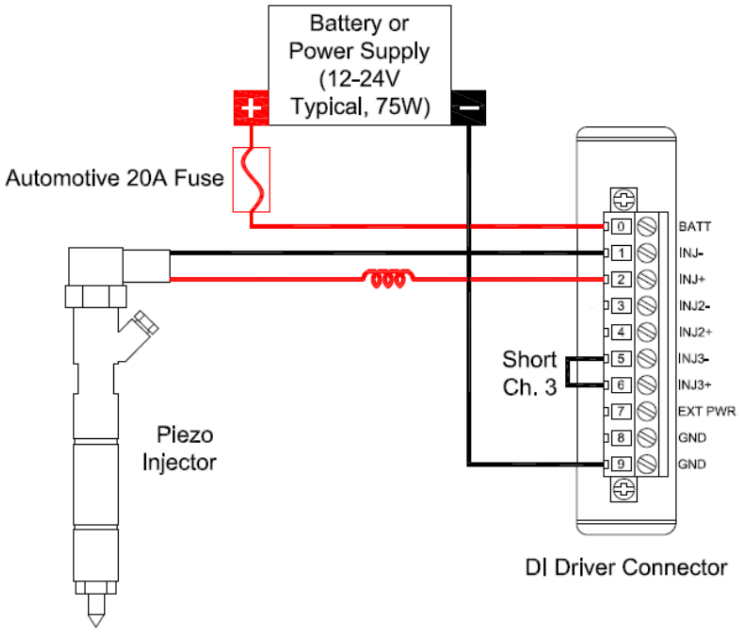

Figure 54. Diagram of wiring of Piezo Injector, reproduced from [89]

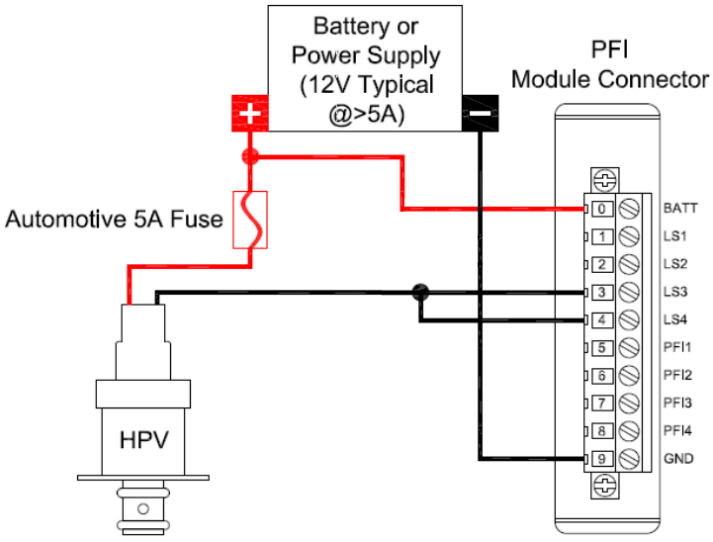

Figure 55. Diagram of wiring of high pressure valve, reproduced from [89]

For interfacing and calibrating the system, the NI Software Calibration Manager (SCM) Toolkit is used [89]. After the configuration of the DI driver module (operating mode, current profile, IPhase array, etc.), the piezo injector can be controlled via interface that enables multiple injections per cycle, and provides the control of the start or end of injection (SOI or EOI) and injection duration. Control interface for a direct injector is shown in Figure 56.

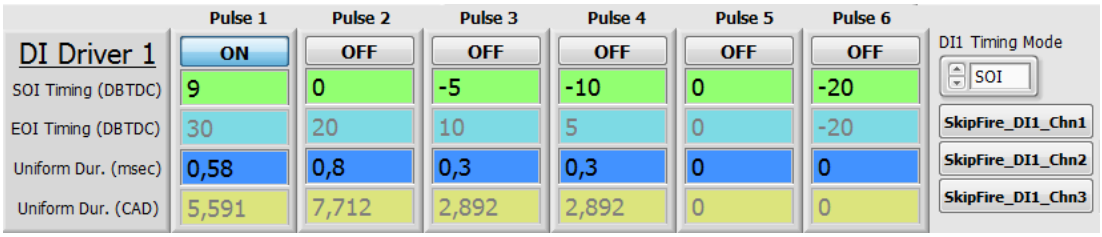

Figure 56. The NI Software window for direct injection control

For the rail pressure control, it is necessary to configure the processing of the analog signal from the rail pressure sensor. The rail pressure sensor has linear characteristic which means that the change in rail pressure proportionally changes the generated voltage. For the proper definition of the linear characteristics of the rail pressure sensor, two points that give a relationship between voltage and pressure should be entered. After configuration of the analog input signal, the rail pressure can be set in the control window. Since the high pressure fuel pump has no inlet metering valve, it needs to be manually overridden. Figure 57 shows the rail pressure control setup.

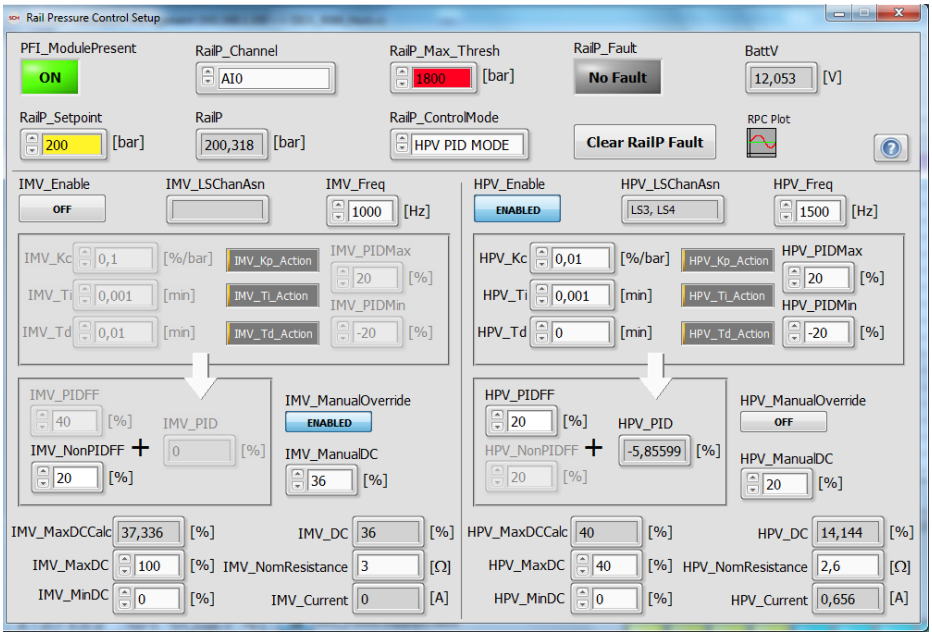

Figure 57. Rail pressure control setup

The installed equipment of the experimental setup that was described above provides full flexibility in selecting engine operating parameters during the experimental research.

3.7. Engine indicating equipment

Besides the described measurement equipment and LabVIEW software, for some of the data acquisition the AVL GmbH equipment is used which primarily includes previously mentioned and described in-cylinder high pressure sensor AVL GH14DK [63] and intake pressure sensor AVL LP11DA [63], encoder AVL 365 C [90] and device AVL IndiSmart Gigabit [91]. This equipment along with the software AVL IndiCom [92] provides monitoring and saving the in-cylinder pressure in dependence of the crank angle. Figure 58 shows the encoder AVL 365 C and the AVL IndiSmart Gigabit, while the sensors were already shown in Figures 22 and 24.

Figure 58. Encoder AVL 365 C (left) and AVL IndiSmart Gigabit (right)

For monitoring of the engine process, the AVL IndiCom allows creation of different display modes which show the acquired and recalculated values such as (Figure 59): in-cylinder pressure, intake pressure, injection timing, spark timing, indicated mean effective pressure (IMEP), Coefficient of variation of IMEP (CoV (IMEP)), CA50, pressure rise rate (dp/dα), etc.

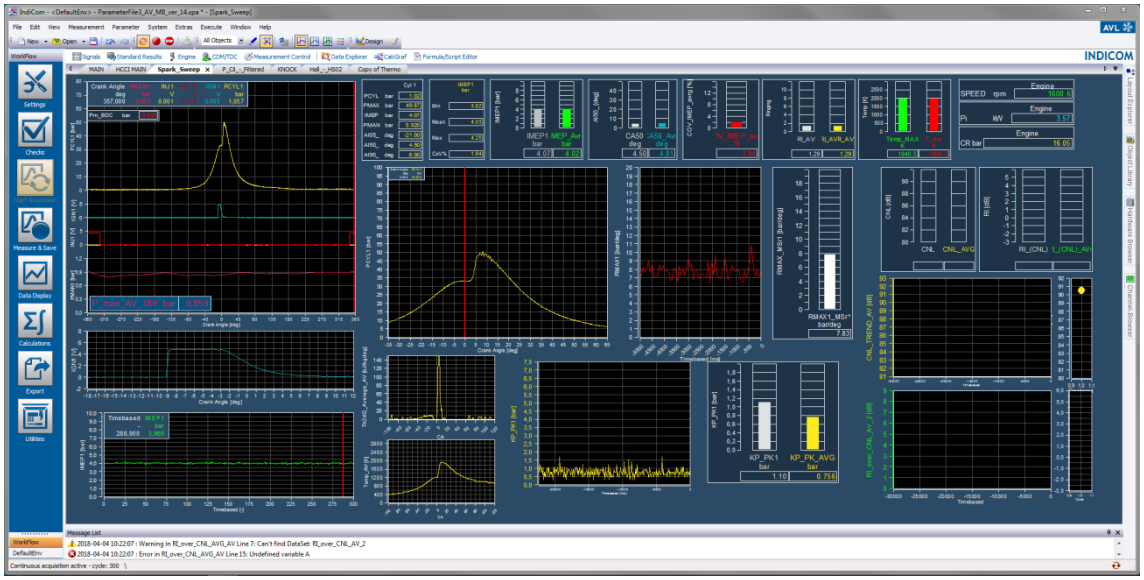

Figure 59. Monitoring window of the AVL IndiCom

3.8. Post processing of the measurement results

The main performance characteristics of engine such as IMEP, CoV(IMEP), thermal efficiency, temperature at IVC, in-cylinder temperature and the rate of heat release (RoHR) are calculated from the measured values by using an in-house developed code. The measured pressure of each individual cycle was smoothed by a Savitzki-Golay filter with 19 points [93] and the calculation of RoHR is based on the first law of thermodynamics and includes changes of mixture composition and properties, with properties calculated by using NASA polynomials, the calculation of wall heat losses by Woschni model and the calculation of the blow by losses. More details about the calculation of RoHR can be found in [61]. From calculated RoHR the code calculates timings of specific mass fraction burned as CA5, CA10, CA50, etc. These values are calculated for each individual cycle and then averaged over 300 consecutive cycles.

The in-cylinder temperature T_{cyl} is calculated with the following equation:

$$T_{\mathrm{cyl}} = \frac{p_{\mathrm{cyl}} \cdot V_{\mathrm{cyl}}}{m_{\mathrm{cyl}} \cdot R_{\mathrm{cyl}}} \tag{13}$$

where p_{cyl} represents the in-cylinder pressure, V_{cyl} represents the total in-cylinder volume, m_{cyl} represents the in-cylinder mass and R_{cyl} represents individual in-cylinder gas mixture constant. The in-cylinder mass is calculated according to the measured intake mass flow and measured fuel flows, with the addition of assumed residual gas concentration.

The in-cylinder volume is calculated with the following equation:

$$V_{\mathrm{cyl}} = \frac{{D_{\mathrm{cyl}}}^2 \cdot \pi}{4} \cdot \left[\frac{H}{(CR-1)} + x_{\mathrm{piston}}\right] \tag{14}$$

where D_{cyl} represents the cylinder bore, H represents the engine stroke, CR represents the compression ratio and x_{piston} represents the current piston position measured from TDC.

The RoHR ($\mathrm{d}Q/\mathrm{d}\varphi$) is calculated from the following equation:

$$\frac{\mathrm{d}Q}{\mathrm{d}\varphi} = m_{\mathrm{cyl}} \cdot c_{\mathrm{v,cyl}} \cdot \frac{\mathrm{d}T_{\mathrm{cyl}}}{\mathrm{d}\varphi} + p_{\mathrm{cyl}} \cdot \frac{\mathrm{d}V_{\mathrm{cyl}}}{\mathrm{d}\varphi} - \frac{V_{\mathrm{cyl}}}{m_{\mathrm{cyl}}} \cdot p_{\mathrm{cyl}} \cdot \frac{\mathrm{d}m_{\mathrm{cyl}}}{\mathrm{d}\varphi} + \frac{\mathrm{d}Q_{\mathrm{wall}}}{\mathrm{d}\varphi} \tag{15}$$

where Q represents the released heat, $c_{v,cyl}$ represents specific heat capacity of the mixture at constant volume and Q_{wall} represents the heat that is transferred to the cylinder walls.

The wall heat losses (Q_{wall}) are calculated by well-known Woschni model which includes heat losses through the cylinder head ($Q_{wall,head}$), heat losses through the piston ($Q_{wall,piston}$) and heat losses through cylinder liner ($Q_{wall,liner}$).

$$\frac{\mathrm{d}Q_{\mathrm{wall}}}{\mathrm{d}t} = \frac{\mathrm{d}Q_{\mathrm{wall,head}}}{\mathrm{d}t} + \frac{\mathrm{d}Q_{\mathrm{wall,piston}}}{\mathrm{d}t} + \frac{\mathrm{d}Q_{\mathrm{wall,liner}}}{\mathrm{d}t} \tag{16}$$

$$\frac{\mathrm{d}Q_{\mathrm{wall,head}}}{\mathrm{d}t} = h_{\mathrm{w}} \cdot A_{\mathrm{head}} \cdot (T - T_{\mathrm{head}}) \tag{17}$$

$$\frac{\mathrm{d}Q_{\mathrm{wall,piston}}}{\mathrm{d}t} = h_{\mathrm{w}} \cdot A_{\mathrm{piston}} \cdot (T - T_{\mathrm{piston}}) \tag{18}$$

$$\frac{\mathrm{d}Q_{\mathrm{wall,liner}}}{\mathrm{d}t} = h_{\mathrm{w}} \cdot A_{\mathrm{liner}} \cdot (T - T_{\mathrm{liner}}) \tag{19}$$

where are:

h_w – Woschni heat transfer coefficient,
A_i – Surface area of *i* element,
T – Average in-cylinder temperature,
T_i – Surface temperature of *i* element.

Woschni heat transfer coefficient (h_w) in high pressure cycle is calculated with the following expression [94]:

$$h_{\mathrm{w}} = 130 \cdot {D_{\mathrm{cyl}}}^{-2} \cdot p^{0.8} \cdot T^{-0.53} \cdot \left[\mathrm{c}_1 \cdot v_{\mathrm{mp}} + \mathrm{c}_2 \cdot \frac{V \cdot T_{\mathrm{IVC}}}{p_{\mathrm{IVC}} \cdot V_{\mathrm{IVC}}} \cdot (p - p_{\mathrm{motored}})\right]^{0.8} \tag{20}$$

where D_{cyl} represents cylinder diameter, p represents the in-cylinder pressure, c_1 and c_2 represent model constants, v_{mp} represents mean piston velocity, V represents displacement volume, T_{IVC} represents temperature at the intake valve closure, p_{IVC} represents pressure at intake valve closure, V_{IVC} represents volume at intake valve closure and $p_{motored}$ represent motored pressure.

4. Spark Ignition Combustion Mode

As mentioned in introduction, natural gas can be used in both SI and CI engine. Before the experimental research of dual-fuel combustion, the short analysis of using the methane (instead of natural gas) in SI engine will be given in this chapter. These results will be used as a benchmark for further dual-fuel combustion. At the beginning, the short analysis of previous research in SI natural gas fuelled engines will also be given.

Most of the available experimental research of using natural gas in the SI engines is performed on the conventional gasoline engines and most of the presented results show the comparison of performances between gasoline and NG fuel. Engine operation with NG shows some advantages compared to the operation with gasoline fuel, but results also with some disadvantages. In [95] the authors showed that the SI engine fuelled with NG produces 18.5% less power compared to the gasoline due to the lower volumetric efficiency, which is caused by the fact that NG has lower molar mass and therefore displaces more air in the intake port. Comparison between NG and gasoline in spark ignition engine in retrofitted gasoline vehicle (CR = 9.2) is given in [96]. The authors showed that the engine fuelled by NG has lower power and lower brake specific fuel consumption (BSFC), emits less CO and HC emissions, but also 33 % more NO_X emission, compared to the engine fuelled by gasoline. Similar conclusions were presented in [97] where SI engine that had compression ratio of 9.5 was tested. An effective method for reducing NO_X emissions and maintaining or improving thermal efficiency is a lean burn strategy, presented in [2] and [98], but an ultra-lean operation ($\lambda > 2$) can result in misfire and unstable operation [2].

The experimental study of influence of compression ratio [99] tested three different compression ratios 8.5, 10.5 and 12.5 and showed that the increase of the heat release rate, power output, thermal efficiency and NO_X emission is obtained with the increase of compression ratio. At excess air ratio near the misfire limit hydrocarbon emission also increases with the increase of compression ratio. In [100] the influences of EGR and three-way catalyst (TWC) on the emissions of SI natural gas heavy-duty Euro VI engine (CR = 11.5) are shown and the results show that the engine without TWC cannot satisfy EURO VI NO_X emission standard while by using the TWC NO_X emission decreases significantly below the allowed value. The authors in [101] and [102] performed experimental research on SI

single cylinder engine with compression ratio 14, and showed that AFR, EGR as well as the SOI and spark timing (ST) have the influence on combustion phasing, fuel consumption, knock and emissions. Direct injection resulted in a better cycle efficiency and extends the lean limits which further extend the knock limit. AFR and EGR were effective parameters for controlling knock and decreasing NO_X emission. Comparison of influence of compression ratios (10.5 and 11.5) in heavy-duty spark ignited NG engine is presented in [103] where the improvement in thermal efficiency with the increased compression ratio is shown, but the increase of CR also leads to the higher NO_X emission. In [104] the comparison of four compression ratios in spark ignition natural gas engine is made (CR between 8 and 14.7) with the emphasis on NO_X and HC emissions. They noticed the increase in NO_X and HC emission with the increase of compression ratio for running with the same spark timing, but with optimised spark timing the engine could achieve high efficiency with low emissions.

The overview of the previous research indicates a lack of experimental results for natural gas fuelled SI engines with compression ratio higher than 14.7 (in the CI engine range), which would be of interest for comparison with dual-fuel operation. Since higher compression ratio could lead to higher efficiency and could enable operation with leaner mixtures, the main objectives of this research are to experimentally investigate behaviour of SI engine fuelled by natural gas at higher compression ratios and at different mixture dilution levels. Therefore, the most attention will be devoted to the analysis of SI combustion mode at higher compression ratios. This research will give the main characteristics of the SI natural gas fuelled engine related to the performance and exhaust gas emissions.

The experimental tests were performed at three different compression ratios, one compression ratio similar to conventional gasoline engine (CR = 12) and two compression ratios similar to conventional diesel engine (CR = 16 and CR = 18) and at three values of air excess ratio (λ), $\lambda = 1$, $\lambda = 1.2$ and $\lambda = 1.4$. These values of air excess ratio are chosen because the literature review showed that the increase of lambda decreases NO_X emission, while lambda higher than 1.54 ($\varphi < 0.65$) causes unstable engine operation in the natural gas fuelled SI engine [105].

Also, all measurements were performed at three different engine speeds (1200 rpm, 1600 rpm and 2000 rpm) and at wide open throttle (WOT) position with ambient conditions at the air inlet. To determine the optimal ST for maximum brake torque (MBT) [106], spark sweep process was performed for every predefined operating point (compression ratio, engine speed and air to fuel ratio). During measurements of all operating points the ambient conditions (temperature, ambient pressure, humidity, etc.) were very similar. The maximum

variations of the average inlet air temperature were within ±3 °C in all operating points, while the average intake pressure varied from 0.97 to 0.99 bars.

4.1. Engine performance

As described in the previous section, for every engine speed, compression ratio and excess air ratio a spark timing sweep was performed in order to determine the optimal combustion phasing, with criteria of maximum efficiency while satisfying the limit on knock. With advancing the spark timing, in all the cases, the maximum IMEP was achieved before the occurrence of knock.

4.1.1 The influence of spark timing on the performance

The spark sweep process performed at different compression ratios and different air excess ratios shows significant influence on the achieved performances. Figures 60 – 62 show the change of indicated mean effective pressure for the change of spark timing for compression ratio 12 and compression ratio 16 at all three lambda values and three engine speeds. The optimal spark timing at CR = 12 and λ =1 is approximately -25 °CA ATDC at 1200 rpm while the increase of lambda value leads to a shift of optimal spark timing towards more advanced values. When comparing the results for compression ratios 12 and 16, the results show that the influence of spark timing on IMEP is greater at higher compression ratio (larger difference in IMEP for smaller change of ST). At higher CR optimal spark timing is more retarded for the same lambda value. As expected, the increase of engine speed requires the change of spark timing to advanced values to achieve maximum IMEP, regardless of the compression ratio and lambda value.

With defined optimal spark timings for every set of conditions it is possible to compare the performance results at optimal operating conditions.

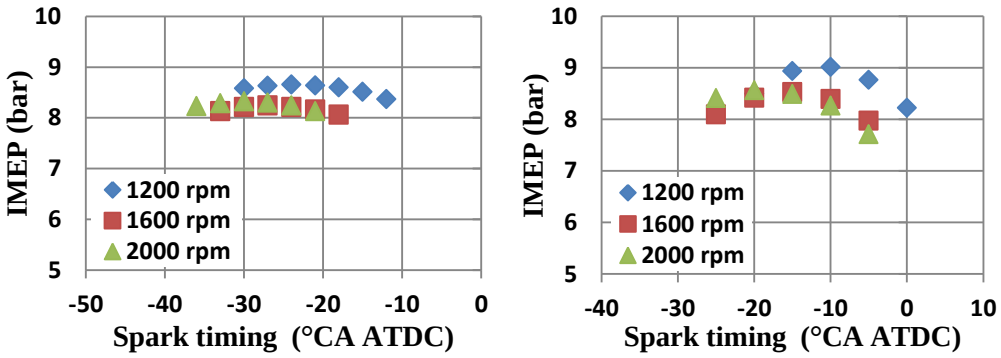

Figure 60. IMEP at λ = 1; CR = 12 (left) and CR = 16 (right)

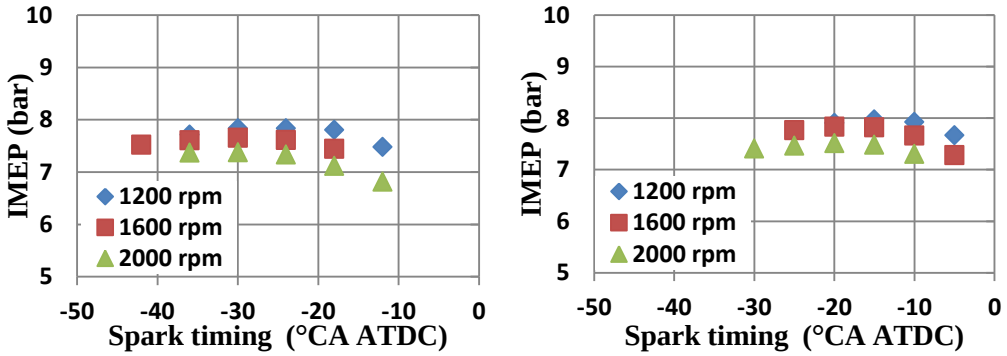

Figure 61. IMEP at λ = 1.2; CR = 12 (left) and CR = 16 (right)

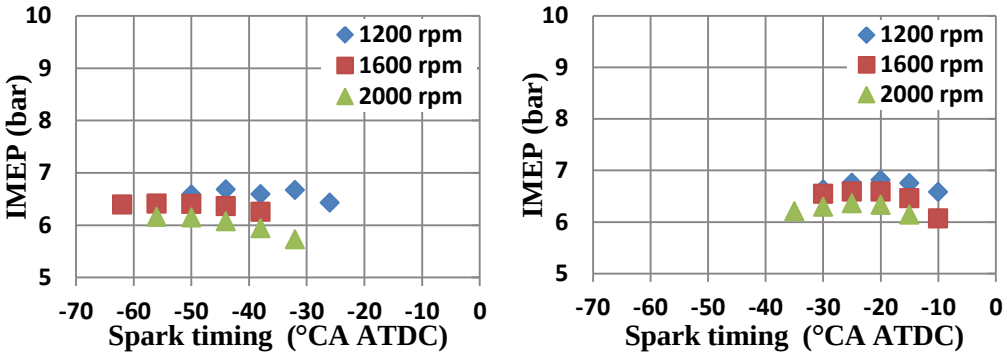

Figure 62. IMEP at λ = 1.4; CR = 12 (left) and CR = 16 (right)

4.1.2 Indicated mean effective pressure (IMEP)

Figure 63 compares the results of IMEP at different engine speeds, compression ratios and excess air ratios at optimal combustion phasing.

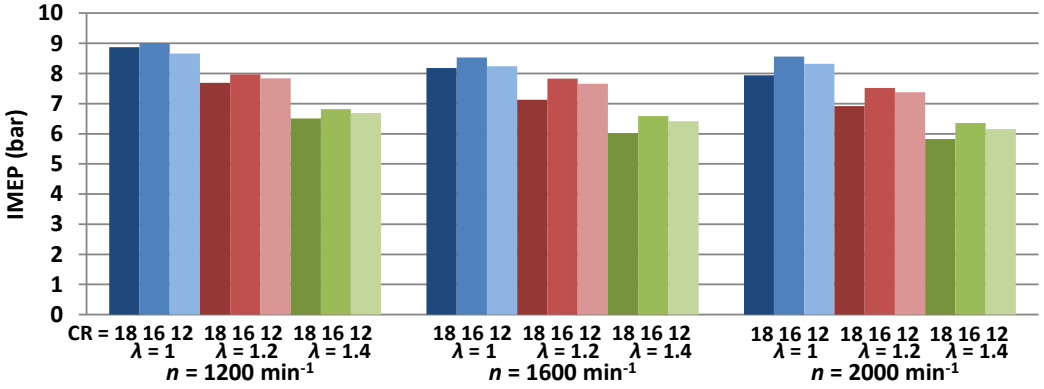

Figure 63. Indicated mean effective pressure – optimised ST

It can be seen that with the increase of compression ratio from CR = 12 to the compression ratio of conventional diesel engine (CR = 16) the IMEP also increases, but further increase to the CR = 18 results in a significant drop in IMEP. This drop in IMEP is more pronounced at higher excess air ratio and higher engine speed. The change in IMEP is mostly the result of changes in indicated efficiency which will be discussed separately. The

results also show that the IMEPs obtained with stoichiometric mixture are higher than the ones obtained with lean mixtures, which is caused by the lower energy supply from the fuel of the lean mixture. Also, trends show a decrease in IMEP value with the increase of engine speed due to the decrease in the volumetric efficiency of the engine.

4.1.3 Ignition delay

The changes of spark timing, of CR and of excess air ratio cause the changes in ignition delay, and in combustion duration since the conditions at the spark discharge change. Figure 64 shows the ignition delay which is calculated as a difference between CA5 and spark timing, where the spark timing is a crank angle at which the spark discharges between the electrodes.

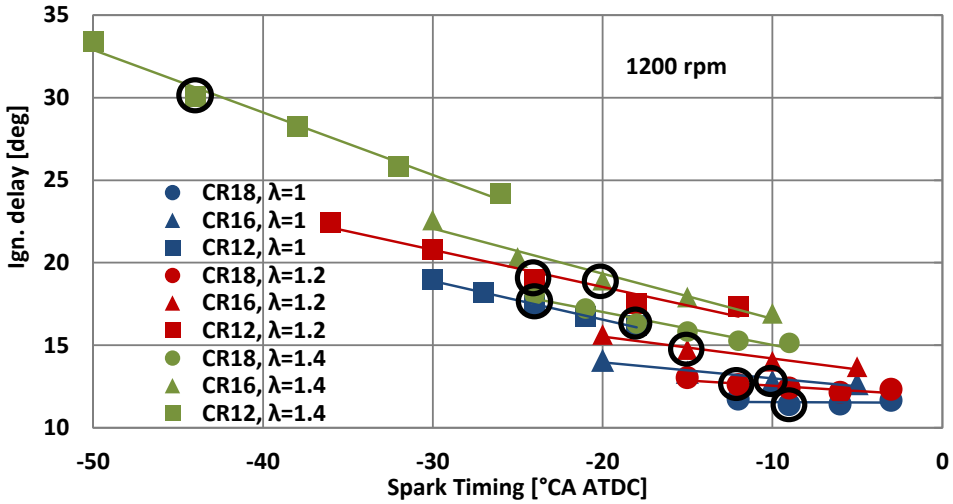

Figure 64. Ignition delay vs. spark timing at 1200 rpm

In Figure 64 the ignition delay is plotted against the spark timing, and for better understanding of the influence of compression ratio and lambda on ignition delay the results are plotted for all spark sweep points. Optimum points for every CR and lambda are marked with a circle. While it can be noticed that the compression ratio and the excess air ratio have influence on ignition delay it seems that the spark timing has the largest influence on ignition delay with more advanced spark timing leading to longer ignition delay. Therefore, since the optimal spark timing change between compression ratio and excess air ratio this leads to the changes in ignition delay. Consequently with the increase of excess air ratio and a decrease of CR the increase of ignition delay is obtained, where this increase is small except for the case with the lowest CR and highest excess air ratio. The similar trend is obtained at other engine speeds, with the only difference that values of ignition delay are larger at increased engine speed.

4.1.4 Combustion duration

With respect to combustion duration, which is defined as the difference between CA90 and CA10, the results show that the increase of compression ratio decreases combustion duration at all lambda values and all engine speeds. Engine speed also has influence on combustion duration. Higher engine speed increases combustion duration in all test cases but its influence is most significant at lower CR and higher lambda (λ = 1.4). By combining results of ignition delay and combustion duration one can notice that at higher lambda and lower CR the increase of combustion duration and ignition delay is very large. This leads to the requirement of very early spark timing to maintain combustion phasing. However, excessively advanced spark timing can lead to the misfire because the spark discharge occurs at the local mixture of low temperature and pressure.

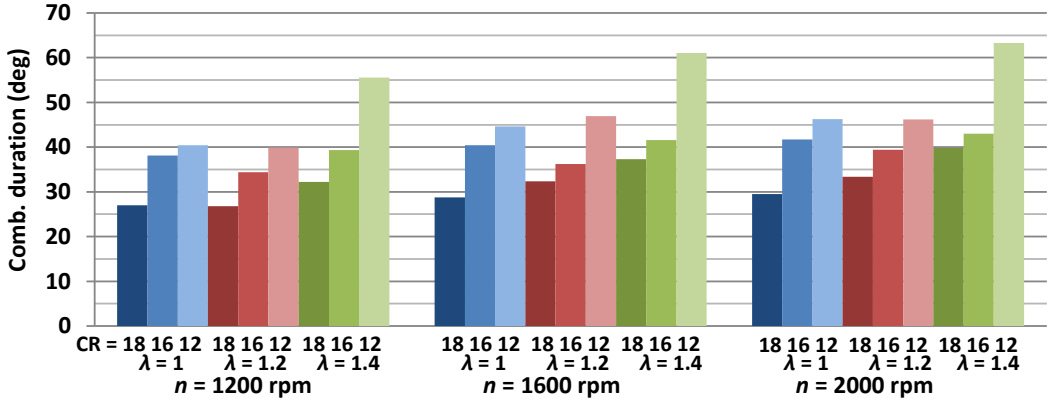

Figure 65. Combustion duration at optimized ST

4.1.5 Indicated efficiency

The consequence of the changes in combustion profile and in thermodynamic cycle caused by the changes in CR, engine speed and excess air ratio is a change in engine efficiency. The indicated efficiencies of all optimal cases are shown in Figure 66.

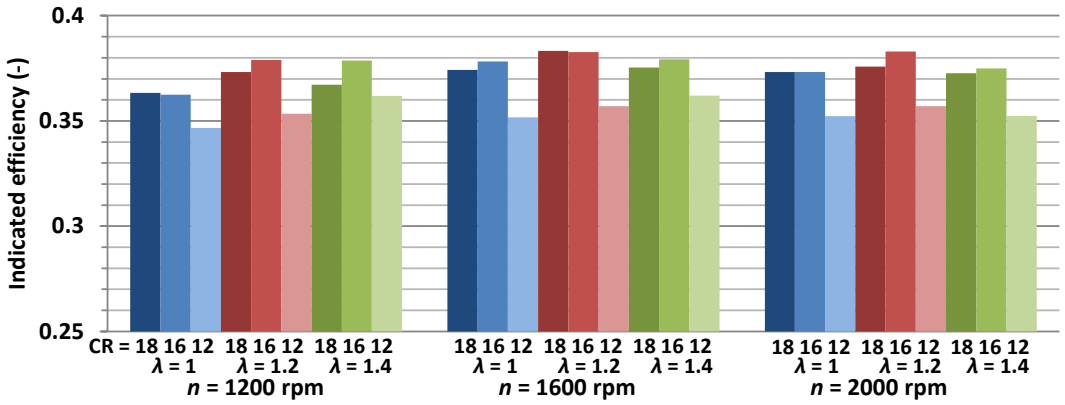

Figure 66. Indicated efficiency – optimized ST

Results show significantly higher indicated efficiency at higher compression ratios (16 and 18) compared to the compression ratio of 12 for the same excess air ratio value. The results also show that at CR = 12 the increase of excess air ratio generally increases indicated efficiency, while at CR = 16 and CR = 18 the increase of excess air ratio from 1 to 1.2 leads to increase of indicated efficiency due to the higher combustion efficiency, which is confirmed by the low level of CO emission and lower or equal levels of HC emission, and lower thermal losses because of lower in-cylinder temperature. Further increase of excess air ratio from 1.2 to 1.4 decreases indicated efficiency due to the slower flame propagation through lean mixture which results in lower combustion efficiency. In these cases crevices also have significant influence. By analysing results at constant excess air ratio one can notice that in general the increase of CR from 12 to 16 results in an increase of indicated efficiency, while further increase to 18 results in decrease of efficiency in most cases. This decrease in efficiency is the consequence of the higher thermal losses caused by the higher in-cylinder temperature as well as the higher influence of crevices since the in-cylinder pressure at TDC is higher. By looking at overall results across engine speed range the best indicated efficiencies are obtained with $\lambda = 1.2$ and CR = 16.

4.1.6 Rate of Heat Release (RoHR)

Figure 67 – 69 show the RoHR for two compression ratios at optimized ST, for all three lambda values and all engine speeds. It can be observed that the increase of compression ratio results with higher peak RoHR values which will lead to larger pressure rise rates and noise, while the increase of lambda value decreases peak RoHR and decreases pressure rise rates. It can also be observed that increasing the compression ratio results in delayed combustion phasing, which means that the higher amount of heat after TDC is released, which ultimately results in increased indicated efficiency.

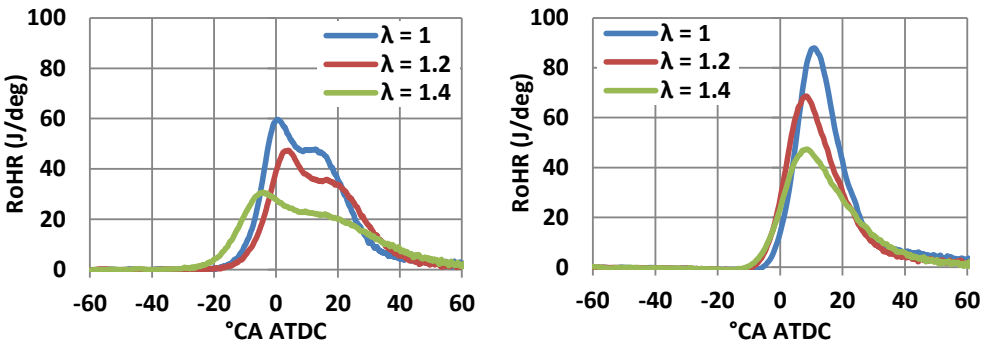

Figure 67. RoHR at *n* = 1200 rpm; CR = 12 (left) and CR = 16 (right)

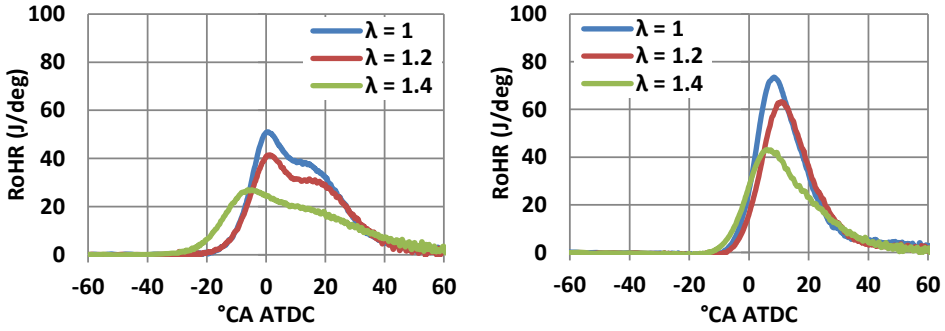

Figure 68. RoHR at *n* = 1600 rpm; CR = 12 (left) and CR = 16 (right)

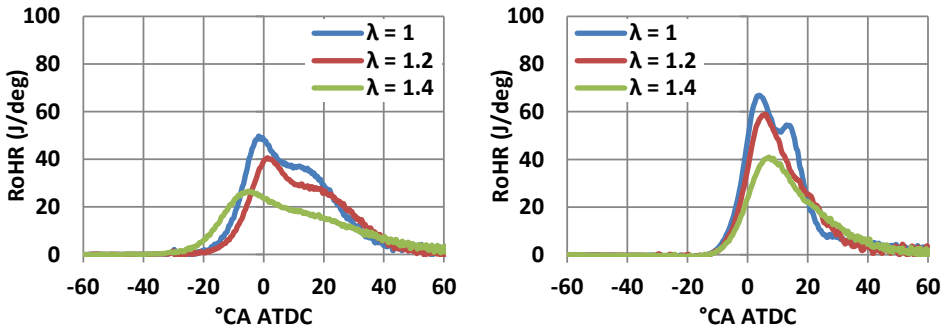

Figure 69. RoHR at *n* = 2000 rpm; CR = 12 (left) and CR = 16 (right)

4.2. Exhaust gas emissions

The changes of harmful exhaust gas emissions (HC, CO and NO_X) of the optimal operating points are shown in this chapter, and in order to put these results into a context of regulations Table 17 shows currently valid European Union (EU) standard for allowed exhaust emissions of heavy-duty engines.

Table 17. Heavy-duty European exhaust emissions standard - Euro VI [107].

	CO	THC	NMHC	CH_4	NO_X	NH_3	PM Mass	PM Number
	mg/kWh	mg/kWh	mg/kWh	mg/kWh	mg/kWh	ppm	mg/kWh	#/kWh
WHSC (CI)	1500	130	/	/	400	10	10	$8x10^{11}$
WHTC (CI)	4000	160	/	/	460	10	10	$6x10^{11}$
WHTC (PI)	4000	/	160	500	460	10	10	Not confirmed yet

The regulation prescribes values for steady-state test cycle (world harmonised stationary cycle - WHSC) for CI engines and Transient test cycle (world harmonised transient cycle - WHTC) for Spark ignited (Positive ignition – PI) and for CI engines. In this research the SI engine was used in steady state conditions. Since there is no regulation for that engine in those

conditions the WHTC (PI) limits will be used as reference for this work, keeping in mind that limits are slightly higher for WHTC than for WHSC.

4.2.1 Total Hydrocarbons (THC) Emission

Figure 70 shows measured values of THC (total hydrocarbons) expressed in g/kWh. It can be noticed that in stoichiometric and slightly lean cases the increase of engine speed results in slight decrease of THC emissions. This could be related to fuel slip since in [108] it was shown that higher amount of fuel slip is obtained at 1000 and 1500 rpm compared to higher engine speeds on the same engine. With constant compression ratio the increase of excess air ratio results in non-monotonic change in THC emission. The change from $\lambda = 1$ to $\lambda = 1.2$ results in slight decrease or no change in THC emissions, while further change from $\lambda = 1.2$ to $\lambda = 1.4$ results in significant increase in THC emissions. This is caused by slower flame propagation and earlier quenching of the flame in significantly leaner mixtures.

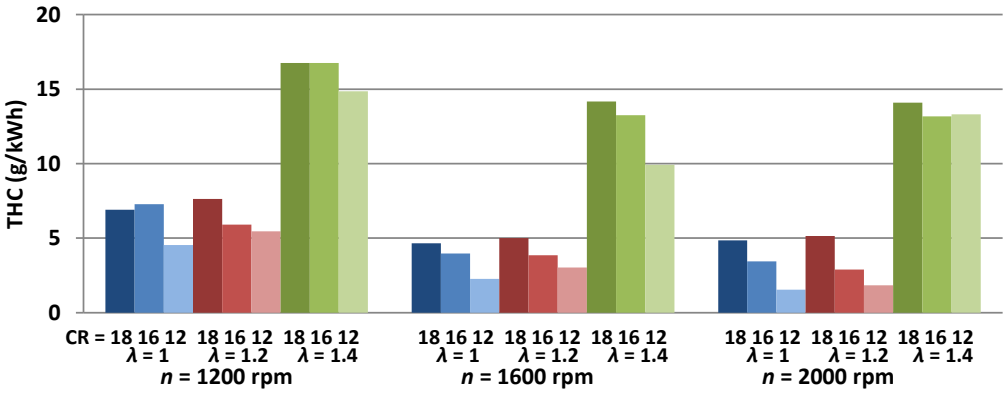

Figure 70. THC emissions (g/kWh) at optimized spark timings

At constant excess air ratio the increase of CR in most of the cases results in slight increase in THC emissions. This is probably related to the larger fraction of air/fuel mixture being pushed into the crevices at higher CR. In all of the cases the values of THC are higher than the limits shown in Table 17 (NMHC + CH_4 = 0.66 g/kWh), which could be expected given that the geometry of combustion chamber is not representative of SI combustion and could cause the flame quenching in boundary layers. The excess of THC values range from 50% to 10 times more which means that some form of after treatment would be required for satisfying limits in these conditions.

4.2.2 Carbon Monoxide Emission (CO)

The measured CO emissions are presented in Figure 71. With constant excess air ratio the increase of CR from 12 to 16 results in lower CO emission. This is caused by the higher in

cylinder temperatures obtained with higher compression ratios. Further increase of compression ratio from 16 to 18 results with higher CO emission at low engine speed and with almost equal CO emission as in CR = 16 at middle and higher engine speed. The increase of CO emission with further increase of CR is probably determined by the whole hydrocarbon oxidation process where higher CR results with slightly higher THC caused by larger fraction of mixture pushed into the crevices, and later in the expansion process some of these hydrocarbons form CO but do not fully react to CO_2. At higher engine speed the CO to CO_2 process is enhanced by the higher in-cylinder temperatures and therefore this pathway is not that influential.

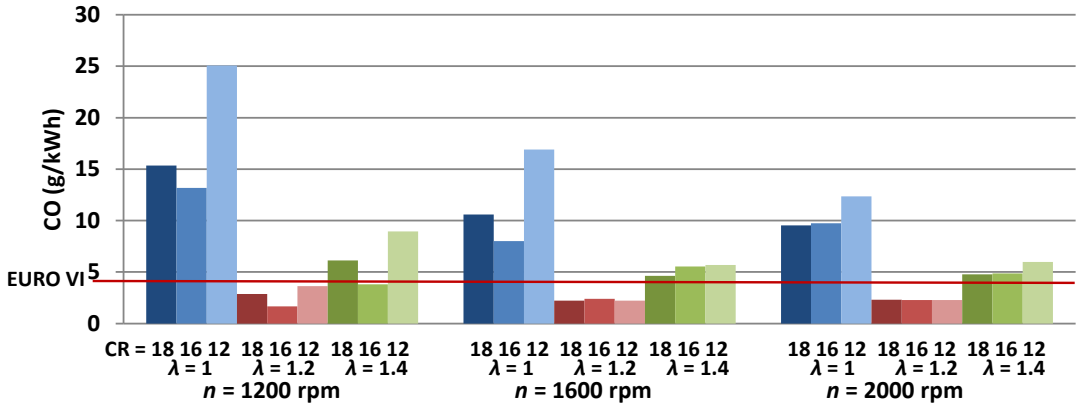

Figure 71. CO emissions at optimized spark timings

With constant CR the increase of excess air ratio from $\lambda = 1$ to $\lambda = 1.2$ results in lower CO emissions. This is caused by the CO – CO_2 oxidation pathway which is enhanced by the increased concentration of O_2. Further increase of excess air ratio from $\lambda = 1.2$ to $\lambda = 1.4$ results in slight increase of CO emission. This increase is smaller than the change when excess air ratio changed from 1 to 1.2, and is probably caused by the lower in-cylinder temperatures (shown in Figure 73) and therefore more advanced quenching and stopping of CO - CO_2 oxidation with smaller change on the side of formation of CO from hydrocarbons. The observed behaviour of the CO emissions with respect to changes in excess air ratio is completely in line with the behaviour shown in literature [2] and [109].

The values of CO emissions are higher than the limits defined in Table 17 (WHSC – 1.5 g/kWh), but with $\lambda = 1.2$ the CO emission limit was satisfied if one looks WHTC limit for PI engines (4 g / kWh). In other cases, $\lambda = 1$ and $\lambda = 1.4$, CO emissions are 1.2 to 10 times higher depending on the other conditions and on the value of the limit (WHTC or WHSC).In lean conditions the values range from satisfying the limit to 3 times higher values. In any case it seems that the use of oxidation catalyst would be required to satisfy the CO emissions. Since

the exhaust gas temperatures are above 396 °C in all measured cases it is expected that the conversion efficiency of 92% is enough to put CO emissions below the limits [110].

4.2.3 Nitrogen Oxides Emission (NO_X)

The results of NO_X emissions are shown in Figure 72. With constant CR the lowest NO_X emissions are achieved with excess air ratio λ = 1.4. In these cases the in-cylinder temperatures are lowest and therefore the formation of NO_X is reduced (Figure 73). With excess air ratio λ = 1.2 the NO_X formation is highest since the temperature is higher and there is enough oxygen to form NO_X. On the other hand, although with stoichiometric mixture the temperature is even higher than at λ = 1.2 the formation of NO_X is limited by the lack of oxygen and therefore the emission of NO_X is lower. But, if compared to the very lean operation λ = 1.4, stoichiometric operation still results with higher NO_X emission.

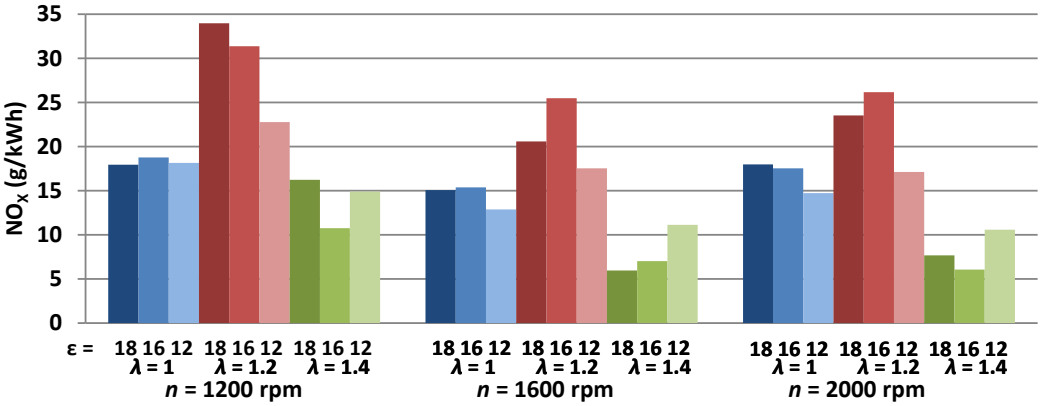

Figure 72. NO_X emission at optimized spark timings

At constant excess air ratio and different CR trends are diverse. The only clear and visible trend is in a change of CR from 12 to 16 at λ = 1.2 where the NO_X emissions increase significantly. All other changes are small and without any trend, although the trends in peak temperatures are quite uniform, higher CR results with higher peak temperature (Figure 73).

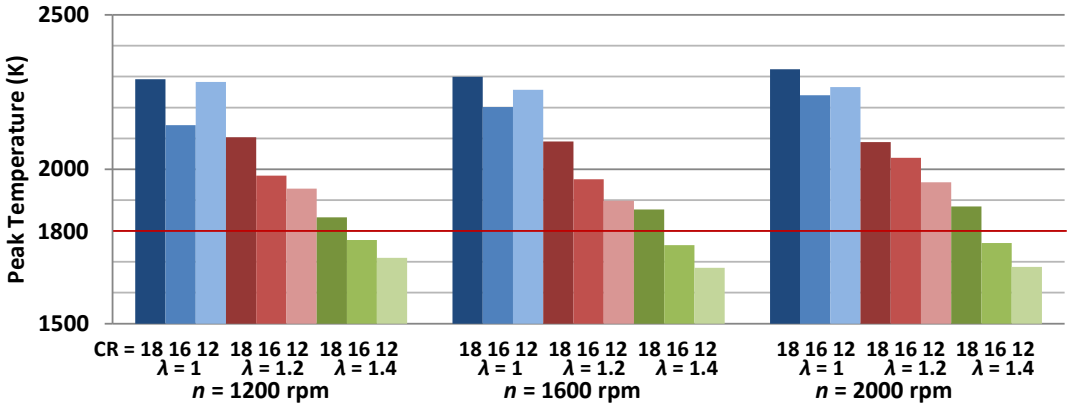

Figure 73. Peak in-cylinder temperatures at optimized spark timings

Peak in-cylinder temperatures shown in Figure 73 are defined as the maximum values from the calculated profile of the average temperature in the cylinder. Although the temperature of the burned zone is the one that influences NO_X formation, the average temperature also indicates the temperature of the burned zone since an increase of the burned zone temperature will lead to the increase of the average temperature as well.

At stoichiometric conditions the change of CR almost has no influence on NO_X. This can be explained by the fact that although the NO_X formation with increase of CR from 12 to 16 is higher (NO_X in ppm is larger), the produced power is also larger and therefore the emissions in g/kWh are almost the same. At λ = 1.4 the change of CR results with non-monotonic change in NO_X emission and the interesting thing is that the emissions does not follow the peak temperature trend. In most of the cases it follows the opposite trend, where with increased peak temperature the emissions are lower. Since the NO_X is formed in the burned part of the cylinder and the average temperature in these cases are below 1800 K (the temperature threshold for NO_X formation) the combustion profile determines the NO_X emissions.

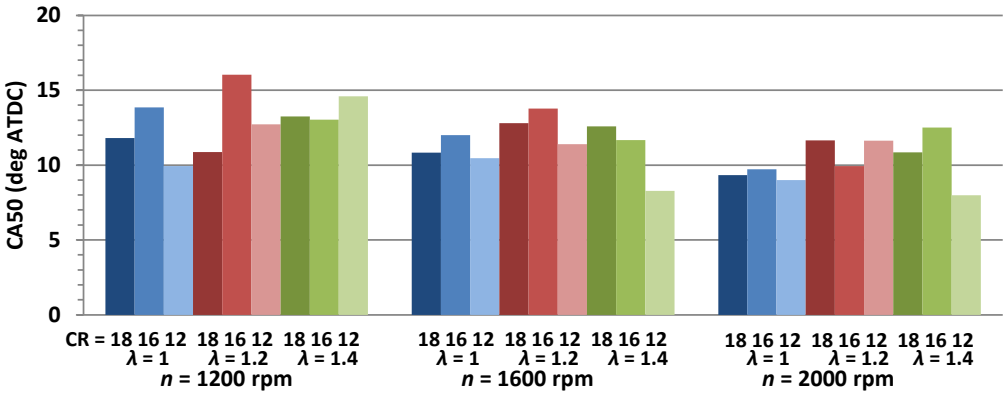

Figure 74. CA50 at optimized spark timings

As it can be seen in CA50 plot shown in Figure 74, the trend of change of NO_X emission with the change of CR at λ = 1.4 corresponds to the results of combustion phasing. This means that the later combustion phasing produces lower NO_X emission.

All measured values of NO_X are significantly higher than the allowed values (0.46 g/kWh) set by the Euro VI standard (Table 17) which means that the engine in these conditions would still need some after treatment system. In stoichiometric conditions the three way catalyst could be used and in these conditions the conversion of 95% would be required which is achievable with today's catalysts [111]. In lean conditions the required efficiency is slightly lower (92%) and can also be achieved with today's NO_X after treatment devices for lean burn combustion systems.

4.3. Conclusions

In this chapter, the effects of compression ratio, excess air ratio and engine speed on the performance and emissions of the natural gas fuelled SI engine are examined. The main objective of the work was to show the advantages and disadvantages of using different compression ratios, especially high compression ratios similar to CI diesel engine. The main conclusions are as follows:

- Indicated efficiency of SI natural gas fuelled engine is highly influenced by CR. There is some influence of lambda and engine speed, but the influence of CR is greater with indicated efficiency increasing as the CR increases from 12 to 16. Further increase of compression ratio leads to decrease of indicated efficiency because of higher thermal losses and higher influence of crevices.
- Increasing of CR decreases ignition delay and combustion duration mainly as a consequence of different spark timings.
- IMEP is higher at lower engine speeds because of the influence of the volumetric efficiency.
- The THC emission is highest at lean mixture (λ = 1.4) which is caused by slower in-cylinder flame propagation, lower temperature and probably flame quenching process. The increase of CR also increases THC emission which is caused by higher influence of crevices. At stoichiometric or slightly lean conditions (λ = 1.2) the influence of CR on THC emissions is significant, but the change to λ = 1.4 significantly increases THC regardless of the CR.
- Although there is some influence of CR on CO emission (the increase from CR = 12 to CR = 16 results in decrease of CO emission, while further increase to CR = 18 slightly increases CO), the dominant factor in CO emissions is the excess air ratio. The change of operation from stoichiometric to slightly lean mixture results in significant decrease of CO emissions.
- The emissions of NO_X are also significantly influenced by excess air ratio and much less by CR, except for λ = 1.2 where CR has strong influence on NO_X. In lean operation the NO_X emission is not exclusively correlated to the peak cylinder temperatures, but depends on the entire combustion profiles, e.g. combustion duration. For the engine operation without catalyst the excess air ratio should be even higher than λ = 1.4, which is not possible with the application of standard type of ignition system used on the presented experimental engine.

With all the above highlighted conclusions, there are three possible modes of operation that would require different hardware in satisfying emission regulations. The stoichiometric mixture provides the highest engine power with drawbacks in exhaust emissions and efficiency, but the emissions can be eliminated with relatively cheap three way catalyst. The highest indicated efficiency in this mode of operation would be 36.2%, 37.8% and 37.3% at 1200 rpm, 1600 rpm and 2000 rpm, respectively. The lean burn concept with $\lambda = 1.2$ achieves the highest indicated efficiency and reduces THC and CO exhaust emissions, however the engine would still require oxidation catalyst and a lean burn NO_X catalyst. The highest indicated efficiency in this mode of operation would be 37.9%, 38.3% and 38.3% at 1200 rpm, 1600 rpm and 2000 rpm, respectively. Finally, the operation with λ higher than 1.4 would probably reduce NO_X below legal limits but would require oxidation catalyst and the ignition system which provides higher source of energy. In all the cases the favourable CR is much higher than the usual CR of SI engines and it is equal to 16.

5. Dual-fuel Combustion Mode

As shown in the previous chapter, CR = 16 provided the best results with respect to the engine performance and emissions. Also, new CI diesel engines for vehicles operate at CR around 16 (mostly with charging systems) which confirm the suitability of this CR for achieving the best engine performances. Therefore the research of dual-fuel combustion is performed with CR = 16 and all following results are displayed for that CR.

5.1. Initial measurement

A first step in the research of dual-fuel combustion mode was to determine initial behaviour of the engine fuelled by diesel and natural gas. For this purpose, engine speed of 1600 rpm and three different loads (IMEP = 2 bars, 4 bars and 7 bars) were selected as baseline operating points. Maximum deviations in achieved IMEP's were within ± 0.04 bars.

The first measurement was performed at engine speed of 1600 rpm at all three loads, with NG mass participation rates: Z = 0%, 35%, 55% and 80%. NG mass participation rate of 0% represents normal diesel operation with single injection during the engine cycle. Start of injection of diesel fuel is optimised with respect to the maximum indicated efficiency while the fuel pressure was maintained at 300 bars. Figure 75 shows the test cases and achieved IMEP. Below each of the column the excess air ratio of the total fuel/air mixture (NG + diesel) is also shown.

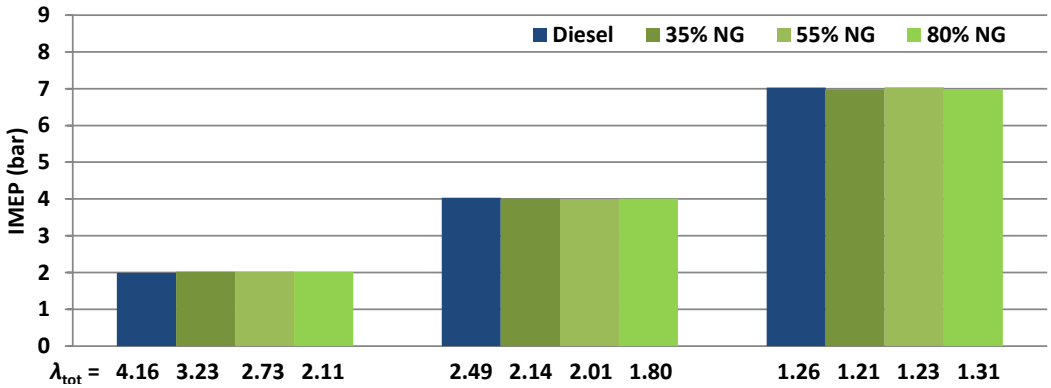

Figure 75. Design of initial experiment (1600 rpm)

As shown in Figure 75, the increase of the NG mass participation rate at low loads (2 and 4 bars of IMEP) reduces the excess air ratio of the total mixture, which means that a

larger amount of fuel is required in dual-fuel mode for achieving the same power output, compared to the normal diesel operation. At high load (7 bar of IMEP), the effect is opposite, which means that with large amount of natural gas results an increase of the total excess air ratio is obtained, which means that the lower fuel amount is required for the same power. The ratios of injected fuel as well as the energy of the injected fuels are shown in Figure 76. Excess air ratio of the total injected fuel and excess air ratio of the premixed charge (NG and air) are also shown in Figure 76.

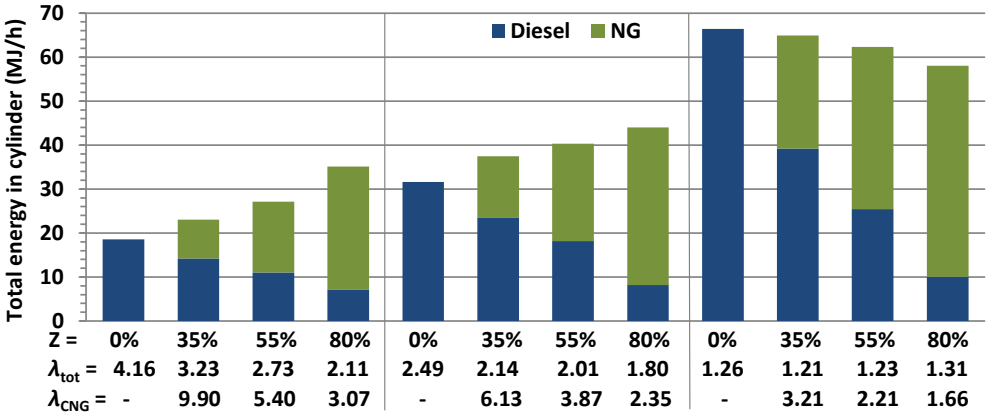

Figure 76. Distribution of energy of fuel in initial tests

The results shown in Figure 76 lead to the conclusion that at low load some amount of natural gas remains unburned, because of the poor flame propagation through the premixed charge. Indicated efficiency, which is shown in Figure 77, confirms that the energy conversion is at the low loads in dual-fuel mode on the low level, and with more natural gas in the mixture of the dual-fuel operation the efficiency is lower. At high load, indicated efficiency in dual-fuel mode is even better than in normal diesel operation and with more natural gas in the mixture of the dual-fuel operation the indicated efficiency is higher.

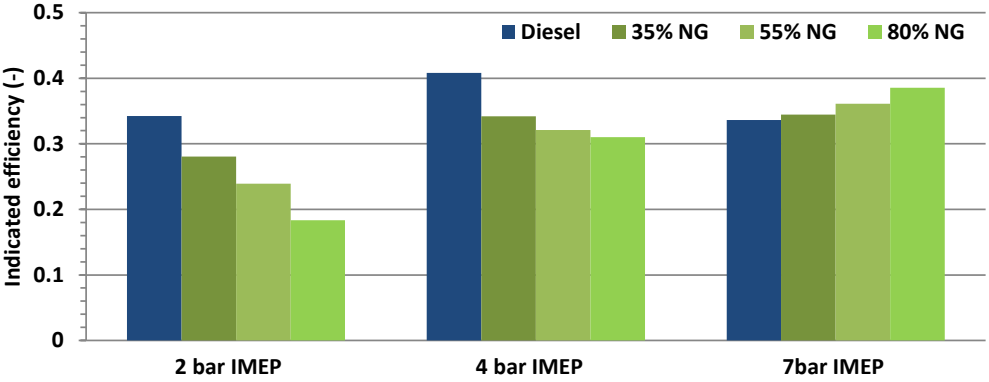

Figure 77. Indicated efficiency in initial test

As shown in Figure 77, at low loads, the indicated efficiency is significantly higher in normal diesel operation than in dual-fuel combustion mode. This confirms the previously

stated drawback of the dual-fuel operation taken from the literature review and the suggestions that at low load the engine should operate in normal diesel mode [26]. Similar behaviour of the dual-fuel combustion is shown in [41], but in all of these results all operating parameters were not optimised.

Further proof of the poor combustion of the premixed fuel at low loads is the result of THC emission which is shown in Figure 78. In the chart the ratio between emitted THC and injected methane (CH_4) in grams of THC per gram of injected methane is added for each dual-fuel result. This result shows that a significant fraction of the NG fuel is unburned at low load. Interestingly at specific load (e.g. 2 bars or 4 bars) the ratio of unburned NG seems to be constant regardless of the mass participation rate and changes as the overall load changes. The high THC emission and high fraction of unburned NG at low load is a result of low combustion efficiency of the lean NG/air mixture, which could be further improved by advanced injection strategies or combustion techniques. Only a small amount of this emission could be attributed to a fuel slip due to the valve overlap.

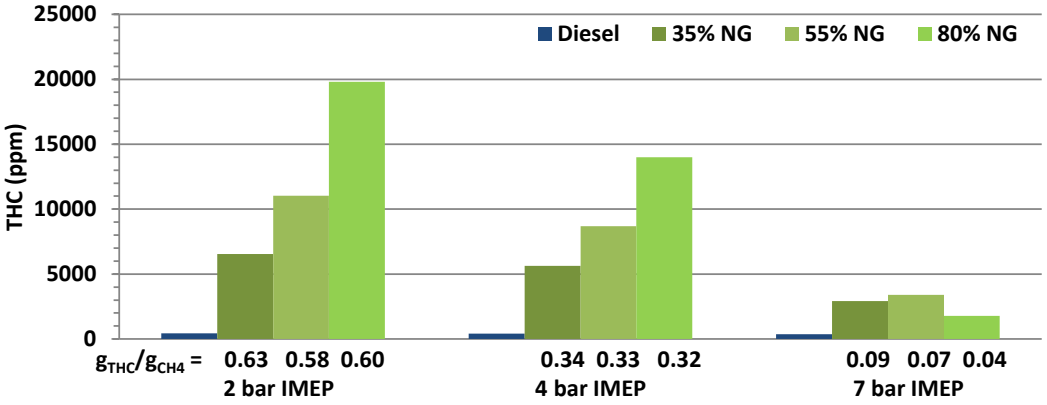

Figure 78. THC emissions in initial tests

As shown in Figure 78, at very low load and high mass participation rate of NG, THC emissions reach 20 000 ppm, which means that a significant amount of NG fuel flows to the exhaust without combustion. In these cases, the NG/air mixture is very lean, and the amount of injected diesel fuel is also very low. This results with a weaker diesel fuel combustion that should initiate further flame propagation through the combustion chamber in a very lean mixture. At higher loads, the NG/air mixture is richer and the diesel fuel mass is higher. The stronger diesel fuel combustion, which results in higher local temperature, promotes flame propagation through the moderately lean NG/air mixture and consequently results in further increase of the in-cylinder temperature and decrease of the THC emissions. Figure 79 shows the average in-cylinder temperatures at various loads and NG mass participation rates.

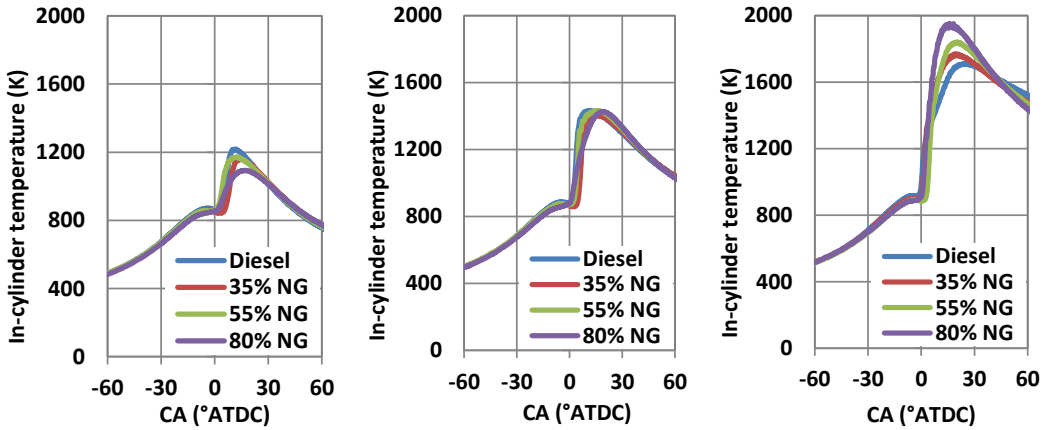

Figure 79. Average in-cylinder temp.: IMEP = 2 bars; IMEP = 4 bars; IMEP = 7 bars

By increasing the in-cylinder temperature, the in-cylinder pressure also increases. Figure 80 shows the significant increase of the in-cylinder pressure at high load in dual-fuel mode compared to the normal diesel operation. This is caused due to the higher temperature and higher amount of natural gas admitted to the engine at high load. Higher temperature and lower excess air ratio allow better flame propagation through the in-cylinder mixture and improve combustion of gaseous fuel. The highest increase of peak pressure (~20%) is obtained at the highest natural gas mass participation rate (Z = 80 %NG). This could represent a challenge in the conversion process from normal diesel operation to the dual-fuel because the higher pressure causes higher stress of the vital parts of the engine, which may shorten the engine life. At low load, the in-cylinder pressure in dual-fuel mode is lower than in the normal diesel operation.

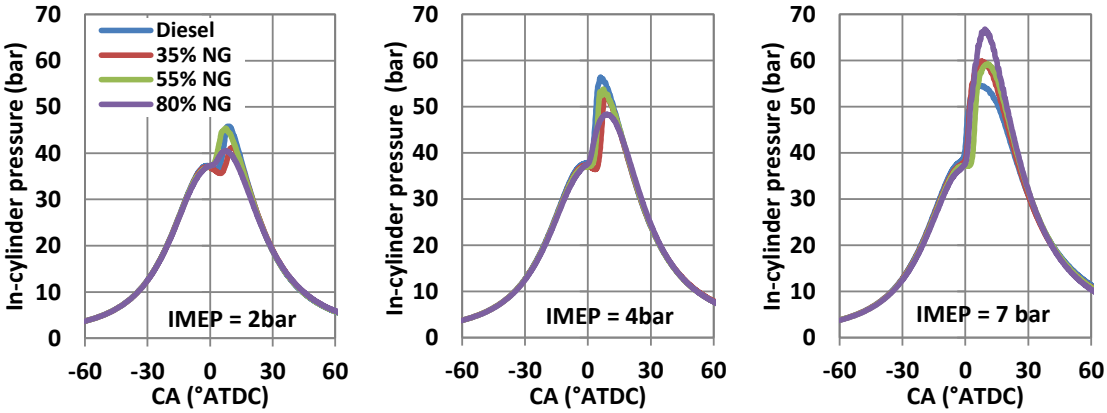

Figure 80. In-cylinder pressure profiles (averaged over 300 cycles)

The CO emissions are shown in Figure 81. They are significantly higher in DF combustion mode compared to the emissions from normal diesel operation. This is expected due to fact that the NG is premixed and can be found in parts of the combustion chamber that have lower temperatures unlike pure diesel operation where the most of the fuel does not

reach colder combustion chamber areas. Also, as it can be seen the CO emissions follow the trend of temperature with lower CO emission in cases with higher in-cylinder temperature.

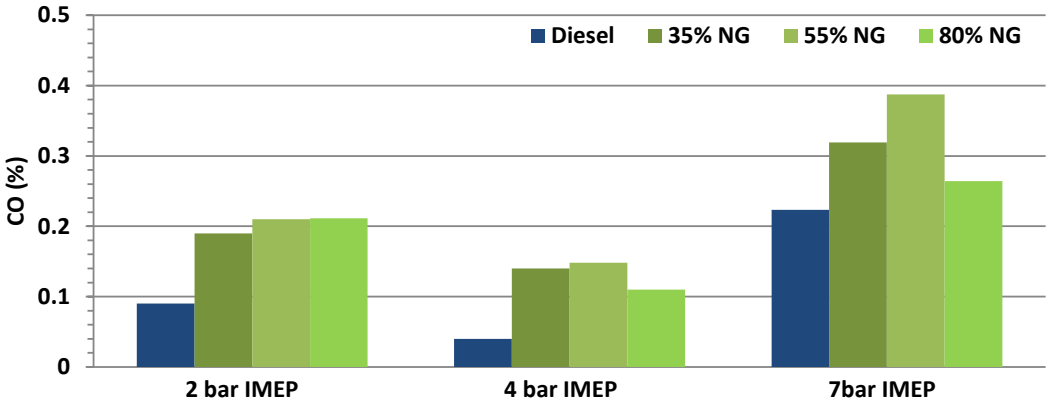

Figure 81. CO emissions in initial tests

As mentioned in the introduction chapter, natural gas has a potential for reducing the CO_2 emission, which is confirmed in the Figure 82. In all the cases, dual-fuel combustion produces less CO_2 compared to the pure diesel operation.

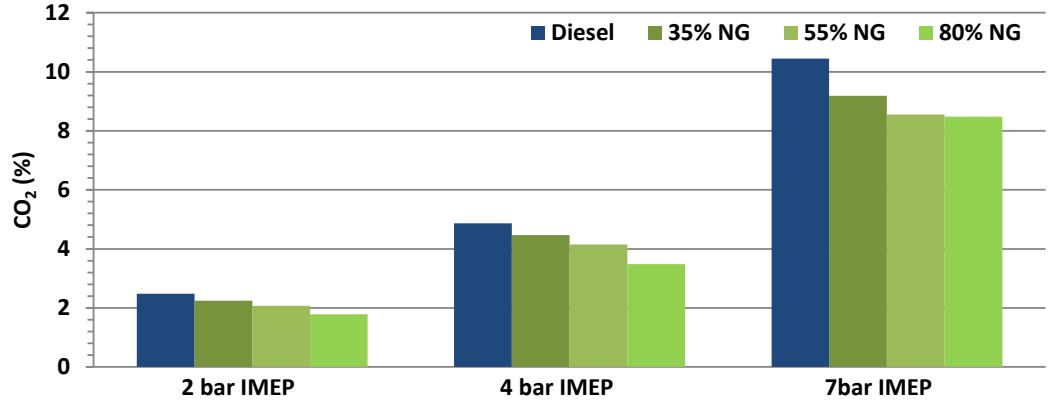

Figure 82. CO_2 emission

Figure 83 shows the NO_X emissions. At the load of 2 bar IMEP, formation of NO_X is very low due to low in-cylinder temperatures. Although the average cylinder temperature (Figure 79) is very low, the local temperature in the spray zone is significantly higher than the average in-cylinder temperature and therefore certain amount of NO_X is generated in the spray zone. As shown in Figure 79, the increase of the NG mass participation rate in the mixture results in a decrease of the in-cylinder temperatures which results in the reduction of NO_X emissions. At high load (IMEP = 7 bars) the average temperatures are higher which result in a higher formation of NO_X. The efficient combustion of methane, which is significantly better promoted at high loads, increases also the temperatures in the propagating flame which then increases the NO_X formation in that part of the cylinder. Thus, the increase of NG mass

participation rate in the mixture at high load significantly increases the overall NO_X emissions accordingly.

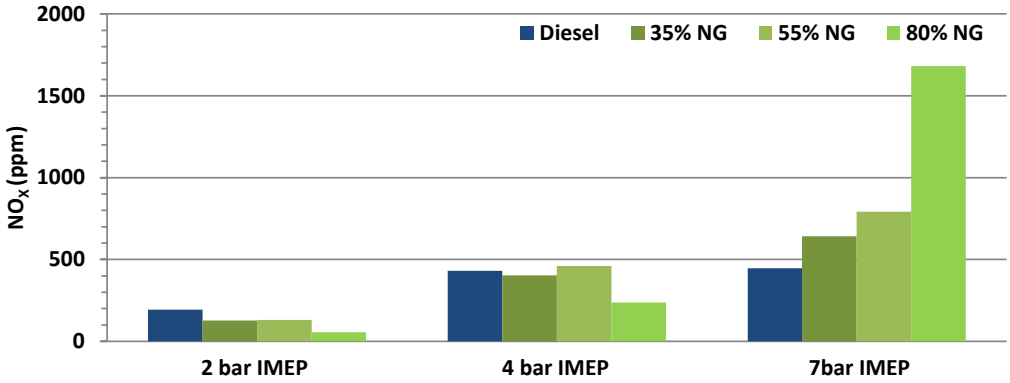

Figure 83. NO_X emissions

Figure 84 shows the RoHR for optimized start of injection timings of operating points at IMEP = 2 bar, IMEP = 4 bar and IMEP = 7 bar. It can be observed that the increase in NG mass participation rate results with lower peak RoHR values at low load, while at high load the trend is reversed, which will also lead to a larger pressure rise rates, as seen in Figure 80. The start of injection are similar in all cases, between 8 °CA BTDC and 14 °CA BTDC, with the increase in natural gas mass participation rate resulting in advanced start of injection.

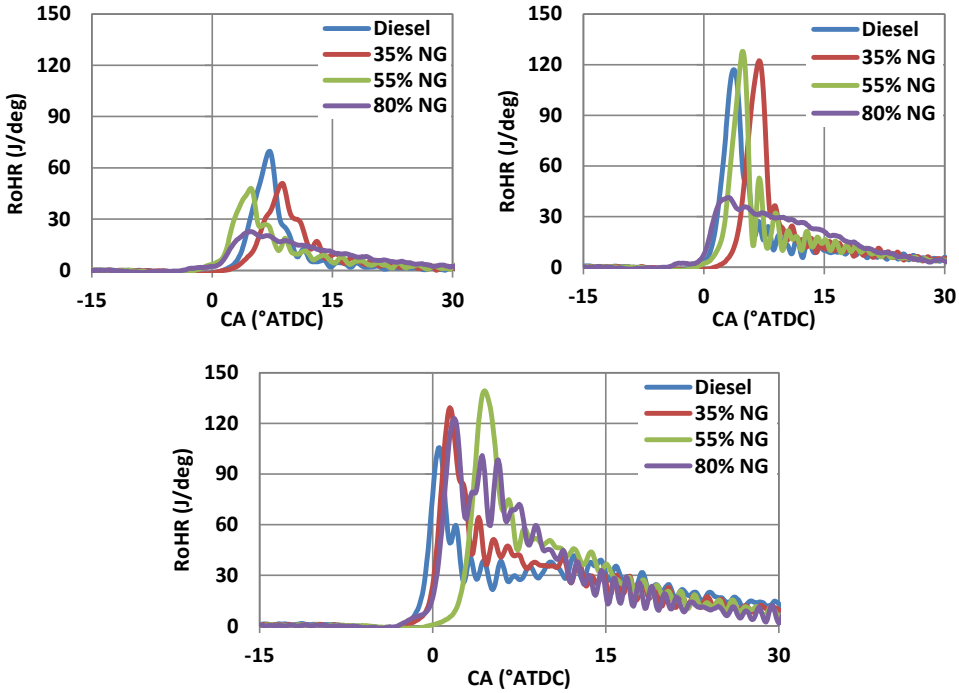

Figure 84. RoHR profiles: IMEP = 2 bars; IMEP = 4 bars; IMEP = 7 bars

All the presented in this chapter show general trends in performance and exhaust gas emissions in conventional dual-fuel combustion mode, and represent the basis for the design of experiment of further measurements and define research areas of possible improvements.

For better understanding of the dual-fuel operation and change in performance and emissions with some changes in operating parameters, the influence of start of injection of diesel fuel in various conditions of dual-fuel operation will be shown in the next chapter.

5.2. The influence of start of injection of diesel fuel on performance

The measurement was performed with one injection per cycle with the fuel pressure maintained at p_{diesel} = 300 bar. For this measurement, three mass participation rates of natural gas were selected: 0 %NG (NDO), 50 %NG and 90 %NG, while loads and engine speed were the same as in the previous measurements (IMEP = 2, 4, 7 bars; n = 1600 rpm). The first step was to find the optimal SOI point with respect to the maximum indicated efficiency and then the influence of advanced and retarded SOI was researched. Fuel quantity is maintained at constant level during the SOI sweep process. The SOI was changed as long as the IMEP did not significantly decrease, or as long as the one of the specific constraints was not crossed: average pressure rise rate dp/dα > 10 bar/°CA or CoV(IMEP) > 10%. These values were selected according to the usual practice shown in available literature. The CoV(IMEP) is defined as:

$$CoV(IMEP) = \frac{\sigma(IMEP_n)}{\mu(IMEP_n)} \cdot 100\ [\%] \tag{21}$$

where $\sigma(IMEP_n)$ [bar] represents standard deviation of IMEP during the n consecutive cycles, and $\mu(IMEP_n)$ [bar] represents mean value of IMEP during the n consecutive cycles.

Figures 85 and 86 show the influence of start of injection of diesel fuel on indicated mean effective pressure for all tested operating points. Since during the SOI sweep the fueling was kept constant the values in the legend shows the total excess air ratio during the sweep. The highest sensitivity on the change in start of injection timing is noticed at low load. The increase in engine load increases the range of SOI points that results in equal or similar value of IMEP, especially at the highest mass participation rate of the natural gas.

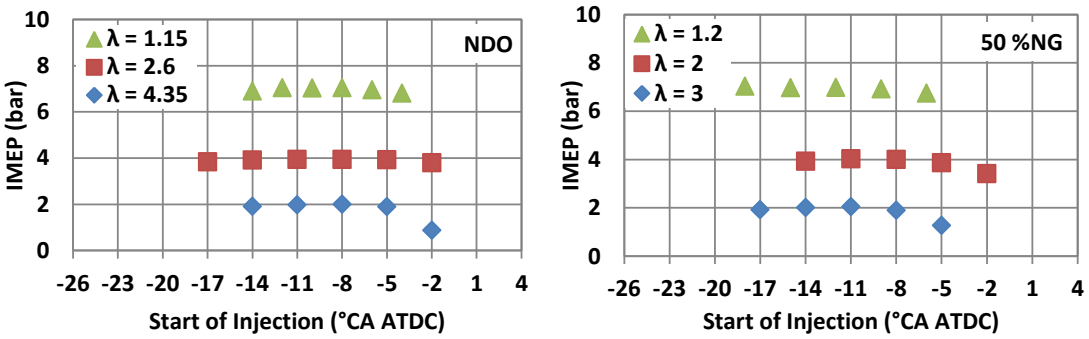

Figure 85. The influence of SOI timing on IMEP; normal diesel operation and 50 %NG

As shown on the above figure, in some cases advancing the SOI timing increases IMEP (e.g. 50 %NG and IMEP = 7 bar) and improves indicated efficiency, but these operating points are not acceptable because of the high maximum cylinder pressure rise rates (dp/dα).

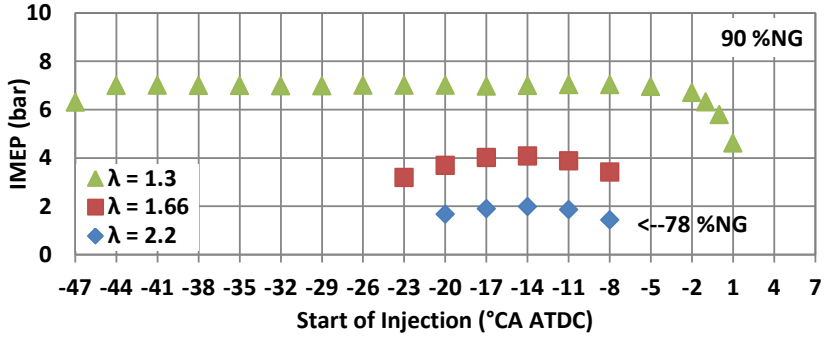

Figure 86. The influence of injection timing of diesel fuel on IMEP at 90 %NG

Considering that the combustion phase influences IMEP and combustion efficiency, the relationship between SOI and combustion phase (CA50) is shown in Figure 87.

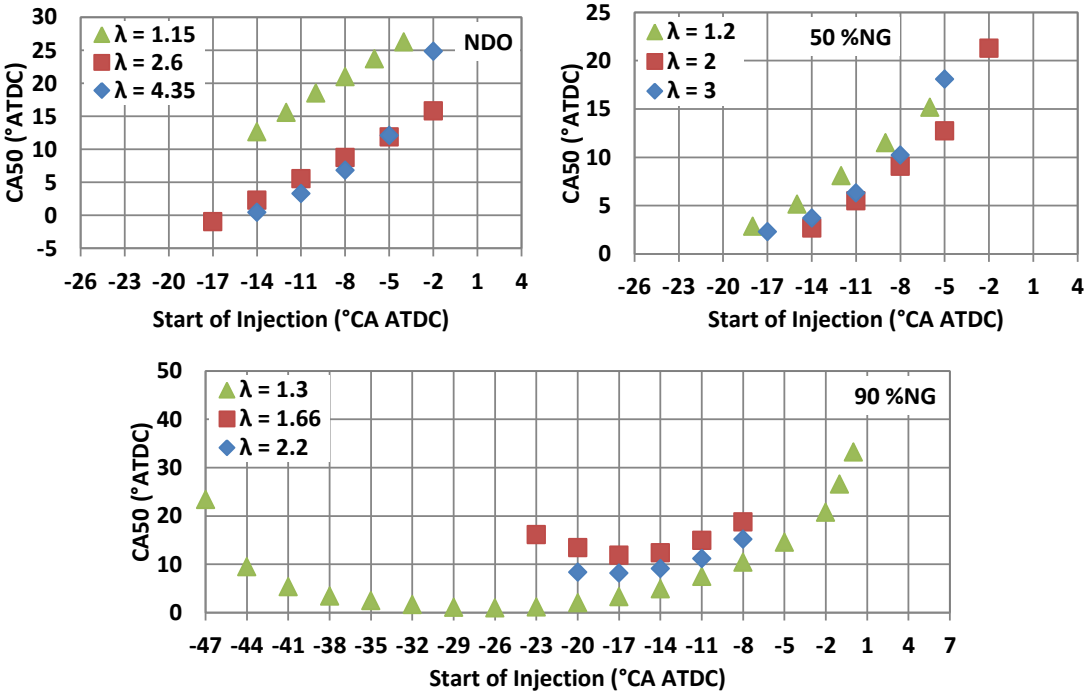

Figure 87. The influence of injection timing on CA50

In normal diesel operation (NDO) and at 50% NG mass participation rate, CA50 shows practically linear dependence of start of injection timing, i.e. the combustion phase is changing as the SOI timing changes. At 90% NG mass participation rate, advancing the SOI timing advances the combustion phase until the SOI reaches SOI = 20 °CA BTDC. Further advancing of SOI up to SOI = 35 °CA BTDC practically doesn't have influence on CA50, while advancing the SOI timing over 35 °CA BTDC retards the combustion phase.

Figures 88 - 90 show the change in indicated efficiency with the change of SOI for all tested operating points. On the charts the values of constraints in terms of dp/dα in bar/°CA and CoV(IMEP) in % are shown to understand why some operating points are not acceptable.

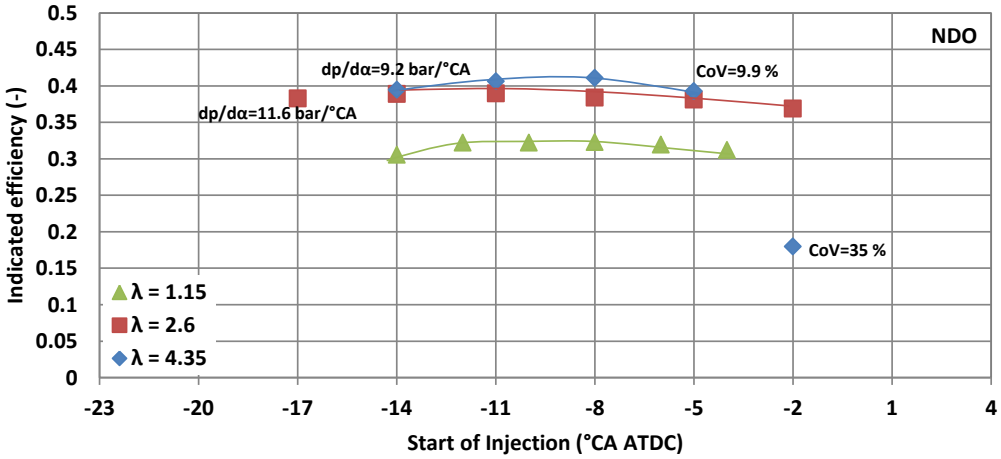

Figure 88. Influence of SOI timing on indicated efficiency for NDO

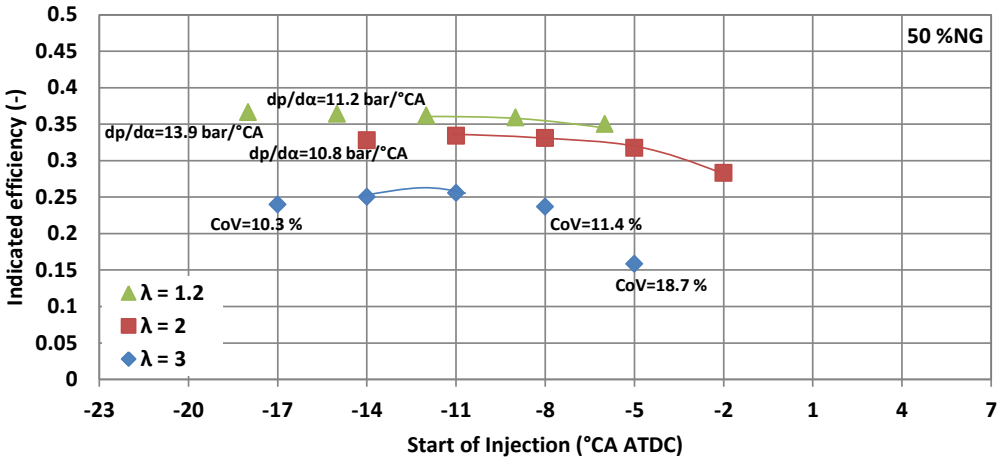

Figure 89. Influence of SOI timing on indicated efficiency for *Z* = 50 %NG

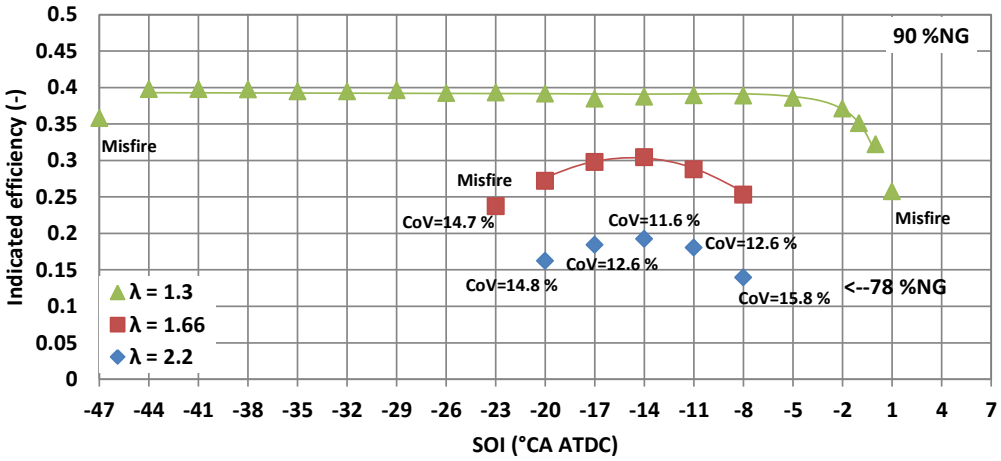

Figure 90. Influence of SOI timing on indicated efficiency for *Z* = 90 %NG

The ranges of acceptable start of injection timings are connected with solid lines. As shown, the range of acceptable SOI timings is very small at low load (IMEP = 2 bars) and decreases with increasing NG mass participation rate, while at high load, the range of acceptable SOI timings is the highest at the highest natural gas mass participation rate. If one compares results with different NG mass participation rates at IMEP = 2 bars, it can be concluded that normal diesel operation (Z = 0% NG) can operate between SOI = -5 and SOI = -14 °CA ATDC, while the increase in NG mass participation rate to Z = 50 % significantly reduces efficiency and reduces the range of acceptable SOI timings. Advancing or retarding the SOI timing from optimum result in unstable operation and high combustion instability. At higher loads (IMEP = 4 bars and IMEP = 7 bars) and at 50% NG mass participation rate, advancing the SOI timing increases indicated efficiency but it is limited by high pressure rise rate. The highest flexibility in SOI timing is obtained at very high mass participation rate (90% NG) and at the high load (IMEP = 7 bar). There is provided stable engine operation and maximum efficiency at a wide range of SOI timing. At low and part loads, using the high amount of NG (Z = 90%) significantly reduces the range of acceptable SOI timings. Also, indicated efficiency is significantly reduced with a small change of SOI timing from the optimal point. At low load (IMEP = 2 bars), maximum NG mass participation rate that was acceptable equals 78%. Higher amount of NG results in misfires due to poor flame propagation and too low energy from diesel fuel for flame initiation.

When compared to the normal diesel operation, the cases with increased natural gas mass participation rates have reduced the indicated efficiency at low and part loads (IMEP = 2, 4 bars), while at high load, the increase in natural gas mass participation rate increases the engine efficiency. Also one can notice that in normal diesel operation the increase of load results in decreased indicated efficiency, while in dual-fuel operation the increase of load results in increased indicated efficiency. The increased efficiency at higher load of dual-fuel operation is a result of better flame propagation due to the higher in-cylinder temperature and lower excess air ratio of NG/air mixture, while at low loads the poor efficiency is a result of lower temperatures and poor flame propagation through NG/air mixture with very high excess air ratio.

Besides on the efficiency the injection timing of diesel fuel also has significant influence on the exhaust gas emissions. The influence of SOI timing on the hydrocarbon emissions is shown in Figure 91. The normal diesel operation results in very low THC emissions at all three loads, around 200 ppm at optimum SOI timings, while the dual-fuel operation results in significantly higher THC emissions.

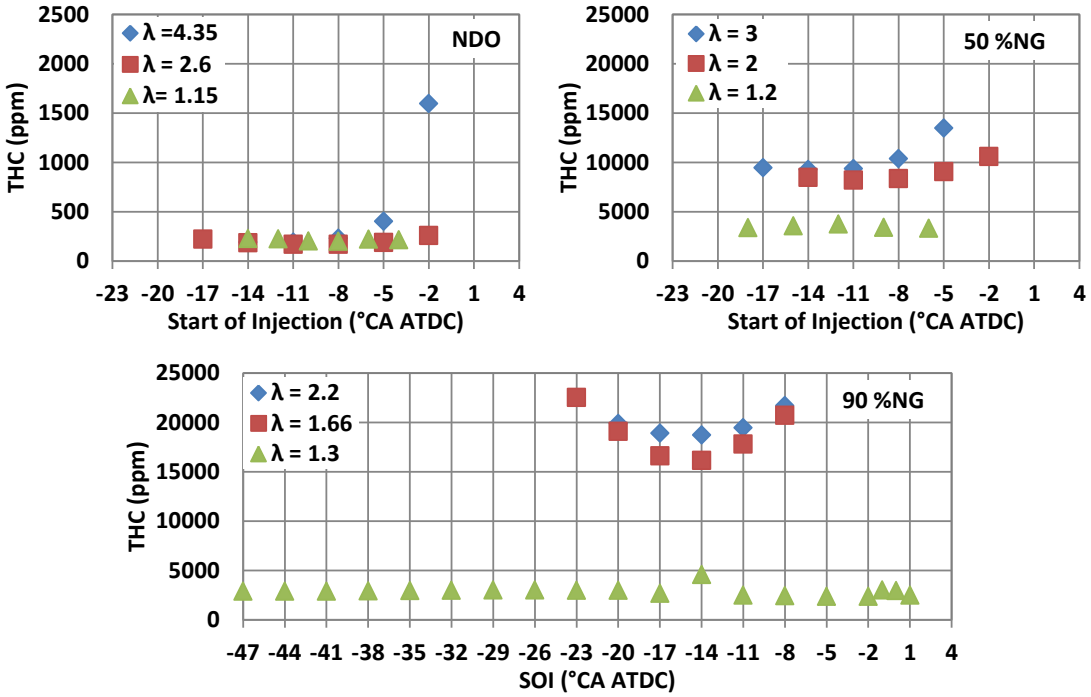

Figure 91. Effect of SOI timing on THC emissions (*Z* = 0%, 50% and 90%)

As shown, with dual-fuel operation at 50 %NG and optimum SOI timing, the THC emission increases from 200 ppm to 3700 ppm and 8500 ppm at high and part load, respectively. Combining the results of THC and indicated efficiency at low and part load, one can notice that significant part of the gas fuel remains unburned in dual-fuel operating mode which explains the low efficiency and high THC emissions. At low and part load a significant influence of SOI timing on THC emissions is also noticed, which means that changing the SOI timing from optimum to more advanced or retarded results in significant increase in hydrocarbon emissions. At high load, the change in SOI timing does not have significant influence on hydrocarbon emissions, especially at NG mass participation rates where THC emission is quite constant throughout the entire range of SOI timings.

With respect to the NO_X emissions, the start of injection timing has significant influence at both, normal diesel and dual-fuel operation, as shown in Figures 92 and 93.

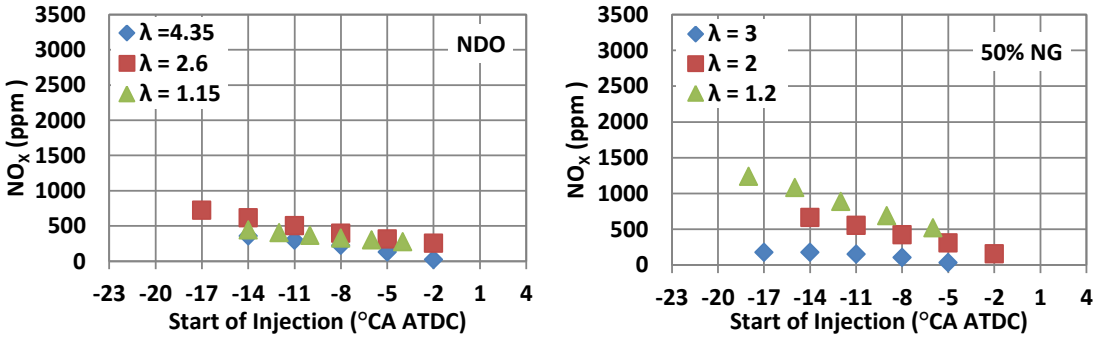

Figure 92. NO_X emissions vs. start of injection timing, NDO and *Z* = 50%

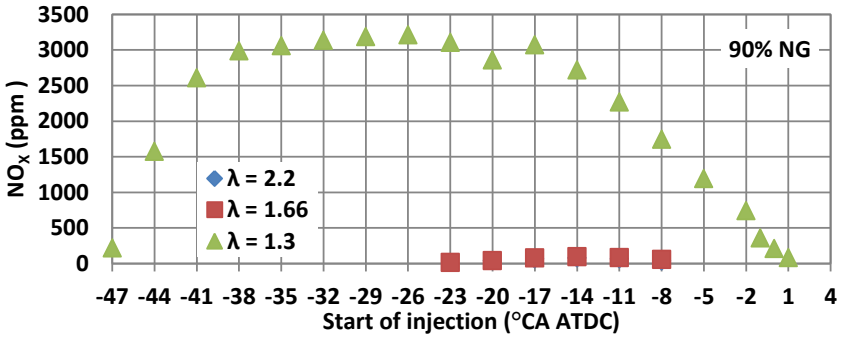

Figure 93. NO_X emissions vs. start of injection timing, *Z* = 90%

At normal diesel operation and at 50% mass participation rate of NG, advancing the start of injection timing increases the maximum temperatures in the charge and promotes NO_X formation. At high load and at 90 %NG, NO_X emissions increase with advancing the SOI timing and reach the maximum value of 3000 ppm around SOI = 17 °CA BTDC. Further advancing the injection timing result in approximately constant NO_X emissions up to SOI = 38 °CA BTDC, whereupon NO_X emission starts to decrease. It is possible to achieve lower NO_X emission with further advancing of SOI timing, or similar as around SOI = 8 °CA BTDC, but probably with significantly lower soot emission, which was not measured during the test. The main reason for reduced NO_X formation could be higher ignition delay, which allows better mixing of diesel fuel with the NG/air mixture resulting in lower maximum temperatures during combustion. However, operation in this area is on the boundary and significantly depends on the intake temperature and temperature of the engine, which means that the misfire can easily occur. With the stable combustion, high engine efficiency is retained in this area.

The same behavior of the duel fuel combustion at high load (IMEP = 7 bar) and high mass participation rate (90% NG mass participation rate) was observed at other engine speeds. Figure 94 shows the comparison of NO_X emissions and indicated efficiencies of dual-fuel combustion with late and early SOI timing.

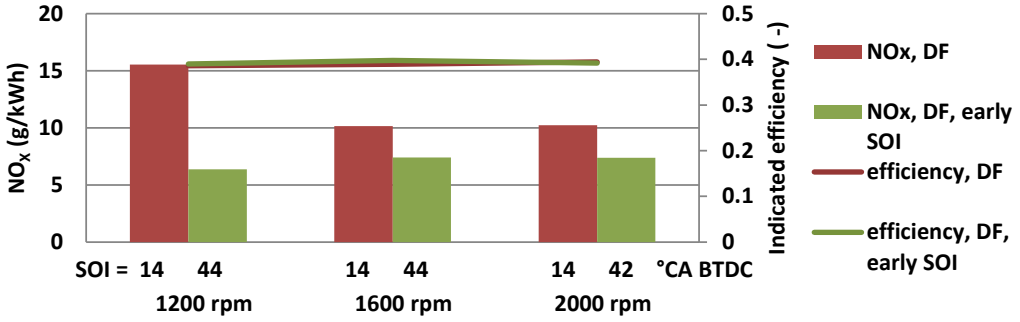

Figure 94. NO_X and indicated efficiency at normal and early SOI timing; IMEP =7 bar; *Z* = 90 %

With early start of injection it seems that the combustion becomes more chemically controlled which then results with more difficult control of combustion timing. Therefore, although the early start of injection of diesel fuel reduces NO_X emissions, it is very difficult to maintain a stable combustion, because the combustion timing now also depend on engine temperature and engine speed.

5.3. The influence of intake air preheating and EGR at low load

The literature review and research presented above show that the dual-fuel combustion mode is significantly inefficient at low load compared to the normal diesel operation. Although the increase in NG mass participation rate decreases NO_X emissions, high THC emission indicates that a large amount of unburned fuel is thrown into the exhaust pipe.

Since the reason for low efficiency is the inability of the spray combustion to initiate and sustain strong flame in the lean NG/air mixture, one of the possible methods for improvement of combustion at low load could be the higher intake temperature that would result in higher temperature of the NG/air mixture which would have a higher flame speed even at the high excess air ratio. The higher intake temperature can be achieved in two ways: a) installation of the heater into the intake pipe and b) hot exhaust gas recirculation, where some of the exhaust gas is returned to the intake without cooling.

The influence of the intake air temperature (without using EGR) on dual-fuel combustion was investigated by taking measurements at the three different intake temperatures: 20 °C, 40 °C and 60 °C, at ambient intake pressure. The operating point that was selected for this research was IMEP = 4 bar and *n* = 1600 rpm, with mass participation rate of natural gas Z = 90 %. As shown above, lower load (IMEP = 2 bars) with high NG mass participation rate does not make sense because it results in an unstable combustion. Results of the influence of intake air preheating (without EGR and optimized SOI with respect to the indicated efficiency) on dual-fuel combustion are shown in Figures 95 and 96.

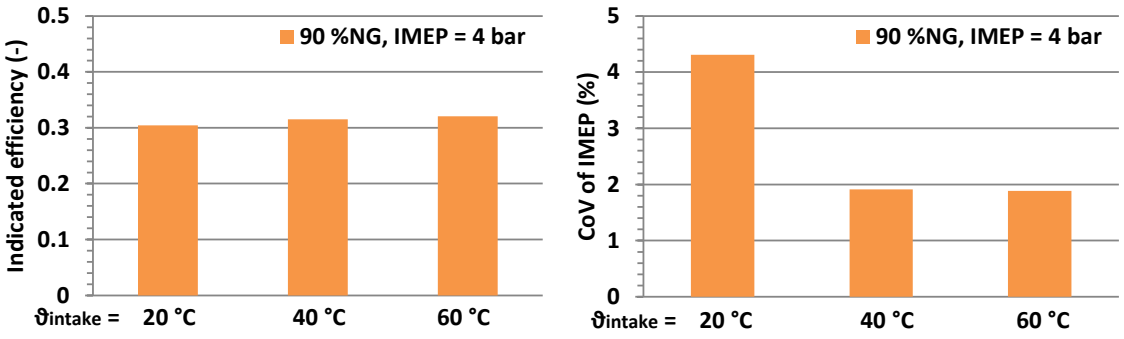

Figure 95. Influence of the intake air preheat on efficiency and CoV(IMEP)

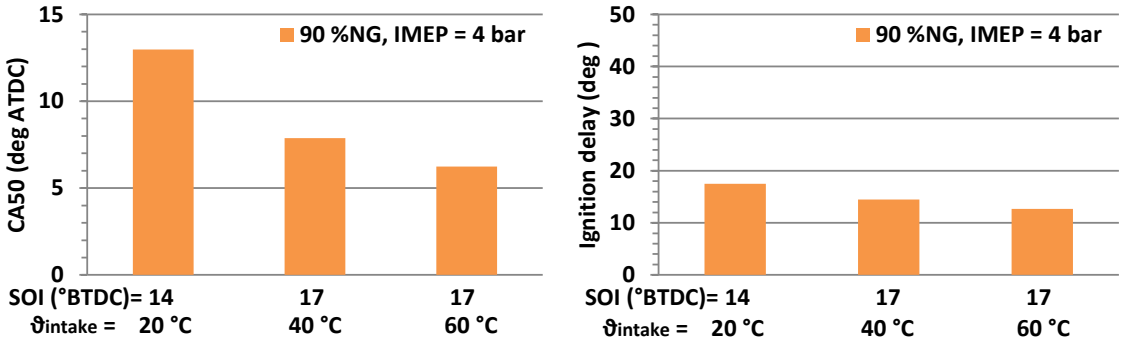

Figure 96. Influence of the intake air preheat on CA50 and ignition delay

Figures 95 and 96 show obvious trends in combustion characteristics caused by an increase in inlet air temperature. Increasing the intake temperature allows advanced SOI timings, lowers the ignition delay and moves CA50 to more advanced angles. The change in intake air temperature from 20 °C to 40 °C results in 1.5% point increase of the indicated efficiency while the change from 20 °C to 60 °C provides 2% point increase of the indicated efficiency. The reason for the increased efficiency is the improvement of the burning rate of the natural gas, caused by the slight reduction of the total excess air ratio (i.e. the air inlet preheating leads to a decrease of the volumetric efficiency) and a slight increase of the unburned zone temperature. These facts lead to a faster flame speed through the combustion chamber. However, in the results of indicated efficiency the energy of the heater is not included. If the real system would provide the intake heating in the same way as the used experimental setup (the electric heater placed in intake line) the real efficiency would be slightly lower because of the energy required to power the electric heater. On the other hand some engine power plants can use the heat from other sources, e.g. the heat from the exhaust gases, considering that the tested intake temperature on the experimental engine was not very high.

From the exhaust gas emission point of view (Figure 97), the preheating of the intake air increases flame speed, improves combustion process and decreases THC emissions, but at the same time, higher in-cylinder temperatures enhance NO_X formation. The effect of intake air temperature on the NO_X formation seems significantly higher than the effect on reduction of THC emissions. With the improvement of the total burning rate due to the increased temperatures, the CO emission slightly decreases with the increase of the intake temperature, while the CO_2 emission increases accordingly.

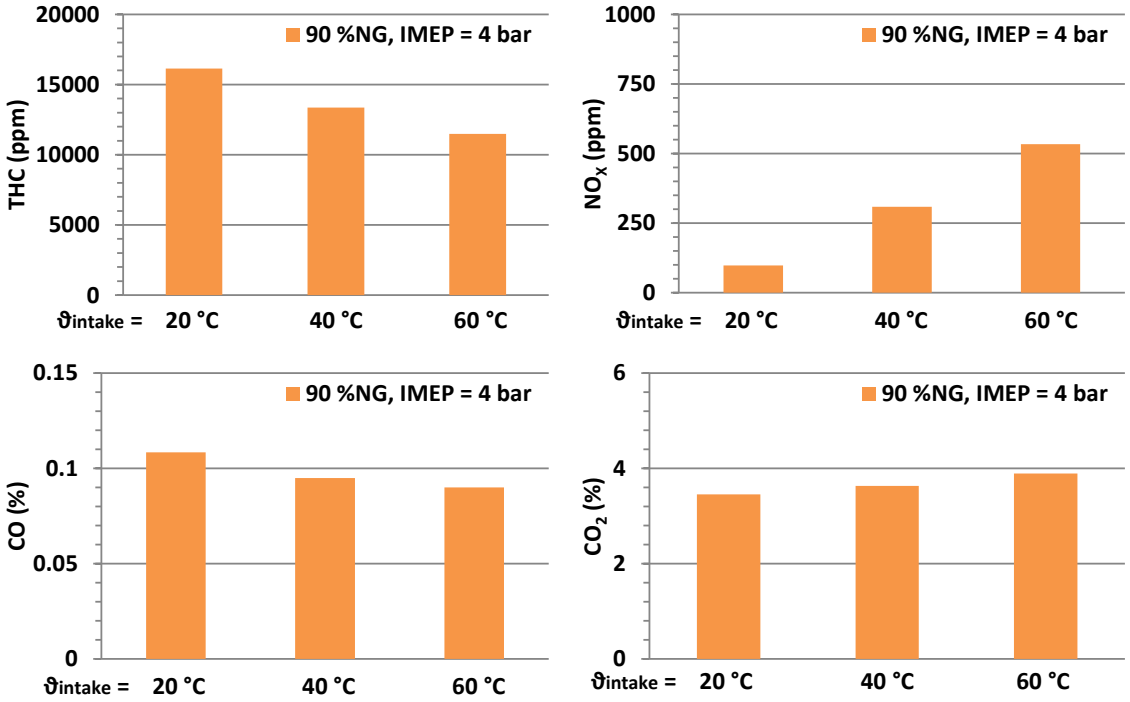

Figure 97. Influence of intake air preheat on exhaust gas emissions

The second method to increase the intake temperature is the recirculation of the hot exhaust gases. Considering the EGR line in experimental setup is fairly long and uninsulated, the intake air heater was still used for control of the intake temperature. In this study the intake temperature was set to two values: 20 °C and 40 °C, where one represents the mixture of intake air and cold EGR and the second representing mixture of air and hot EGR. The results are again shown for IMEP = 4 bar and 1600 rpm, with mass participation rate of natural gas Z = 90 % and exhaust gas recirculation set to four different levels: EGR = 0%, 5%, 10% and 15%. Figures 98 and 99 shows the effects of cold and hot EGR on the performance of dual-fuel engine, whereas Figure 100 shows the influence of hot and cold EGR on exhaust gas emissions. In the charts, cases without EGR (EGR = 0%) are also shown, which represent the dual-fuel operation at 20 °C intake temperature and dual-fuel operation at 40 °C intake temperature.

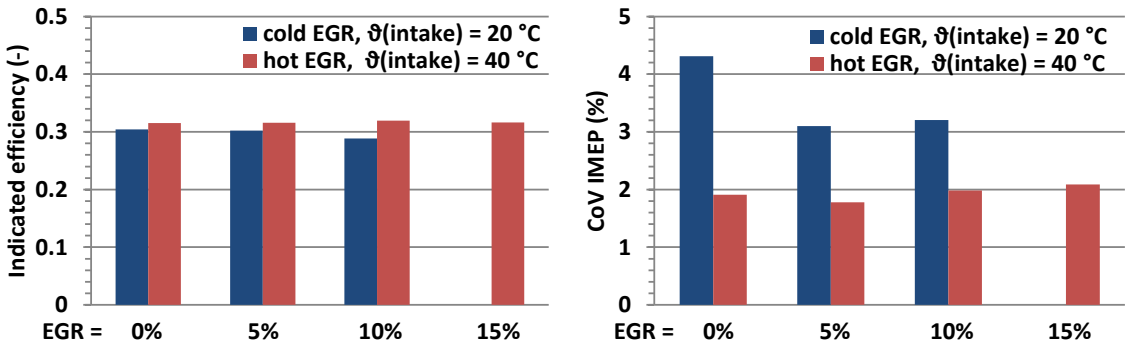

Figure 98. Effects of EGR on performance, IMEP = 4 bar, Z = 90%

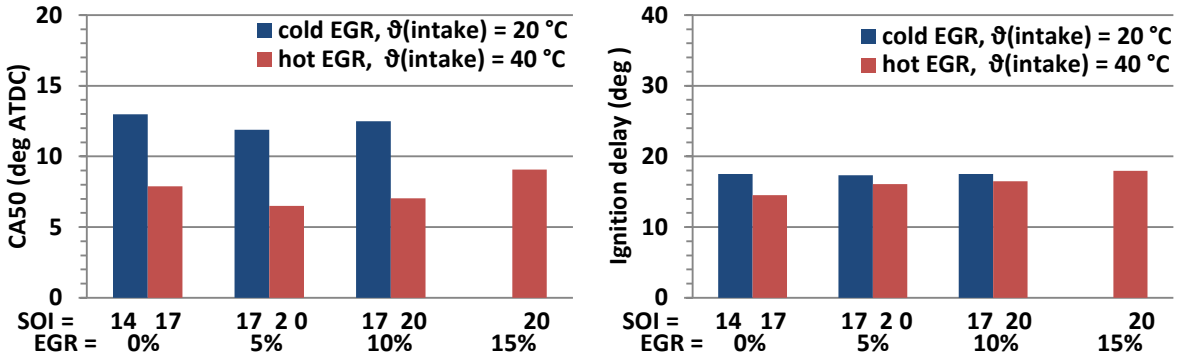

Figure 99. Effects of EGR on CA50 and ign. delay, IMEP = 4 bar, *Z* = 90%

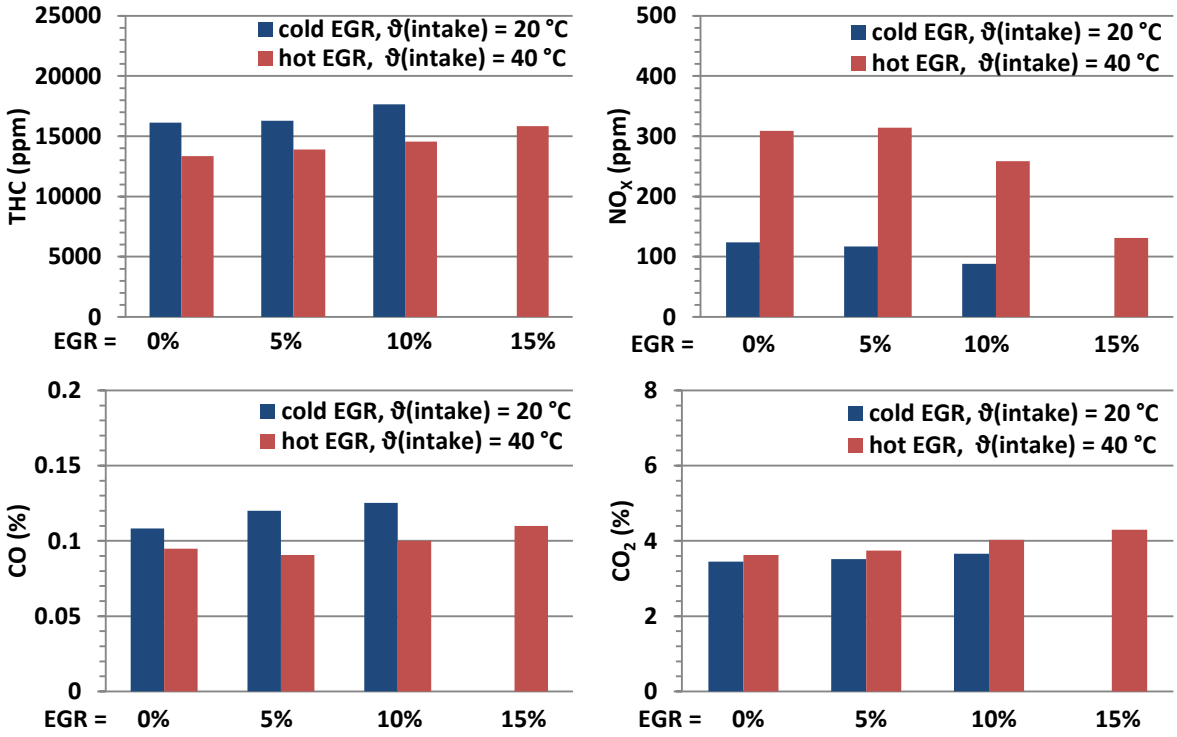

Figure 100. Influence of EGR on exhaust gas emissions, IMEP = 4 bar, *Z* = 90%

The maximum achievable amount of hot EGR which still guarantees a stable operation for this operating point is 15% EGR, while with cold EGR limit is at 10%. Higher amounts of EGR in specific cases cause misfires and unstable operation.

As shown in Figure 99, the ignition delay increases as the EGR percentage increases for both hot and cold exhaust gas recirculation, but with hot EGR the ignition delay is shorten than with the cold EGR. The increase in EGR percentage increases the overall specific heat capacity of the in-cylinder mixture, thus resulting in a decrease of the cylinder charge temperature at the point of direct fuel injection and therefore in an increase of the ignition delay. On the other hand, the increase of the EGR percentage decreases the total excess air ratio, which should reduce the ignition delay. Since the ignition delay has slightly increased, it

can be concluded that the reduction of the temperature of the mixture has the dominant influence on ignition delay.

Comparing the achieved indicated efficiency (Figure 98) when using the hot and cold EGR, one can notice that these two parameters have different effect. The application of cold EGR lowers the indicated efficiency due to a longer ignition delay period of the pilot fuel, which affects negatively the total heat release rate during the premixed controlled combustion phase. On the other hand, the application of the hot EGR increases indicated efficiency, compared with the case without EGR at intake temperature ϑ_{intake} = 20 °C. This is due to the fact that the higher intake charge temperature combined with the lower total air excess ratio, caused by the presence of EGR, promotes the flame propagation through combustion chamber and improves the combustion quality of gaseous fuel. Since the indicated efficiency is maintained with an increase in EGR percentage, it can also be concluded that the intake temperature has a higher influence on efficiency than the EGR percentage.

If one looks at the effect of EGR on NO_X emissions, it can be concluded that the increase in EGR percentage results in a decrease of NO_X emissions, regardless of the use of cold or hot EGR. Increasing the EGR percentage decreases the charge temperature due to the higher specific heat capacity of the cylinder charge and also decreases the oxygen availability in the cylinder charge. These phenomena restrain the NO_X formation mechanism. By looking at Figures 97 and 100, it seems that NO_X emission is more sensitive to the inlet air temperature than to the EGR percentage. Presented results lead to the conclusion that one could slightly reduce NO_X emission by application of cold EGR, but with penalty in indicated efficiency, while application of hot EGR cannot reduce NO_X emission below the emission achieved without EGR at intake temperature ϑ_{intake} = 20 °C. The only benefit of hot EGR application is slightly increased indicated efficiency, which is practically a result of increased intake temperature, and not of the presence of EGR.

On the other hand, very high THC emissions (> 10.000 ppm) at low load and high mass participation rate of NG are further deteriorated by using the EGR. Figure 100 shows an increase in THC emissions with an increase of cold or hot EGR. The higher intake temperature has a positive influence on THC emissions, which can be seen in case without EGR, but increases in EGR percentage deteriorates THC emissions. Similar behavior is noticed in CO emission.

The overall conclusion regarding the intake preheat can be that increased intake temperature improves combustion with a slightly positive effects on the indicated efficiency, THC and CO emissions, but with a very negative effect on NO_X emissions. The only way to

reduce the NO_X formation is by introducing the cold EGR, which results in a penalty in the indicated efficiency, while introducing the hot EGR in order to reduce the NO_X emissions does not have any sense, because the negative effect of increased intake temperature is significantly higher than the effect of presence of exhaust gas. However, any significant improve of the dual-fuel combustion cannot be achieved only by the application of mentioned operating parameters.

5.4. Influence of the HCCI/RCCI combustion process for improving operation at low load

The previous measurements showed a significant disadvantages of the dual-fuel operation at low and mid load, where THC emissions at Z = 50% NG are around or even higher than 10000 ppm, the NO_X emissions are similar to normal diesel operation and indicated efficiencies are significantly lower than at normal diesel operation. The higher amount of NG results with extremely high emissions of THC. These results suggest that the conventional dual-fuel is not suitable for low loads (i.e. engine should operate only with diesel fuel or with very small addition of NG). Therefore, the improvement of dual-fuel operation at low load should be sought in a different combustion process. One of the possible combustion processes could be Reactivity Controlled Compression Ignition (RCCI).

RCCI is a dual-fuel engine combustion technology that is a variant of Homogeneous Charge Compression Ignition (HCCI) and provides more control over the combustion process. It has the potential to dramatically lower the fuel consumption and emissions. In general definition, RCCI uses in-cylinder fuel blending with at least two fuels of different reactivity and multiple injections to control in-cylinder fuel reactivity to optimize combustion phasing, duration and magnitude. The process involves introduction of a low reactivity fuel into the cylinder to create a well-mixed charge of low reactivity fuel, air and recirculated exhaust gases. The high reactivity fuel is injected before ignition of the premixed fuel by using a single or multiple injections directly into the combustion chamber. The difference between RCCI and conventional dual-fuel is that the RCCI combustion is chemically controlled combustion of the air/fuel mixture and there is no diffusion flame or flame propagation through a premixed mixture. In order to enable RCCI the injection of the high reactivity fuel has to be more advanced than in conventional dual-fuel operation, and the conditions in the cylinder (temperature and pressure) have to be adequate to enable the start of chemical reactions.

5.4.1 RCCI combustion technology at IMEP = 4 bars

Since the RCCI combustion is supposed to improve the dual-fuel operation at low load the first test point is set to:

- IMEP = 4 bars and n = 1600 rpm.

Measurement was performed at the following intake conditions:

- p_{intake} = ambient,
- ϑ_{intake} = 60 °C,
- Z = 50% CNG,
- EGR = 0%.

Injection pressure of diesel pilot fuel was set to 300 bars and there are three different injection strategies applied:

- Conventional dual-fuel: injection of diesel pilot fuel at 10 °CA BTDC,
- Premixed dual-fuel: injection of diesel fuel at 85 °CA BTDC,
- Splitted injection of diesel fuel: (75 % of fuel injected early and 25 % late).

Fuel quantities of natural gas and diesel fuel were maintained constant through all the test cases. Figure 101 shows the injection strategies and mass flows of the directly injected diesel fuel.

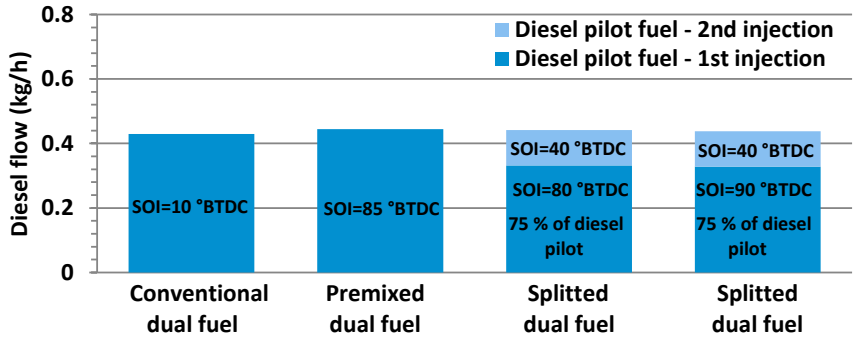

Figure 101. Injection strategies of diesel pilot fuel

As shown, in the first two cases the diesel fuel is injected in a single injection per cycle with the main difference in the start of injection timing. Increased intake temperature allows very early injection (SOI = 85 °CA BTDC) which results in similar IMEP that is achieved and in similar indicated efficiency, compared to the conventional dual-fuel operation (SOI = 10 °CA BTDC). The first case with SOI timing (10 °CA BTDC) is optimized with respect to the maximum indicated efficiency, while the second SOI timing (85 °CA BTDC) is optimised with respect to the indicated efficiency and NO_X emissions. In the other two cases, diesel fuel injection is divided into two injections: in the first injection, 75% of diesel fuel is injected,

while the rest of 25% is injected later in the compression stroke. These fuel amounts as well as injection timings of each injection were also optimised with respect to the indicated efficiency and NO_X emissions. In this way, the higher amount of diesel fuel is premixed and ignited later by the second injection phase. Through the optimization phases it has been observed that the best results related to the NO_X emissions are obtained when the second injection contains as little fuel as possible to maintain the indicated efficiency. Too little fuel mass in the second injection results in a drop of IMEP and increase in NO_X emissions. Also, for the reduction of NO_X emissions, both injections should be advanced as much as possible. The detail process of optimisation of each injection phase will be described in next chapter (5.4.2). Figure 102 shows the obtained IMEP and indicated efficiencies, while Figure 104 shows CA50's, coefficients of variation, ignition delay and exhaust temperatures for all measured cases.

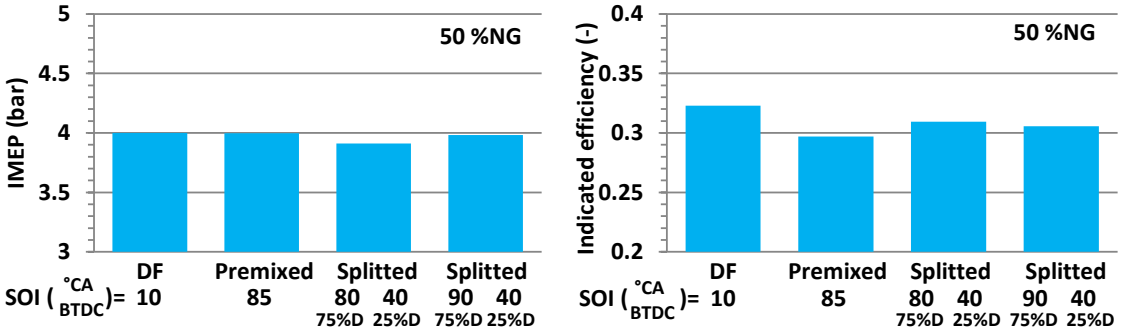

Figure 102. Influence of different injection strategies on IMEP and indicated efficiency

Results in Figure 102 show that similar performance is achieved by applying different injection strategies of diesel fuel. The IMEP is maintained almost constant (within 0.1 bar) throughout all cases, while the higher drop in indicated efficiency (2.5% point) is noticed in the second case, where all of the diesel fuel is injected at 85 °CA BTDC. Figures 103 and 104 compare the other characteristics of different injection strategies.

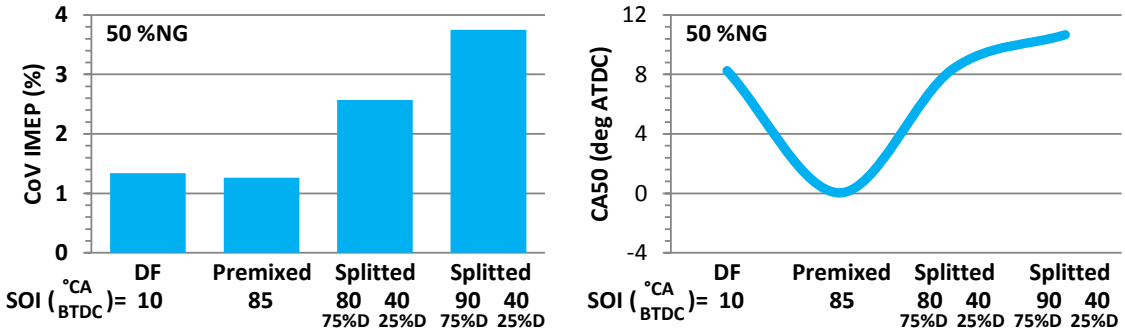

Figure 103. Influence of injection strategies on CoV and CA50

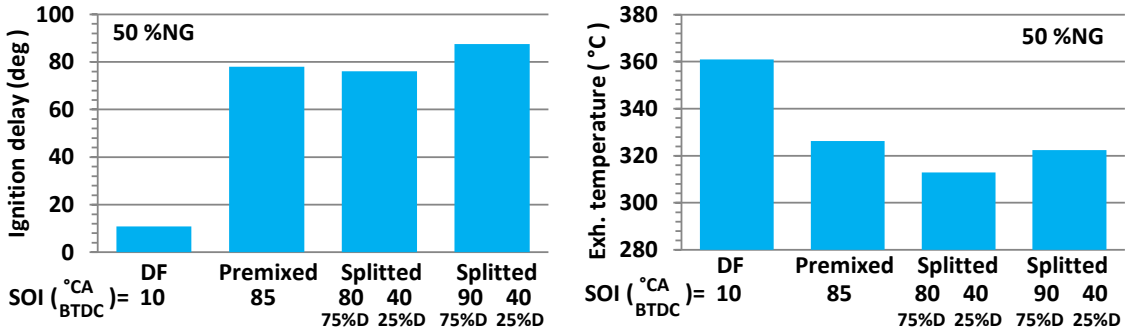

Figure 104. Influence of injection strategies on ign. delay and exhaust gas temp

The comparison of recalculated results shows that premixed case has CA50 around TDC, while other cases have similar CA50 at 8 - 10 °CA ATDC. The combustion phasing (CA50 point) could be a possible reason for the reduced indicated efficiency of this case. The advanced injection of diesel fuel in low in-cylinder temperature prolongs the ignition delay and allows better mixing of the diesel fuel with air-CNG mixture, which results in more homogenous mixture at start of combustion and avoiding the rapid combustion phase and high exhaust gas temperatures. The RoHR and in-cylinder temperatures profiles are shown in Figure 105.

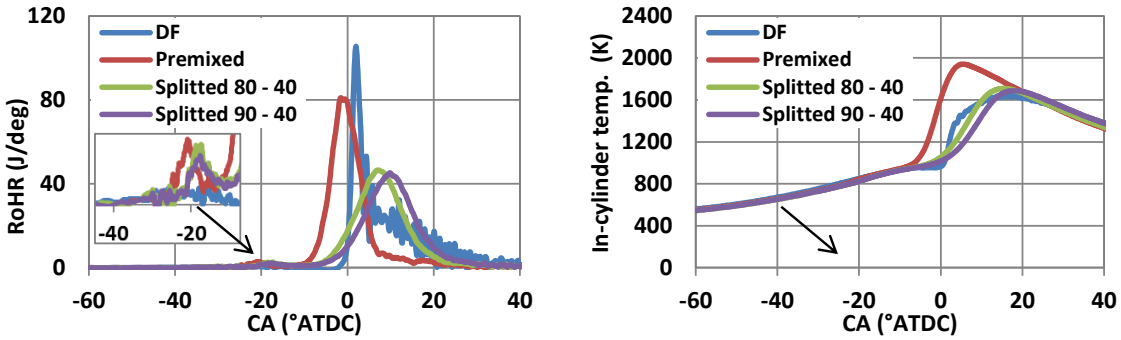

Figure 105. RoHR and average in-cylinder temperature

As shown, advancing of the start of injection timing lowers the peak RoHR, especially in cases with split injection. At around 20 °CA BTDC some low temperature heat release (LTHR) can be observed in premixed cases. Depending on the pressure and temperature of the operating point the main heat release may be preceded by the LTHR of the diesel fuel. During this phase, the radicals are formed which accelerate the main heat release. In the premixed case, the early start of main combustion results in high in-cylinder temperatures before TDC and high thermal losses. The splitting of the diesel fuel injection allows for a fair amount of the fuel to be premixed with the air-CNG mixture. Compared to the premixed case, it results in slower combustion after the combustion start, which is triggered by the second injection due to the lower excess air ratio of the charge in the cloud of the second injection.

This strategy decreases the combustion intensity, maintains the indicated efficiency and shows the strong effects on exhaust gas emissions. Figure 106 shows the measured exhaust gas emissions, while Figure 107 shows THC and NO_X emissions, expressed in g/kWh.

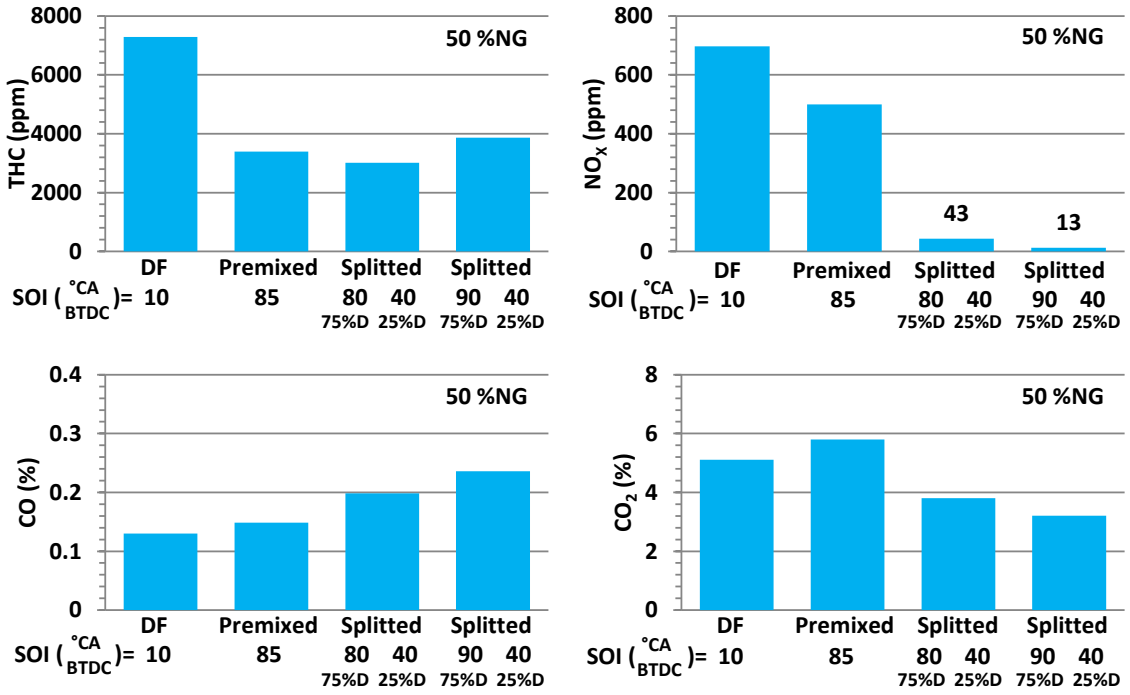

Figure 106. Influence of injection strategies on exhaust gas emissions

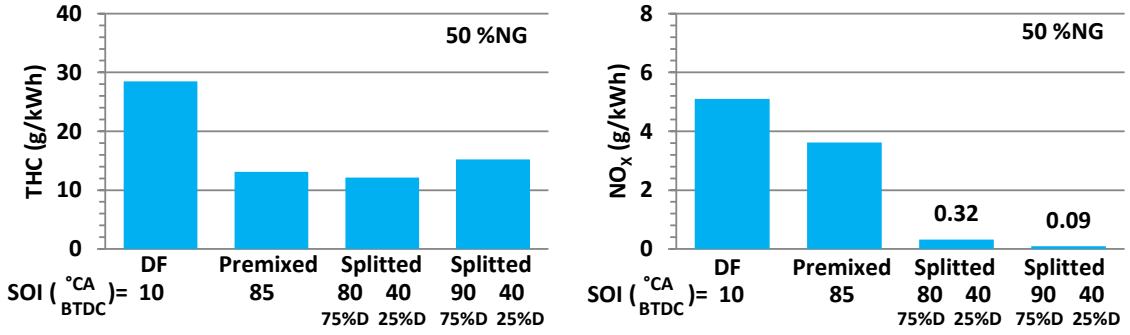

Figure 107. THC and NO_X emissions

From the exhaust gas emissions point of view, the first significant effect of advanced diesel fuel injection is observed in THC emissions. As shown, the reduction in THC emission is around 53% in premixed case, 58% in first split case and 47% in the second split case. This can be attributed to a better combustion of the premixed charge, which is now richer in larger combustion chamber part. This means that in these cases the natural gas is better used in the combustion process. Obviously the high THC emissions in conventional dual-fuel come from the unburned NG due to the poor flame propagation through the air/NG mixture. When the significant amount of diesel fuel is also premixed, excess air ratio is decreased and the

combustion is more efficient. On the other hand, the reduction in combustion temperature as well as the change from the mixing controlled combustion to the chemically controlled combustion in the last two cases decreases the CO – CO_2 conversion and results in an increase of CO emission. However, the remaining THC and CO emission do not represent a significant problem because they could be reduced with an oxidation catalyst.

If one looks at the CO_2 emission, it can be seen that the highest value is achieved in the premixed case. This means that this injection strategy completely burns the highest amount of fuel, but does not show the highest efficiency due to the large thermal losses. However, lower CO_2 emission in other cases is an indication that there is some amount of fuel that is not efficiently used and converted into the thermal energy.

The main benefit of premixed and split strategies is related to the NO_X emissions. It is shown that NO_X emissions could be significantly reduced by the application of appropriate injection strategy of diesel fuel. It has previously been shown that increased intake temperature increases NO_X emissions, but this measurement shows that the use of intake preheating and appropriate injection strategy could significantly reduce or practically eliminate NO_X emissions. Also, it can be concluded that the majority of NO_X emissions in conventional dual-fuel at low load ($\lambda_{premixed} > 1.8$) comes from the spray region, where the combustion temperature is over 1800 K. In premixed case, diesel fuel is injected early and due to the long ignition delay, it is well premixed with air/NG mixture, which eliminates the spray region and lowers the NO_X emissions accordingly. However, the bulk in-cylinder temperatures in this case are high, because of the combustion timing, which promotes formation of NO_X. Significant reduction in NO_X emissions is noticed in the split injection strategy. There is a majority of the diesel fuel injected in early phase which ensures good premixing and moderate combustion intensity after the start of combustion caused by the second fuel injection. In these cases, the second injection contains a small amount of diesel fuel which practically reduces local in-cylinder temperatures, prolongs ignition delay and causes smooth combustion without high local temperatures which would promote NO_X formation.

If one compares the recalculated results shown in Figure 107 with the European exhaust emission regulations defined for the Heavy-duty vehicles - Euro VI, which is previously mentioned in chapter 4.2, Table 17, it can be seen that the applied split injection strategy satisfies the defined regulation related to the NO_X emissions. Both split cases achieve NO_X emissions below the required value, which equals 0.4 g/kWh.

THC emissions do not satisfy defined regulations (0.13 g/kWh) as well as CO emission (1.5 g/kWh), shown in Figure 108, but they could be reduced by the application of the after treatment system (catalytic converter).

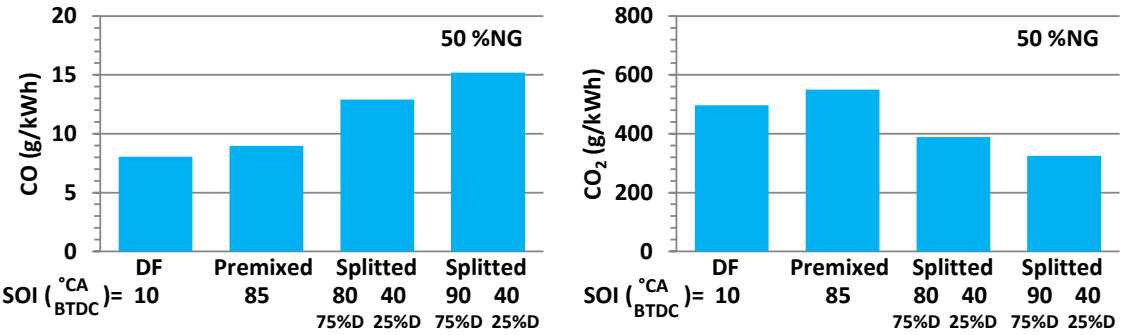

Figure 108. CO and CO_2 emissions in g/kWh

5.4.2 RCCI combustion technology at IMEP = 3 bars

Considering that the experiment performed at IMEP = 4 bars showed great benefits with respect to the exhaust gas emissions in comparison to the conventional dual-fuel operation, the next experiment was performed with the aim of analyzing the RCCI combustion at even the lower load. The operating point defined for that test is described in Table 18.

Table 18. Operating point, low load, RCCI combustion

Operating point	IMEP	3 bars
	n	1600 rpm
Intake conditions	ϑ_{intake}	60 °C
	p_{intake}	ambient
	EGR	0%
Fuels	Z	50% NG
	p_{diesel}	300 bars

In the following results the conventional dual-fuel operation will be compared to the three different split injection strategies. Diesel fuel quantity as well as NG quantity is maintained constant in all the test cases. Considering that two phase injection strategy is optimized with respect to the two criteria, the maximum efficiency and the minimum NO_X emissions, the optimization method will also be explained.

Figures 109 and 110 show measured and recalculated values related to the performance and exhaust gas emissions (THC, NO_X, CO and CO_2). The results follow the same trend that was noticed in the previous experiment at IMEP = 4 bars, which confirms that the split

injection strategy of the diesel fuel is beneficial in dual-fuel engine at low load. Indicated efficiency is maintained or slightly increased in all the cases, while the THC and NO_X emissions are significantly reduced compared to the conventional dual-fuel operation.

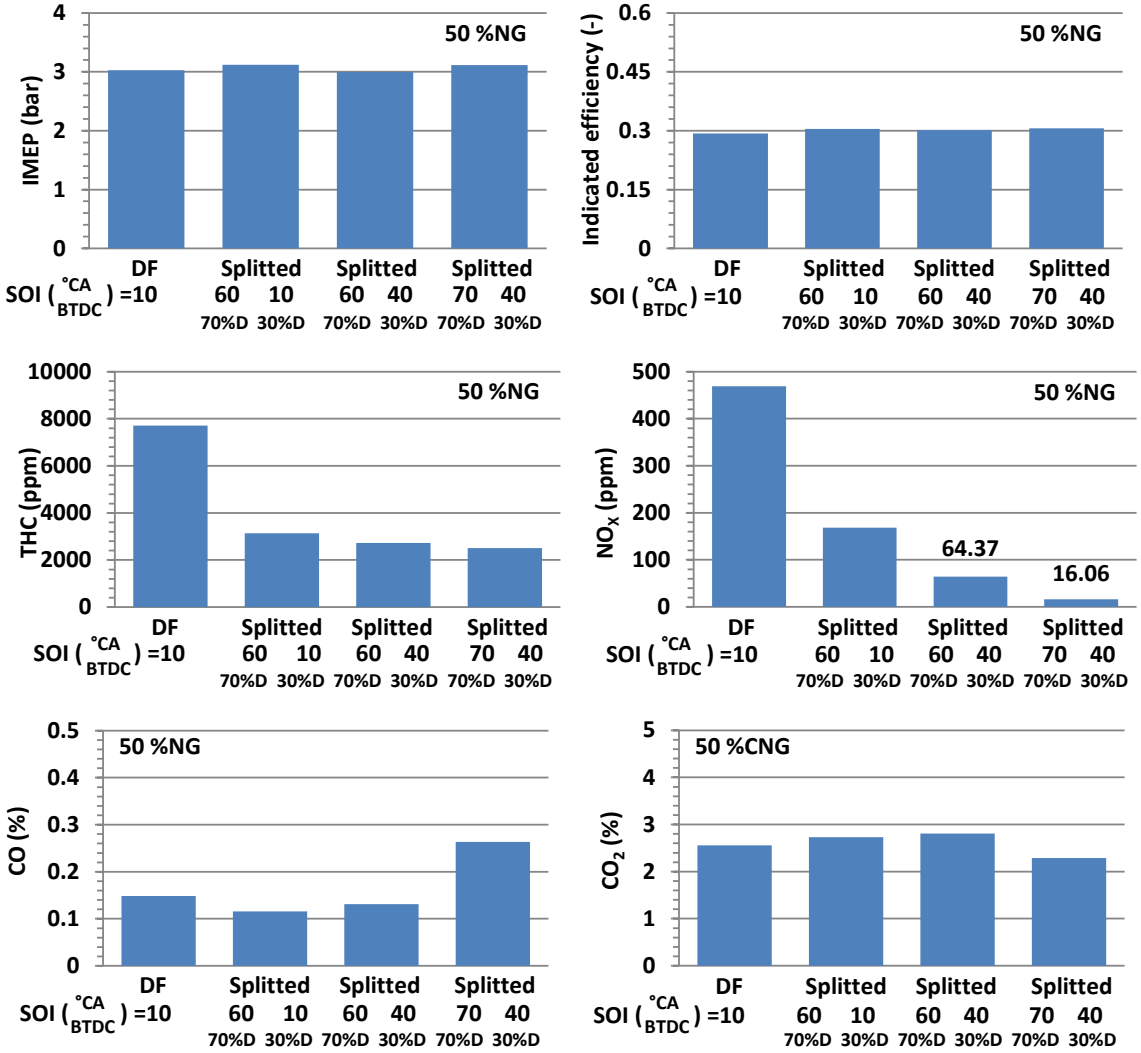

Figure 109. Performance and emissions at IMEP = 3 bar, *Z* = 50%

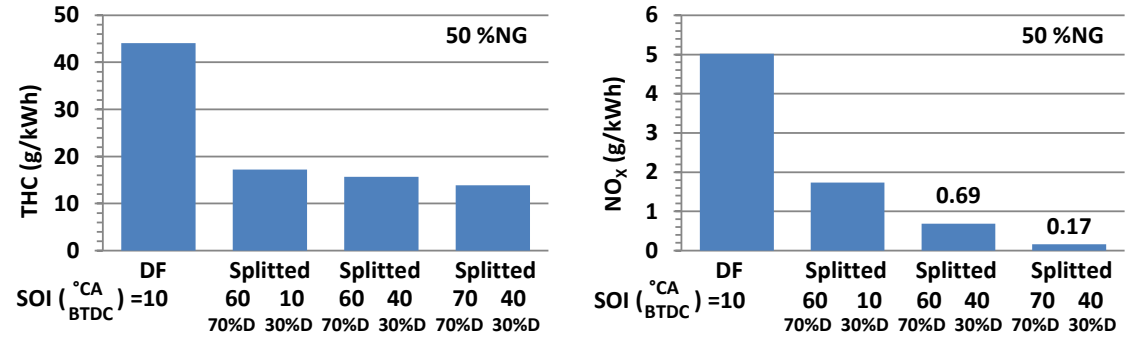

Figure 110. THC and NO_X emissions (g/kWh)

The main challenge in the optimization process of split injection strategy is the determination of the optimum injection phases as well as fuel quantities for each injection.

The optimization process of the above presented measurement results will be explained in the following text.

Once the operating point was selected (IMEP and engine speed), the first step is to find the optimum start of injection point with respect to the highest indicated efficiency in conventional dual-fuel operation. In the case of IMEP = 3 bars this was achieved at SOI =10 °CA BTDC. The next step is to divide the diesel fuel injection into two injections (e.g. 70% first phase and 30% second phase). In this step, the second injection is maintained at SOI = 10 °CA BTDC, while the first injection was advanced to the farthest SOI point which maintained the indicated efficiency and ensured stable engine operation. This was achieved at SOI = 60 °CA BTDC. The next step was advancing the second injection up to the point at which NO_X emissions reached a minimum value, while maintaining the indicated efficiency at similar level and keeping stable engine operation. This was achieved at SOI = 40 °CA BTDC. The last two steps have to be iteratively repeated and injection timings shifted to the more advanced values until the NO_X emissions reach minimum while the indicated efficiency is maintained at similar level.

In addition to the definition of the injection timings, the diesel fuel quantities also had to be optimized. Figure 111 shows the optimization process of diesel fuel quantity in each phase.

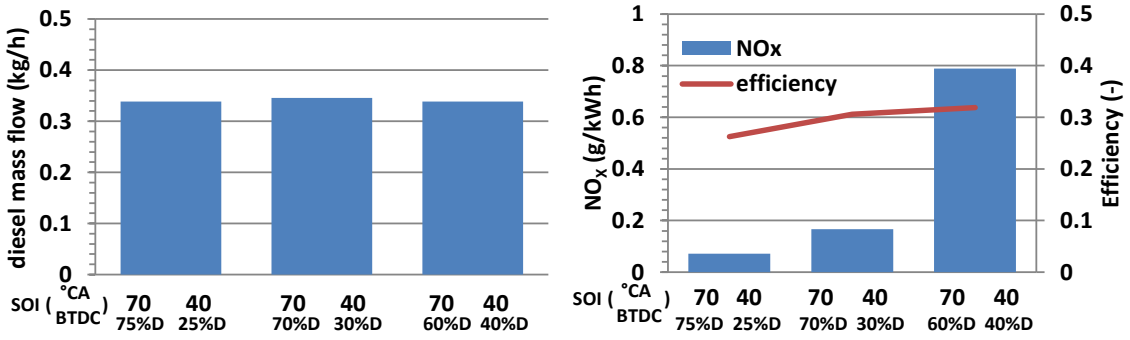

Figure 111. Optimization of diesel fuel quantities

As shown, in this part the total diesel fuel quantity and the SOI points were maintained constant, while the fractions of fuel injected in each phase are varied. Changing the fuel quantities in each injection phase causes changes in indicated efficiency and NO_X emissions. Optimum injection quantities for this operating point are 70% of the total injected diesel fuel in the first phase and the remaining 30% in the second phase. The smaller amount of liquid fuel in the second phase results in significantly reduced indicated efficiency while the higher amount increases NO_X emissions. Excessively large amount of fuel in the second injection promotes NO_X formation in spray region which is previously explained, while too low amount prolongs ignition delay period, lowers peak RoHR and reduces in-cylinder

temperature, which then result in lower indicated efficiency. The RoHR curves and the average in-cylinder temperatures for different fuel quantity distributions between injections are shown on Figure 112.

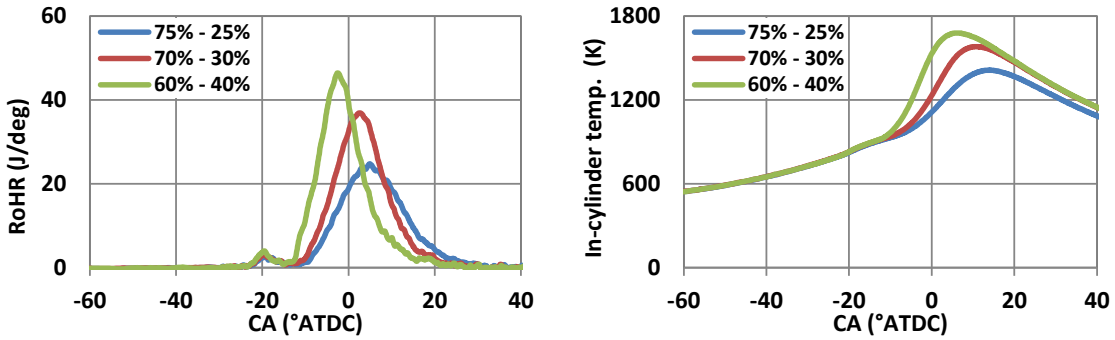

Figure 112. RoHR and average in-cylinder temperature for different fuel quantity distributions

In all three cases some LTHR activity around 20 °CA BTDC can be observed. After the LTHR, the main combustion starts in dependence on fuel quantity in the second injection. The higher amount of fuel in second injection causes earlier main combustion, higher pressure rise rate and higher in-cylinder temperatures, while lower amount of fuel prolongs ignition delay, lowers pressure rise rate and retards combustion phase.

Relationship between NO_X formation and in-cylinder temperature can also be noticed. Case with higher in-cylinder temperatures results in higher NO_X emissions. Although NO_X formation depends on local temperatures, lower average temperature indicates lower local temperatures. However, the low level of NO_X emissions in all the cases is the result of low in-cylinder temperatures that are below 1800 K.

After detail analysis of the presented result, it can be concluded that RCCI combustion strategy is also suitable for a lower load (IMEP = 3 bars) operation. The application of this technology can significantly reduce THC and NO_X emissions, while maintaining or even increasing indicated efficiency.

5.4.3 RCCI combustion technology at various NG mass participation rate

Both of the previous research showed that RCCI combustion technology and split injection strategy, supported by the intake preheating, have great potential for use in dual-fuel engines. Considering that both measurements were performed at Z = 50% NG, the operating points with a higher amount of NG remains to be researched. For that purpose, an additional measurement set was performed with the same operating parameters as previous

measurement, with only a difference in the mass participation ratio which was equal to Z = 50, 70 and 90% NG. The operating parameters used in that test are given in Table 19.

Table 19. Operating parameters, RCCI combustion at various *Z*

Operating point	IMEP	4 bars
	n	1600 rpm
Intake conditions	ϑ_{intake}	60 °C
	p_{intake}	ambient
	EGR	0%
Fuels	Z	50, 70, 90% NG
	p_{diesel}	300 bars

In the following results the main characteristics of the optimized split injection strategy related to performance and emissions will be compared for three different mass participation rates of NG. These optimized split injection strategy results will be compared to the conventional dual-fuel results. Note that conventional dual-fuel was optimized with respect to maximum efficiency, while the split injection strategy was optimized with respect to the two criteria, maximum efficiency and minimum NO_X emissions.

Figure 113 shows the mass flow rates of fuels as well as the injection strategies of diesel fuel. Although the intention was to keep diesel fuel quantity constant in both combustion modes, the small deviations are noticed in test cases, but they do not significantly change the trends of results.

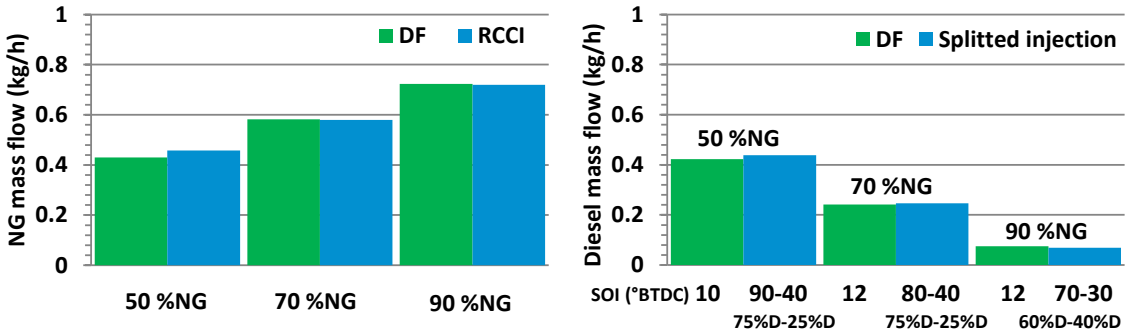

Figure 113. NG and diesel mass flow rates

The obtained IMEP's and indicated efficiencies for both combustion modes (conventional dual-fuel and split strategy) are shown in Figure 114.

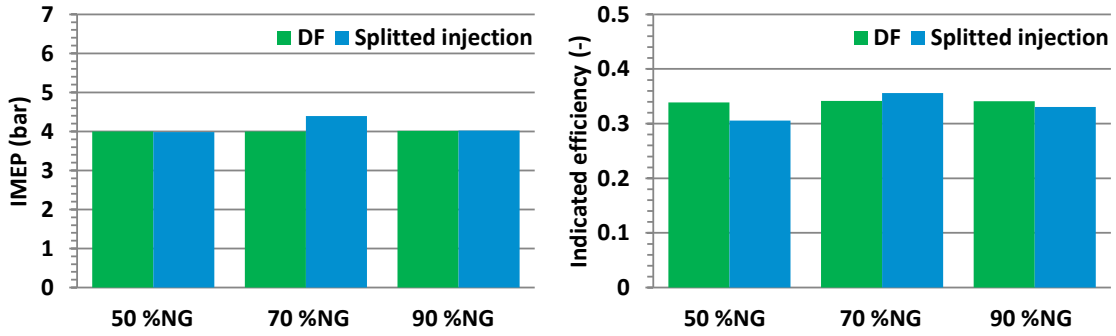

Figure 114. Comparison of IMEP and indicated efficiency – RCCI and conventional DF

As shown, the RCCI combustion technology using the same fuel quantities achieves the same IMEP as conventional dual-fuel. Reached IMEP at 70% NG is even better in RCCI mode than in conventional dual-fuel, which results in higher indicated efficiency. At 50% NG, the RCCI combustion mode results in 3% point reduced indicated efficiency, while in the third case (90% NG), the reduction of indicated efficiency is equal to 1% point and can be practically neglected.

The more significant criteria in the search of the split injection strategy than the indicated efficiency were NO_X emissions. Reduced exhaust gas emissions from RCCI combustion mode (NO_X and THC) that are compared to the emissions from conventional dual-fuel operation are given in Figure 115.

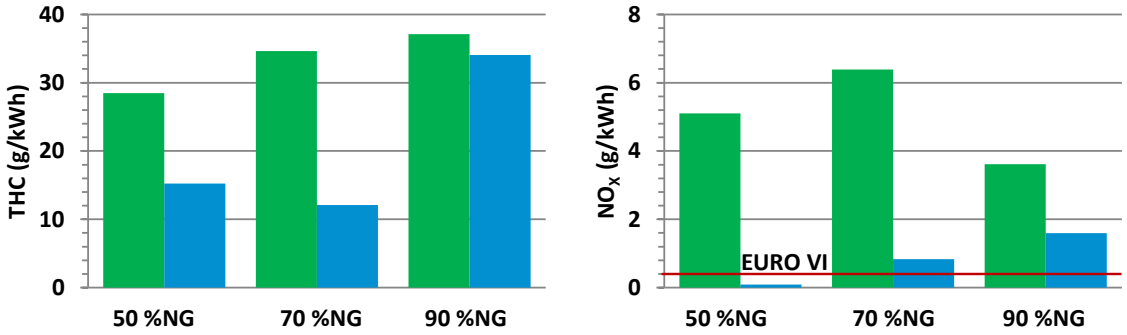

Figure 115. Comparison of THC and NO_X emissions - conventional DF and RCCI

The split injection strategy shows benefits in all three cases, both in THC and NO_X emissions. As expected, the effect of split injection is the lowest in the third case, where the total liquid fuel quantity is the smallest. However, significant improvement of dual-fuel combustion is achieved at 50% NG, where the NO_X emissions meet the EURO VI regulation. At higher natural gas mass participation rate (Z = 70 %), it is not possible to achieve NO_X emissions below permissible limit, but the split injection strategy resulted in significant gain in terms of indicated efficiency, THC and NO_X emissions. It can be concluded that the highest natural gas mass participation rate, which could still meet the NO_X emissions regulation, is

somewhere between Z = 50% and 70%, for the split injection strategy and for the used operating conditions.

5.4.4 RCCI combustion – conclusion

After the extensive analyses of the experimental results, it can be concluded that RCCI combustion technology (i.e. strategy of multiple injections per cycle), supported by the intake preheating provides significant improvements of dual-fuel combustion at low loads.

The mentioned technology enables dual-fuel operation using the significant amount of NG at low load, resulting in very low NO_X emissions, which meet the Heavy-duty European exhaust emissions standard - Euro VI, without any need for after treatment system. Additionally, THC emissions are significantly reduced, but they cannot satisfy EURO VI regulation without the application of after treatment system. The slight disadvantage, compared to conventional dual-fuel operation, is related to the CO emission, but this emission is significantly above the allowed value (1.5 g/kWh) even with the conventional dual-fuel operation and requires after treatment. Indicated efficiency obtained with RCCI combustion technology is practically equivalent to efficiency of the conventional dual-fuel. However, compared to the normal diesel operation, efficiency of any dual-fuel combustion mode is still lower at low load operation.

The conclusion obtained in this work opposes some conclusions of some previous research where it was stated that because of the issues at low load the dual-fuel engine at low loads should operate in normal diesel operation [26] and that higher fractions of diesel fuel at low load will cause higher NO_X emissions [13].

Further research of this injection and combustion strategy should be directed towards the implementation of hot EGR, which could help to easily obtain the increased intake temperature, but on the other side, as seen before, will influence the RoHR and combustion duration. In order to achieve better mixing of the diesel fuel in premixed combustion strategy, higher injection pressures should be tested.

5.5. Influence of EGR on the performance and emissions at high load

Based on the literature review shown in introduction, it was found that the dual-fuel combustion shows some disadvantages at high loads. In this context, preignition and knock occurrence are the main problems, while further disadvantages are related to the slightly increased THC, CO and NO_X emissions.

At the beginning of the research, the initial measurements were performed both at low and high load (Figures 75 - 84) and results did not show any preignition and knock at high load. This phenomenon could be attributed to the two main reasons: first is a relatively low compression ratio (CR = 16) for ambient intake conditions and the second is the use of methane instead of real natural gas. Octane number of pure methane is very high (120), and it is slightly higher than the octane number of natural gas, which except the methane contains ethane, propane and some other components that have lower octane number and therefore lower the octane number of the mixture. This leads to the conclusion that the use of pure methane, instead of natural gas, is not a fully representative solution. Therefore, since the engine in used conditions operated at high load without preignition and knock, these two challenges are removed from research and only the influence of EGR on emissions will be shown.

The disadvantages that are going to be addressed in this part are increased NO_X emission as well as higher THC and CO emission, compared to the normal diesel operation at high load. However, the measured THC and CO emissions at high load are similar to the best achieved with RCCI combustion technology at low load, which means that the after treatment will be required anyway. Therefore, the main focus of this part of research at high load will be on improving the NO_X emissions while maintaining the indicated efficiency.

Although the operating parameters such as inlet air preheating, pilot fuel quantity, EGR and increased intake air pressure are discussed separately in previous investigations, there is a need to combine the operating parameters that could result in different combustion techniques, which could improve performance and exhaust gas emissions. In this context, the effect of cold EGR and different injection strategies on performance and exhaust gas emissions at high load were explored. Considering that the main idea of dual-fuel is to use natural gas as much as possible, and the fact that initial measurements showed that the best indicated efficiency in dual-fuel combustion was obtained by using the highest mass participation rate of NG, the measurements were performed with NG mass participation rate

of 90%. Table 20 shows the operating point and the main intake conditions set for the experiment.

Table 20. Operating parameters at high load

Operating point	IMEP	7 bars
	n	1600 rpm
Intake conditions	ϑ_{intake}	20 °C
	p_{intake}	ambient
	EGR	0%, 5%, 10%, 15%
Fuels	Z	90% NG
	p_{diesel}	300 bars

Considering that a wide range of SOI timings of diesel fuel could be used (Figures 86 and 90), the effect of cold EGR will be compared at two different combustion modes, one with late SOI timing and one with very early SOI timing. The research is performed up to EGR levels of 15%. The higher fractions of EGR resulted in unstable engine operation, which means that 15% of EGR represents the maximum feasible recirculation of the exhaust gas for this intake conditions. Figure 116 shows IMEP and indicated efficiency at both injection strategies for all EGR levels.

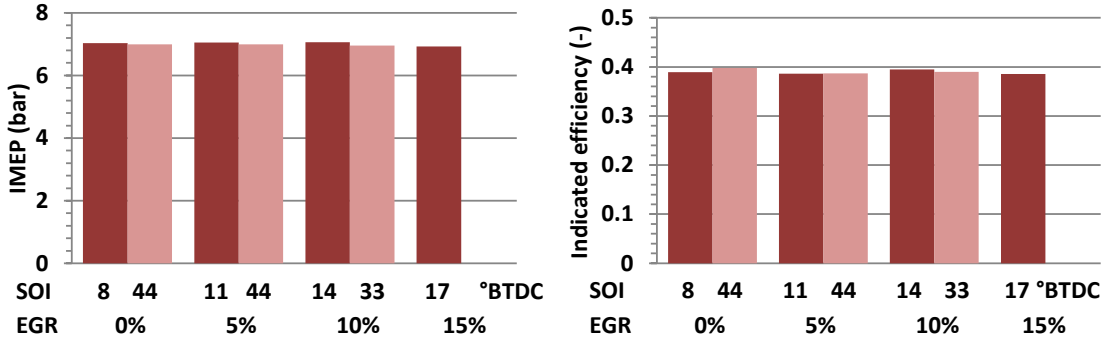

Figure 116. Influence of cold EGR at high load on IMEP and indicated efficiency

In the first case, IMEP = 7 bars is optimized in conventional dual-fuel combustion mode (SOI = 8 °CA BTDC) without exhaust gas recirculation (EGR = 0%). Fuel flows were maintained constant, while SOI timing and EGR percentage were changed through the test cases. At each EGR percentage, the first SOI timing (late) was optimized in conventional dual-fuel mode with respect to the indicated efficiency, while the second SOI timing was sought as earlier as possible, maintaining the stable engine operation. This advanced SOI timing shows benefits related to NO_X emissions. As shown, the indicated efficiency is maintained through all test cases, while the stable engine operation at 15% of EGR and

advanced SOI timing was not possible to achieve it. SOI = 17 °CA BTDC is optimum timing with respect to both criteria, indicated efficiency and NO_X emissions. The advance of the SOI timing decreases IMEP and indicated efficiency accordingly.

As shown in Figure 116, the increase of the EGR percentage slightly influences the indicated efficiency (all efficiencies are within 1.3% point). The main benefits of the EGR and appropriate injection strategy are shown in the Figure 117 that shows the measured exhaust gas emissions.

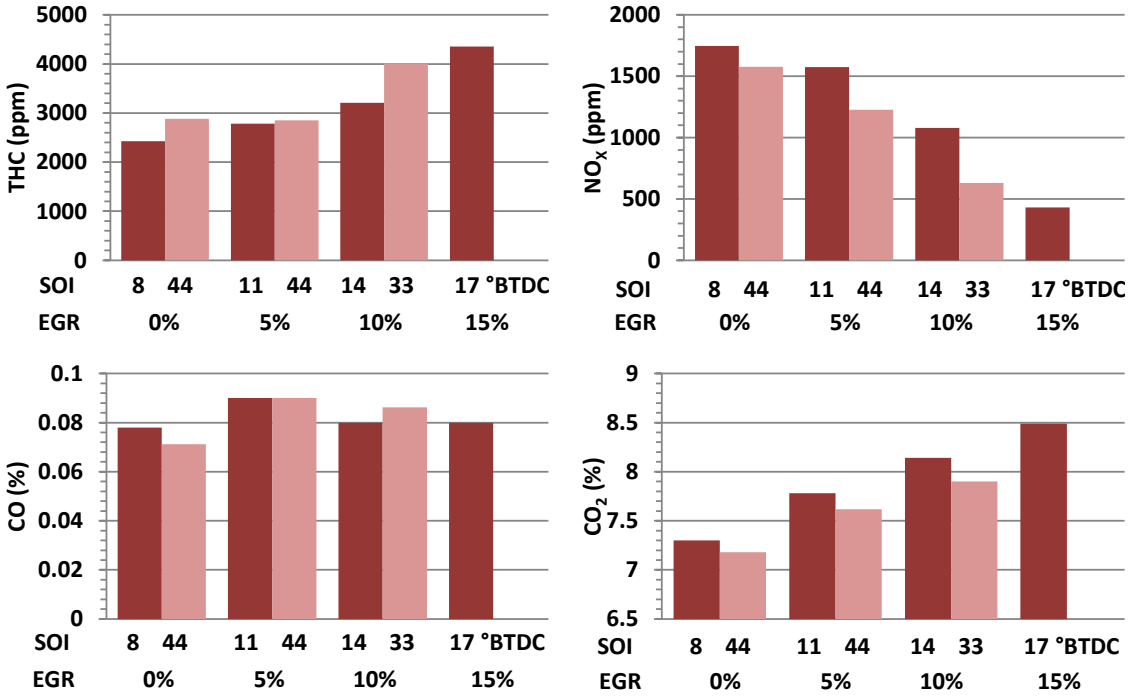

Figure 117. Influence of EGR on exhaust gas emissions at high load

The application of EGR, as expected, has significant influence on NO_X emission, but in this measurement it is shown that EGR in combination with significantly advanced diesel fuel injection can reduce NO_X emissions even more. The additional reduction in the case of 10% EGR with SOI = 33 °CA BTDC is up to 40% compared to the conventional dual-fuel (SOI = 14 °CA BTDC). On the other hand, the increase of EGR percentage increases THC emission and CO emission. However, none of the measured emissions (THC, CO and NO_X) still cannot meet the Heavy-duty European exhaust emissions standard - Euro VI, without an after treatment system. Recalculated values of exhaust gas emissions are given in Figure 118. For satisfying the Euro VI regulation and by using 15% of EGR at SOI = 17 °CA BTDC, after treatment systems should reduce the NO_X emissions for 73%, THC emissions for 86%, and CO emission for 40%.

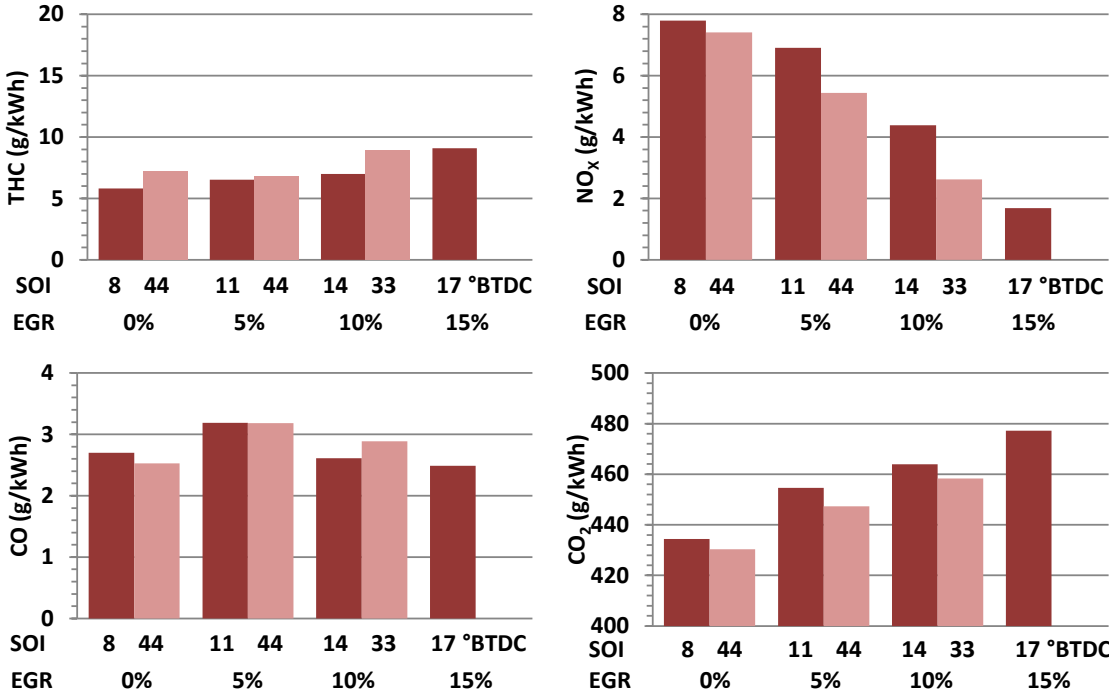

Figure 118. Exhaust gas emissions at high load

The changes in combustion caused by the change in SOI timing and EGR percentage are shown in Figure 119. The higher amount of EGR dilutes the mixture and slows down flame propagation, which results in decreased peak RoHR and decreased pressure rise rate. Slower combustion intensity together with the change in heat capacity decreases peak temperatures and reduces NO_X formation.

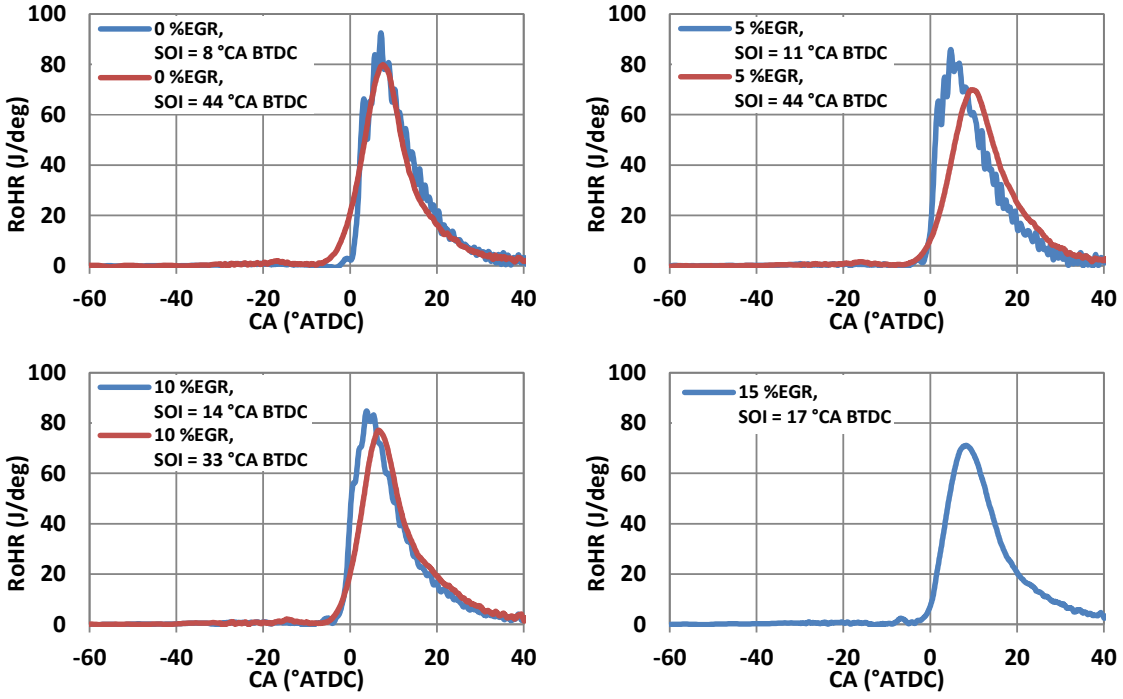

Figure 119. Influence of EGR and injection timing on RoHR profiles

The additional effect of lowering peak RoHR and of smoothing the combustion profile is achieved by advancing the SOI of diesel fuel. Also, advancing the SOI timing results in LTHR around 20 °CA BTDC in three cases (0%, 5% and 10% EGR). This LTHR is not noticed in conventional dual-fuel mode (late injection timing). However, in the last case (15% EGR) some LTHR is also noticed before main combustion, even though the SOI timing is not very early. In this case, SOI is at 17 °CA BTDC, which is somewhere on the boundary between two different combustion modes. Since there is 15% EGR which results with longer ignition delay the LTHR is pronounced. If one compares the trends of injection timings in dependence of the EGR percentage, it can be concluded that the increase in EGR percentage results with advanced optimal SOI timing in conventional dual-fuel, while for combustion with early injection timing, the increase in EGR percentage results with retarded SOI timings. The changes in SOI timing and the application of EGR result with changes in achieved combustion modes. By using EGR and advancing the SOI timing the combustion will gradually change from combustion of diffusion flame followed by the premixed turbulent flame propagation to a premixed chemically controlled combustion of stratified mixture with different levels of stratification.

5.6. Comparison of dual-fuel and SI combustion modes

Since the SI combustion mode was analyzed at wide open throttle and excess air ratios λ = 1, λ = 1.2 and λ = 1.4, only the results of dual-fuel measurement at high load are roughly comparable. The comparison of achieved significant values related to the performance and emissions is shown in Table 21. Results refer to CR = 16 and engine speed n = 1600 rpm.

Table 21. Comparison of SI and dual-fuel combustion modes

	λ (-)	IMEP (bar)	Indicated efficiency (%)	THC (g/kWh)	NO_X (g/kWh)	CO (g/kWh)
SI	1	8.5	37.8	4	15.4	8
SI	1.2	7.8	38.3	3.9	25.5	2.4
SI	1.4	6.6	37.9	13.2	7	5.5
DF (EGR = 0%)	1.4	7	39.7	7.2	7.4	2.5
DF (EGR = 15%)	1.13	6.93	38.5	9.1	1.7	2.5

It can be seen that dual-fuel combustions achieves higher indicated efficiencies, while exhaust gas emissions cannot be classified together. The best comparable cases are SI at λ = 1.4 and dual-fuel without EGR, where the NO_X emissions were similar, while THC and CO emission were lower in dual-fuel combustion. Generally, according to the above mentioned

comparable case, dual-fuel represent better solution for using natural gas, especially at leaner mixtures due to the better combustion quality that is confirmed by higher efficiency and lower THC and CO emissions. In addition, introducing the EGR to dual-fuel mode significantly reduces NO_X emissions, maintaining the indicated efficiency even higher than achieved in the SI combustion mode.

5.7. Dual-fuel conclusions

The experimental investigation of dual-fuel operation is comprised of several different tests, each resulting with some conclusions that are summed up in the following text.

The first set of investigated operating parameters included the injection timings of diesel fuel and natural gas mass participation rate (Z). It was shown that injection timing has significant influence in all of the cases, both on the indicated efficiency and on the exhaust gas emissions. It was also shown that only one SOI timing results with the highest indicated efficiency, while advancing or retarding the injection timing from that optimal timing decreases indicated efficiency or results with excessive pressure rise rate (usually at higher mass fractions of diesel fuel). Only at high load and high NG mass participation rate (Z = 90%), the wide range of SOI timings provided similar (highest) efficiency and therefore enabled optimization with respect to the second parameter, in this case NO_X emission. On the other hand, it was noticed that high NG mass participation rate is not suitable for low and part load operation due to the very high emissions of THC. Moreover, large amount of NG at very low load (IMEP = 2 bars) caused misfires and unstable engine operation. The results showed that at low load dual-fuel engine should operate with larger fractions of diesel fuel, while the large fractions of NG should be used at high loads.

The second experimental test was related to the effects of inlet air preheating and exhaust gas recirculation on the performance and emissions at low load. It was observed that higher intake air temperature improves combustion and results with lower THC and CO emissions, but at the same time significantly increases NO_X emissions.

The standard measure of reducing the NO_X emissions in IC engines is the application of EGR strategy. EGR was implemented on the experimental engine in the form of cold and hot EGR. However, the research showed that the influence of the intake temperature on NO_X formation is significantly higher than the effect of EGR. The cold EGR slightly decreases NO_X formation, but also decreases the indicated efficiency and increases the THC and CO emissions. On the other hand, hot EGR causes higher NO_X formation due to the higher intake temperature, which cannot be removed by the further increase in EGR percentage.

Considering that the highest achievable amount of EGR was 15% and 20% at cold and hot EGR respectively, it is concluded that the NO_X formation cannot be significantly reduced, maintaining the indicated efficiency, only by the application of exhaust gas recirculation.

A further improvement of the dual-fuel operation at low load was sought in a RCCI combustion process. In these measurements, two different injection strategies of diesel fuel were used: early single injection per cycle (injection at 80 °CA BTDC) and two injections per cycle (e.g. 1st injection at 80 °CA BTDC and second injection at 40 °CA BTDC). The measurements were performed at Z = 50% NG, at low loads and intake temperature of 60 °C. The results showed significant improvements in the NO_X emissions that were below the permitted value of EURO VI regulation. Indicated efficiency was maintained at similar level throughout all cases, while the THC emissions were also significantly reduced. This combustion technology showed significant improvement of the dual-fuel combustion and should be in the focus of further investigations.

Final tests were performed at high load, where the cold exhaust gas recirculation was used to reduce the NO_X emission. In this measurement it was shown that EGR in the combination with very early pilot fuel injection can achieve higher reduction of NO_X emission than conventional dual-fuel operation with only the addition of EGR. The reduction of NO_X emission in this case (SOI = 33 °CA BTDC) reaches the value of up to 40% compared to the conventional dual-fuel operation (SOI = 14 °CA BTDC). On the other hand, the increase of EGR increases THC emission and CO emission. However, it has to be noted that none of the measured emissions (THC, CO and NO_X) would not meet the Euro VI standard at high load, without the application of an after treatment system.

Finally, it can be concluded that the appropriate combination of operating parameters, which have partial effect on dual-fuel combustion, can result in significant reductions in individual emissions of exhaust gas, e.g. intake temperature and split injection of diesel fuel can significantly reduce NO_X emissions.

In addition to the effects on performance and emissions, it was also shown, that by using the fully flexible fuel injection systems for diesel fuel and NG, and by using the exhaust gas recirculation and conditioning of the intake charge, it is possible to achieve diffusion flame combustion, premixed flame propagation, and premixed chemically controlled combustion of homogeneous or stratified mixture in dual-fuel engine.

6. General Conclusions

The research presented in this thesis shows experimental research of the influence of operating parameters on combustion, efficiency and exhaust gas emissions in conventional diesel/NG dual-fuel engine, and compares the results with the standard combustion mode (SI) running with pure NG on the same engine.

Dual-fuel engine is an engine that operates with NG and diesel fuel simultaneously. NG is used as the primary source of energy and it is ignited by a certain amount of diesel fuel directly injected into the combustion chamber. The value that defines the relative amount of natural gas in the total fuel mixture is usually a diesel substitution ratio [10] or a NG mass participation rate [25], [26]. The combustion process in conventional dual-fuel engine has both CI engine and SI engine characteristics, which means that the combustion process is a blend of mixing-controlled combustion and flame propagation process.

Extensive literature review showed that dual-fuel combustion have some benefits related to the NO_X and soot emissions [13], [26], [31], [38]-[40], but it also showed some disadvantages related to the increased HC and CO emissions, to reduced efficiency at low loads [26], [31], [38], [40], [41] and to pre-ignition and knock occurrence at high loads [10], [42]. The noted disadvantages were the main motivation for the preparation of the experimental setup and for further research of dual-fuel combustion.

Through the research, the existing experimental setup was upgraded with the installation of a common rail fuel supply system, the addition of a fuel supply system for gaseous fuels and the development of software for the management, control and monitoring of the fuel injection parameters. The installation of a fully flexible injection system for both fuels enabled investigation of the influence of different injection parameters, which in combination with other changeable operating parameters results in different combustion modes that provide improvement in the dual-fuel engine performance and emissions.

6.1. The main achievements

In the first phase of the research the numerical investigation of the influence of the injection timing of the gaseous fuel on the fuel slip through the cylinder to the exhaust pipe due to the positive valve overlap, which is the characteristic of the used diesel engine, was

performed. In this research, it was established that the fuel slip from cylinder due to valve overlap is the highest at low engine speed (1000 rpm) and equals 0.6% of the injected fuel in the case of naturally aspirated engine, and 2.3% at intake pressure of 2.2 bars. It is also shown that at higher engine speeds (2000 rpm, 3000 rpm) the fuel slip becomes very low and can be neglected. In comparison of different injection timings, research shows that the appropriate intermittent injection timing can reduce fuel slip up to 43% compared to the continuous injection at defined excess air ratio, while inappropriate intermittent injection timing can result with an increase of fuel slip up to 62% in charged conditions, which means that optimized intermittent injection can improve thermal efficiency of the engine as well as exhaust gas emissions. In addition, the research showed that the fuel slip is more dependent on the end of injection timing than on the start of injection timing, which means that injection duration does not have any influence if the fuel is injected before the critical point after which the fuel slip starts to increase.

The above listed conclusions were applied to the injection strategy of the experimental setup. The obtained results indicate that the fuel slip at engine speed of 1600 rpm and ambient intake pressure are 0.12% and therefore does not have significant influence on the total exhaust gas emissions, i.e. the influence of fuel slip in the performed measurement of THC could be neglected. The results also indicate that, this influence should be taken into account in charged conditions.

In the second phase, the effects of compression ratio, excess air ratio and engine speed on the performance and emissions of natural gas fuelled spark ignition engine are examined. The main objective of the work was to show the advantages and disadvantages of using different compression ratios, especially higher compression ratios, similar to diesel engine and to give some benchmark results of conventional natural gas engine.

The performed research showed that the indicated efficiency of the spark ignited NG fuelled engine is highly influenced by the CR. The main improvement in indicated efficiency is achieved by increasing the CR from 12 to 16, independently of excess air ratio, while the further increase of the compression ratio leads to the decrease of indicated efficiency in most of cases because of the higher thermal losses and higher influence of crevices. The highest indicated efficiency at CR = 16 and stoichiometric mixture equals 36.2%, 37.8% and 37.3% at 1200 rpm, 1600 rpm and 2000 rpm, respectively, while at leaner mixture (λ = 1.2) equals 37.9%, 38.3% and 38.3% at 1200 rpm, 1600 rpm and 2000 rpm, respectively.

Analysis of the results showed that CR also has significant influence on THC emission that is the highest at lean mixture (λ = 1.4) due to the slower in-cylinder flame propagation, lower temperature and probably flame quenching. The increase of compression ratio also increases THC emission which is caused by higher influence of crevices. The achieved THC emissions at CR = 16 and 1600 rpm equal 4 g/kWh, 3.8 g/kWh and 13.2 g/kWh at λ = 1, λ = 1.2 and λ = 1.4, respectively.

CO emission is also slightly influenced by CR (the increase from CR = 12 to CR = 16 results in decrease of CO emission, while further increase to CR = 18 slightly increases CO), but the dominant factor in CO emissions is excess air ratio. The change of the mixture from stoichiometric to lean, results in significant decrease of CO emissions.

The emissions of NO_X are also significantly influenced by excess air ratio and much less by CR, except for λ = 1.2 where CR has strong influence on NO_X. In lean operation the NO_X emission is not exclusively correlated to peak cylinder temperatures, but depends on full combustion profiles. For operation without catalyst the excess air ratio should be even higher than λ = 1.4, which is not possible with this type of ignition system. The measured values of NO_X emissions at CR = 16 and 1600 rpm were 15 g/kWh, 25 g/kWh and 7 g/kWh at λ = 1, λ = 1.2 and λ = 1.4, respectively.

The test cases in SI mode showed that the favourable CR is much higher than the usual CR of SI engines and is equal to CR = 16. Considering that the CR = 16 provides the best results with respect to the performance and emissions and that state of the art CI diesel engines for vehicles operate at compression ratio close to 16 (mostly with charging), the research of dual-fuel combustion was performed at CR = 16.

In the last phase of the research, the experimental investigation of the influence of operating parameters on combustion, efficiency and exhaust gas emissions in conventional dual-fuel engine was performed. After the initial measurements, which confirmed all of the expected drawbacks (except pre-ignition and knock at high loads), the main influences of dual-fuel operating parameters on combustion, efficiency and exhaust gas emissions were investigated.

The first set of investigated operating parameters included the injection timings of diesel fuel and natural gas mass participation rate (Z). The results showed:

- Injection timing of diesel fuel has significant influence on the efficiency and on the exhaust gas emissions.
- The flexibility in injection timing exist only at high load and high natural gas mass participation rate (Z = 90%), where the optimization with respect to the two criteria

(indicated efficiency and NO_X emission) is enabled. In this case, the highest indicated efficiency is retained in a wide range of injection timing (SOI = 5 °CA BTDC – SOI = 44 °CA BTDC), while NO_X emissions depend on injection timing. The lowest achieved NO_X emissions are around 6 g/kWh.

- High natural gas mass participation rates are not suitable for low and part load operation due to the very high emissions of THC, which at 50% NG mass participation rate reaches 10000 ppm.
- The maximum achieved efficiencies in dual-fuel combustion mode at low loads and at 50% NG mass participation rate reach 25% and 34% at IMEP = 2 bars and IMEP = 4 bars, respectively.
- The maximum achieved efficiency at high load and at 90% NG mass participation rate reaches 39%.

The second experimental test was related to the effects of inlet air preheating and exhaust gas recirculation on the performance and emissions at low load. The main conclusions derived from this study are:

- Increased intake air temperature improves combustion and results with lower THC and CO emissions, but with the penalty in NO_X emissions.
- The influence of the intake temperature on NO_X formation is significantly higher than the effect of EGR.
- The cold EGR slightly decreases NO_X formation, but also decreases the indicated efficiency and increases the THC and CO emissions.
- Hot EGR causes higher NO_X formation due to the higher intake temperature, which cannot be removed by the further increase in EGR percentage.
- The highest achievable amount of EGR in researched test cases was 15% and 20% at cold and hot EGR, respectively.
- NO_X formation cannot be significantly reduced by the application of EGR if the indicated efficiency should be maintained.

In a research of RCCI combustion mode, two different injection strategies of diesel fuel were used: early single injection per cycle (injection at 80 °CA BTDC) and two injections per cycle (e.g. 1st injection at 80 °CA BTDC and second injection at 40 °CA BTDC). The measurements were performed at Z = 50% NG, at low loads and intake temperature of 60 °C. The results showed:

- Significant improvements in the NO_X emissions that were below the permitted value of EURO VI regulation (e.g. at IMEP = 4 bars, achieved NO_X emissions were 13 ppm, or 0.09 g/kWh)
- Indicated efficiency in RCCI was maintained at similar level as in conventional dual-fuel combustion mode (> 30 %)
- THC emissions were significantly reduced (e.g. from 44 g/kWh to 14 g/kWh at IMEP = 3 bars, which means reduction of 68%)
- RCCI combustion technology enables combustion of higher amounts of NG at low load and shows significant improvement of the dual-fuel combustion

It should be mentioned that two injections per cycle represents the first step in the improvement process of dual-fuel combustion using the splitted injection strategy. There is a space for further splitting of diesel fuel quantity on 3 or more injections per cycle which could ensure even better mixing of diesel fuel with air/NG mixture and improve combustion efficiency.

At high load, the main challenge was related to the decrease of NO_X emission. Therefore, the cold exhaust gas recirculation was used to reduce NO_X formation. The main conclusions of this study are as follows:

- EGR in the combination with very early pilot fuel injection can achieve reduction of NO_X emission up to 40% compared to the conventional dual-fuel operation with only the addition of EGR.
- The increase of EGR increases THC and CO emission.
- At high load, none of the measured emissions (THC, CO and NO_X) would not meet the Euro VI standard at high load, without an after treatment system.

- Comparing the dual-fuel and SI combustion mode at high load, dual-fuel represent better solution for using NG, especially at leaner mixtures due to the better combustion quality that is confirmed by higher efficiency and lower THC and CO emissions. In addition, introducing the EGR to dual-fuel mode significantly reduces NO_X emissions, maintaining the indicated efficiency even higher than achieved in the SI combustion mode.

Finally, it can be concluded that the appropriate combination of operating parameters, which have partial effect on dual-fuel combustion, can result in significant reductions in

individual emissions of exhaust gas, e.g. intake temperature and split injection of diesel fuel can significantly reduce NO_X emissions.

In addition to the effects on performance and emissions, it was also shown, that by using the fully flexible fuel injection systems for diesel fuel and NG, and by using the EGR and conditioning of the intake charge, it is possible to achieve diffusion flame combustion, premixed flame propagation, and premixed chemically controlled combustion of homogeneous or stratified mixture in dual-fuel engine.

6.2. Original scientific contribution

The performed research on dual-fuel engine fulfilled all previously defined objectives and confirmed both stated hypotheses:

- By using the fully flexible fuel injection systems for diesel fuel and NG, and EGR, it was possible to achieve diffusion flame combustion, premixed flame propagation, and premixed chemically controlled combustion of homogeneous or stratified mixture in dual-fuel engine.
- By using the appropriate mode of combustion, it was possible to achieve high efficiency and low harmful exhaust gases emissions in the dual-fuel engine operation both at low and high loads.

The presented research explains the unknowns that are related to the different dual-fuel combustion technologies (conventional dual-fuel and RCCI) and therefore provides the knowledge that will help in further development of dual-fuel engines. From this research the following original scientific contributions are achieved:

- The recommendations for selection of injection strategies and of operating parameters in dependence of expected operating conditions, which will enable highest engine efficiency with as low as possible exhaust gas emissions (especially NO_X emissions).
- The definition of influences of changes in diesel fuel mass participation rates, injection timings, air excess ratios and EGR percentages on changes in achieved combustion modes.
- The explanation of the impact of the achieved combustion mode, on the obtained efficiency and exhaust gas emissions.

6.3. Possible directions of further work

Although the achieved RCCI combustion technology, assisted by the intake air preheating shows significant benefits related to THC and NO_X emissions at low loads, as well as the cold exhaust gas recirculation on the NO_X emission at high load, there are still some disadvantages that should be further investigated.

The indicated efficiency at low load is still lower compared to the normal diesel operation, which means that further investigations should be in the direction of improving the combustion efficiency and further increase of the indicated efficiency. One of the ways of further research of RCCI combustion should be further splitting of diesel fuel quantity into smaller quantities (diesel-like multiple injection strategy), which could lead to improved combustion efficiency and provide benefits in THC emissions as well as in CO emissions. As shown, these two emissions still cannot meet the EURO VI regulation without an after treatment system.

At high load, the influence of the increased intake pressure in combination with cold EGR should be investigated. The main focus should be on reducing the NO_X emissions which are in these cases higher than in normal diesel operation.

Additionally, since all investigations and conclusion of this work are derived from the measurements performed with pure methane from the pressure cylinder the further work should investigate the influence of NG composition on performance, especially at high load and increased intake pressure. The changes in composition of NG, which results in different octane rating, may change the engine performance as well as the range of its application.

Bibliography

[1] Population Matters, https://www.populationmatters.org/the-issue/overview/facts/?gclid=Cj0KCQjwuMrXBRC_ARIsALWZrIjcIpxV1U2vfwddlCgQoXo6_oSjxHHsuK_3n3sQzS2LfLNi8wDsDgEaAtNFEALw_wcB, available on date 8.5.2018

[2] Korakianitis, T., Namasivayam, A.M. and Crookes, R.J., Natural-gas fueled spark-ignition (SI) and compression-ignition (CI) engine performance and emissions, Progress in Energy Combustion and Science, Vol. 37, pp. 89-112, 2011

[3] Kozarac, D., Taritas, I., Sjeric, M., Krajnovic, J. et al., "The Optimization of the Dual Fuel Engine Injection Parameters by Using a Newly Developed Quasi-Dimensional Cycle Simulation Combustion Model," SAE Technical Paper 2018-01-0261, 2018

[4] Ilinčić P, Multi zone simulation model for HCCI engine with a segregated solver, Doctoral thesis, Faculty of mechanical engineering and naval architecture, Zagreb, 2015

[5] Directive 2005/55/EC of the European Parliament and of the council of 28 September 2005 on the approximation of the laws of the Member States relating to the measures to be taken against the emission of gaseous and particulate pollutants from compression-ignition engines for use in vehicles, and the emission of gaseous pollutants from positive-ignition engines fuelled with natural gas or liquefied petroleum gas for use in vehicles

[6] Regulation (EC) No 595/2009 of the European Parliament and of the council of 18 June 2009 on type-approval of motor vehicles and engines with respect to emissions from heavy duty vehicles (Euro VI) and on access to vehicle repair and maintenance information and amending Regulation (EC) No 715/2007 and Directive 2007/46/EC and repealing Directives 80/1269/EEC, 2005/55/EC and 2005/78/EC

[7] World Energy Outlook 2010, IEA Publications, ISBN: 978-92-64-08624-1, Pariz, 2010.

[8] BiogasWorld, https://www.biogasworld.com/news/cng-perspectives-as-an-alternative-fuel-for-transportation/, available on date 10.5.2018

[9] Serrano, D., Bertrand, L., Exploring the Potential of Dual Fuel Diesel-CNG Combustion for Passenger Car Engine, Proceedings of the FISITA 2012 World Congress

[10] Konigsson, F., Advancing the limits of Dual Fuel Combustion, Licenciate thesis, Royal Institute of Technology Stockholm, 2012

[11] Shodhganga : a reservoir of Indian theses, http://shodhganga.inflibnet.ac.in/bitstream/10603/40880/13/13_chapter3.pdf, available on date 22.5.2018

[12] Isidoro Martinez, Fuel Properties, http://webserver.dmt.upm.es/~isidoro/bk3/c15/Fuel%20properties.pdf, available on date 22.5.2018

[13] Abd Alla, G. H., Soliman, H. A., Badr, O. A. and Abd Rabbo, M. F., Effect of Pilot Fuel Quantity on the Performance of a Dual Fuel Engine, Energy Conversion & Management, Vol. 41, No. 6, pp 559-572, 2000, https://doi.org/10.1016/S0196-8904(99)00124-7
[14] Union Gas, https://www.uniongas.com/about-us/about-natural-gas/chemical-composition-of-natural-gas, available on date 23.5.2018
[15] Kozarac, D. Višezonski model izgaranja u HCCI motoru primjenom kemijske kinetike, Doctoral thesis, Faculty of mechanical engineering and naval architecture, 2008
[16] František, P. Dynamic Behaviour of NOx Storage Catalysts and Combined Exhaust Gas Aftertreatment Systems, Annotation of PhD Thesis, Prague, November 2011
[17] Green, R., and Pearce, S. Alternative transport fuels. Energy World, Oct 1994, pp 8-11.
[18] Pirker, G., Wimmer, A., Sustainable power generation with large gas engines. Energy Conversion and Management, Vol.149, 2017, pp. 1048-1065
[19] Dahodwala, M., Joshi, S., Koehler, E., and Franke, M., "Investigation of Diesel and CNG Combustion in a Dual Fuel Regime and as an Enabler to Achieve RCCI Combustion," SAE Technical Paper 2014-01-1308, 2014
[20] May, A.A., Nguyen, N.T., Presto, A.A., Gordon, T.D., Lipsky, E.M., Karve, M., et al., 2014a.Gas- and particle-phase primary emissions from in-use, on-road gasoline and diesel vehicles. Atmos. Environ. 88, 247–260.
[21] Sandhu, G.S., Frey, H.C., Bartelt-Hunt, S., Jones, E., 2016. Real-world activity, fuel use, and emissions of diesel side-loader refuse trucks. Atmos. Environ. 129, 98–104.
[22] Yang, L., Franco, V., Campestrini, A., German, J., Mock, P., 2015a. NOx control technologies for Euro 6 Diesel passenger cars. Market penetration and experimental performance assessment. International Council on Clean Transportation Europe (ICCT).
[23] Pischinger, F., Lepperhoff, G., Houben, M., Soot Formation and Oxidation in Diesel Engines. In: Bockhorn H. (eds) Soot Formation in Combustion. Springer Series in Chemical Physics, vol 59. Springer, Berlin, Heidelberg, 1994
[24] Jong Hun Kim, Man Young Kim & Hyong Gon Kim, NO_2-Assisted Soot Regeneration Behavior in a Diesel Particulate Filter with Heavy-Duty Diesel Exhaust Gases, Numerical Heat Transfer, Part A: Applications, 58:9, 725-739, 2010, DOI: 10.1080/10407782.2010.523293
[25] Papagiannakis, R. G. and Hountalas, D. T., Combustion and Exhaust Emission Characteristics of a Dual Fuel Compression Ignition Engine Operated with Pilot Diesel Fuel and Natural Gas, Energy Conversion and Management, Vol. 45, No. 18-19, pp 2971-2987, 2004, https://doi.org/10.1016/j.enconman.2004.01.013
[26] Lounici, M.S., Loubar, K., Tarabet, L., Balistrou, M., Niculescu, D.C., and Tazerout M.: Towards improvement of natural gas-diesel dual fuel mode: An experimental investigation on performance and exhaust emission. Energy Vol. 64, pp. 200-211, 2014
[27] Selim, MYE. Sensitivity of dual fuel engine combustion and knocking limits to gaseous fuel composition. Energy Conversion and Management, 45(3):411–25, 2004
[28] Sahoo, B.B., Sahoo, N., Saha, U.K., Effects of engine parameters and type of gaseous fuel on the performance of dual-fuel gas diesel engines – A critical review. Renewable and Sustainable Energy Reviews Vol. 13, pp. 1151-1184, 2008

[29] Nwafor OMI. Knock characteristics of dual-fuel combustion in diesel engines using natural gas as primary fuel. Sadhana [Internet]. Springer India; 2002 Jun [cited 2018 May 15];27(3):375–82. Available from: http://link.springer.com/10.1007/BF02703658
[30] Taritaš, I., et al., The Effect of Operating Parameters on Dual Fuel Engine Performance and Emissions – An Overview. Trans FAMENA [Internet]. 2017 Apr 26;41(1):1–14.
[31] Shah, A., Thipse, S.S., Tyagi, A., Rairikar, S.D., Kavthekar, K.P., Marathe, N.V., Literature Review and Simulation of Dual Fuel Diesel-CNG Engines, SAE International, Symposium on International Automotive Tehnology, 2011-26-0001, India, 2011
[32] Taritaš, I., The development of a quasi-dimensional model for dual fuel combustion in engine cycle-simulation, Doctoral thesis, Faculty of Mechanical Engineering and Naval Architecture, Zagreb, 2018
[33] Westport, http://www.westport.com/is/core-Technologies/combustion/hpdi; available on date 4.11.2015
[34] YANMAR Technical Review, https://www.yanmar.com/global/technology/technical_review/2015/0727_2.html, available on date 18.5.2018
[35] IGS CNG services, https://www.igscngservices.com/cng-101/, available on date 21.5.2018
[36] NGV knowledgebase, http://www.iangv.org/current-ngv-stats/, available on date 21.5.2018
[37] Nat, G., CNG solutions, http://www.nat-g.com/why-cng/bi-fuel-dual-fuel-dedicated/, available on date 21.5.2018
[38] Mustafi, N.N., Raine, R.R., Verhelst, S., (2013), Combustion and emission characteristics of a dual fuel engine operated on alternative gaseous fuels, Fuel, 109, pp. 669-678
[39] Gharehgani, A., Mirsalim, S.M., Jazayeri, S.A., (2012), Numerical and Experimental Investigation of Combustion and Knock in a Dual Fuel Gas/Diesel Compression Ignition Engine, Journal of Combustion, 2012
[40] Papagiannakis, R.G., Hountalas, D.T. and Kotsiopoulos, P.N., (2005), Experimental and Theoretical Analysis of the Combustion and Pollutants Formation Mechanisms in Dual Fuel DI Diesel Engines, SAE Technical Paper 2005-01-1726.
[41] Papagiannakis, R.G., Rakopoulos, C.D., Hountalas, D.T. and Rakopoulos, D.C., (2010), Emission characteristics of high speed, dual fuel, compression ignition engine operating in a wide range of natural gas/diesel fuel proportions, Energy, 89, pp. 1397-1406.
[42] Gharehgani, A., Mirsalim, S.M., Jazayeri, S.A., (2012), Numerical and Experimental Investigation of Combustion and Knock in a Dual Fuel Gas/Diesel Compression Ignition Engine, Journal of Combustion, 2012
[43] Dishy, A., Takahashi, Y. Iwashiro, Y., Nakayama, S., Kihara, R., Saito T., Controlling Combustion and Exhaust Emissions in a Direct-Injection Diesel Engine Dual-Fueled with Natural Gas. SAE Technical Paper 952439, 1995
[44] Zhang, Q., Li, N., Li, M.: Combustion and emission characteristics of an electronically-controlled common-rail dual-fuel engine. Journal of the Energy Institute, 2015

[45] Yang, B., Wei, X., Xi ,C., Liu, Y., Zeng, K., Lai, M-C., Parametric investigation of natural gas port injection and diesel pilot injection on the combustion and emissions of a turbocharged common rail dual-fuel engine at low load. Applied Energy, Vol. 143, pp. 130-137, 2015

[46] Abd Alla, G., Soliman, H., Badr, O., Abd Rabbo, M., Effect of injection timing on the performance of a dual fuel engine. Energy Convers Manag [Internet]. Pergamon; 2002 Jan 1 [cited 2018 May 21];43(2):269–77

[47] Shu, J., Fu, J., Liu, J., Zhang, L., Zhao, Z., Experimental and computational study on the effects of injection timing on thermodynamics, combustion and emission characteristics of a natural gas (NG)-diesel dual fuel engine at low speed and low load. Energy Convers Manag [Internet]. Pergamon; 2018 Mar 15 [cited 2018 May 21];160:426–38.

[48] Selim, M. Y. E., Pressure-time Characteristics in Diesel Engine Fuelled with Natural Gas, Renewable Energy, Vol. 22, No. 4, pp 473-489, 2001, https://doi.org/10.1016/S0960-1481(00)00115-4

[49] Gharehghani, A., Mirsalim, S.M., Jazayeri, S.A., Numerical and Experimental Investigation of Combustion and Knock in a Dual Fuel Gas/Diesel Compression Ignition Engine. Journal of Combustion, Vol. 2012, 2012

[50] Papagiannakis, R.G., Study of air inlet preheating and EGR impacts for improving the operation of compression ignition engine running under dual fuel mode. Energy Conversion and Management, Vol. 68, pp. 40-53, 2013

[51] Daisho, Y., Yaeo, T., Koseki, T., Saito, T., Kihara, R., Quiros, E.N., Combustion and Exhaust Emissions in a Direct-Injection Diesel Engine Dual-Fueled with Natural Gas. SAE Technical Paper SAE 950465, 1995

[52] Cameretti, M. C., Ciaravola, U., Tuccillo, R., De Simio, L. and Iannaccone, S., A Numerical and Experimental Study of Dual Fuel Diesel Engine for Different Injection Timings, Applied Thermal Engineering, Vol. 101, pp 630-638, 2016 , https://doi.org/10.1016/j.applthermaleng.2015.12.071

[53] Scott Guerry, E., Mostafa, S. R., Kalyan, K. S., Sundar, R. K. and Sohail, A., Injection Timing Effects on Partially Premixed Diesel-methane Dual Fuel Low Temperature Combustion, Applied Energy, Vol. 162, pp 99-113, ISSN 0306-2619, 2016, https://doi.org/10.1016/j.apenergy.2015.10.085

[54] AVL Boost™ v2013, Users Guide

[55] Hatz Diesel, http://www.hatz-diesel.com/en/products/diesel-engines/d-series/1d81/, available on date 6.2.2018.

[56] Hatz Diesel, http://www.hatz-diesel.com/fileadmin/tx_hatzproducts/ebook_BA_SUPRA_CARB_EPAIV_11.pdf, available on date 6.2.2018.

[57] Prasad, B.V.V.S.U., Sharma, C.S., Anand, T.N.C., Ravikrishna, R.V., High swirl-inducing piston bowls in small diesel engines for emission reduction. Appl Energy [Internet]. Elsevier; 2011 Jul 1 [cited 2018 Mar 8];88(7):2355–67.

[58] Arcoumannis, C., Bicen, A.F., Whitelaw, J.H., Squish and swirl–squish interaction in motored model engines. ASME J Fluid Mech 1993:105–12.

[59] Arcoumannis, C., Bicen, A..F, Vafidis, C., Whitelaw JH. Three-dimensional flow field in four-stroke model engines. SAE Paper 841360
[60] Mahalec, I., Lulić, Z., Kozarac, D., Motori s unutarnjim izgaranjem; Internal book, FSB, 2012
[61] Heywood, J.B., International combustion engine fundamentals. New York: McGraw-Hill Book Company; 1988.
[62] Hatz Diesel, http://www.hatz-diesel.com/fileadmin/user_upload/hatz-diesel.com/ersatzteillisten/Archiv/1D41-90/EL_1D_43420026.pdf, [Internet], available on date 9.3.2018.
[63] AVL pressure sensors for combustion analysis, Product Catalog – Edition 2011, available via https://shop.avl.com
[64] Hatz Diesel, Workshop manual 1D.., http://vi.dzima.com/wp-content/uploads/2015/01/Hatz-1D-Repair-manual.pdf
[65] Bernecic, D., Martinović, D., Tudor, M., The effect of multiple fuel injection on combustion profiles in slow-speed two-stroke marine diesel engines. Transactions of FAMENA. 36. 49-62. 2012.
[66] Anand, K., Reitz, R.D., Exploring the benefits of multiple injections in low temperature combustion using a diesel surrogate model. Fuel [Internet]. Elsevier; 2016 Feb 1 [cited 2018 Mar 29];165:341–50. Available from: https://www.sciencedirect.com/science/article/pii/S0016236115010972
[67] DieselNet, https://www.dieselnet.com/tech/diesel_fi.php, available on date 30.3.2018.
[68] Nurchi, L., Sales Developer at RABOTTI Diesel Equipment/Diagnostic https://www.slideshare.net/LucaNurchi/common-rail-injectors-bosch, Published on Jan 22, 2016
[69] Purić d.o.o. company, http://www.puric.hr/index.php/en/
[70] DieselNet, https://www.dieselnet.com/tech/diesel_fi_common-rail_control.php, available on date 12.4.2018.
[71] Bosch, Diesel engine management, SAE International, 2nd edition, September 1999
[72] Bosch ESI [tronic] v2013, Service and technical data, Electronic part catalogue, Wiring diagrams, Diagnostic Software
[73] Ohaus Explorer, https://us.ohaus.com/en-US/ExplorerPrecision
[74] Petrić, J.: Hidraulika i pneumatika, 1. dio: Hidraulika; FSB, 2012
[75] Siemens, Industry mall, available on date 13. 4.2018. https://mall.industry.siemens.com/mall/en/us/Catalog/Product/1FL60641AC610AA1
[76] Škrtić, A., Konstrukcija električnog pogona visokotlačne pumpe za ubrizgavanje goriva, Bachelor thesis, Faculty of mechanical engineering and Naval Architecture, Zagreb, 2016
[77] Maschinenfabrik Guido GmbH, Berliner Straße 6, 93073 Neutraubling near Regensburg, Germany, http://www.guido.de/en/contact-us.html
[78] Bosch automotive catalog, http://www.bosch-automotive-catalog.com/en_GB/product-detail/-/product/0281002706
[79] Bosch pressure sensors, available on date 14.4.2018, http://redbarontnt.altervista.org/alterpages/files/sensors_highpressure.pdf

[80] Endresas+Hauser, www.endress.com/en/Field-instruments-overview/Flow-measurement-product-overview/Coriolis-flowmeter-Promass-A100, available on date 2.5.2018
[81] Hana Injectors, www.hana-injectors.com/product-category/hana-lpg-cng-autogas-injectors, available on date 16.4.2018
[82] Siemens - Industry mall, https://mall.industry.siemens.com/mall/en/WW/Catalog/Product/1PH8137-1DG00-1BA1, available on date 28.4.2018
[83] Environment S.A., http://www.environnement-sa.com/products-page/en/graphite-52m-4/, available on date 2.5.2018
[84] Environment S.A., http://www.palgo.se/uploads/documents/635719/Model%20MIR2M%20uk%20s%20p.pdf, available on date 2.5.2018
[85] Engine control and monitoring, http://www.ecm-co.com/product.asp?5210t, available on date 3.5.2018
[86] National Instruments, http://www.ni.com/en-rs/shop/compactrio.html, available on date 3.5.2018
[87] National Instruments, http://www.ni.com/en-rs/shop/labview.html, available on date 3.5.2018
[88] National Instruments,http://sine.ni.com/nips/cds/view/p/lang/en/nid/210732, available on date 3.5.2018
[89] National Instruments, http://www.ni.com/pdf/manuals/NIDIDriver.pdf, available on date 3.5.2018
[90] AVL, https://www.avl.com/combustion-measurement1/-/asset_publisher/gYjUpY19vEA8/content/crank-angle-encoder-of-365-series, available on date 4.5.2018
[91] AVL, https://www.avl.com/documents/10138/2699442/Datasheet+IndiSmart.pdf, available on date 4.5.2018
[92] AVL, https://www.avl.com/-/indicom-indicating-software, available on date 4.5.2018
[93] Savitzky, A., Golay, M.J.E., Anal. Chem. 36 (8) (1964) 1627–1639
[94] Woschni, G., No Title, Universally Applicable Equation for the Instantaneous Heat Transfer Coefficient in the Internal Combustion Engine,‖ in SAE Technical Paper 670931, 1967.
[95] Tahir, M.M., et al., Performance Analysis of A Spark Ignition Engine Using Compressed Natural Gas (CNG) as Fuel. Energy Procedia [Internet]. 2015 Apr;68:355–62.
[96] Aslam, M.U., et al., An experimental investigation of CNG as an alternative fuel for a retrofitted gasoline vehicle. Fuel [Internet]. 2006;85(5):717–24.
[97] Jahirul, M.I., et al., Comparative engine performance and emission analysis of CNG and gasoline in a retrofitted car engine. Appl Therm Eng [Internet]. 2010;30(14):2219–26
[98] Cho, H.M., He, B-Q, Spark ignition natural gas engines - A review. Energy Convers Manag [Internet]. 2007;48(2):608–18
[99] Raju, A.V.S.R., et al., Experimental investigations on a lean burn natural gas fuelled si engine at different compression ratios. J Inst Eng Mech Eng Div. 2000;80(4).

[100] Zhang, Q., et al., Combustion and emissions of a Euro VI heavy-duty natural gas engine using EGR and TWC. J Nat Gas Sci Eng. 2016;28.
[101] Zoldak, P., Naber J., Spark Ignited Direct Injection Natural Gas Combustion in a Heavy Duty Single Cylinder Test Engine - Start of Injection and Spark Timing Effects. SAE Tech Pap. 2015;2015–Septe.
[102] Zoldak, P., Naber, J., Spark Ignited Direct Injection Natural Gas Combustion in a Heavy Duty Single Cylinder Test Engine - AFR and EGR Dilution Effects. SAE Tech Pap. 2015;2015–Septe.
[103] Lim, G., et al., Effects of compression ratio on performance and emission characteristics of heavy-duty SI engine fuelled with HCNG. Int J Hydrogen Energy. 2013;38(11).
[104] Takagaki, S. and Raine, R., "The Effects of Compression Ratio on Nitric Oxide and Hydrocarbon Emissions from a Spark-Ignition Natural Gas Fuelled Engine," SAE Technical Paper 970506, 1997, doi:10.4271/970506.
[105] Asar, G.M.M., et al., Study of Natural Gas in an AIR-Cooled Spark Ignition Engine. SAE Technical Paper SAE 1997-10-972113, p291-p296. 1997
[106] Zhu, G., et al., "MBT Timing Detection and its Closed-Loop Control Using In-Cylinder Pressure Signal," SAE Technical Paper 2003-01-3266, 2003, https://doi.org/10.4271/2003-01-3266.
[107] Delphi Technologies, http://delphi.com/docs/default-source/worldwide-emissions-standards/2016-2017-heavy-duty-amp-off-highway-vehicles.pdf?status=Temp&sfvrsn=0.03636262961639791
[108] Sremec, M., et al., Numerical Investigation of Injection Timing and Knock on Dual Fuel Engine. Proceedings of 2nd SEE SDEWES Conference, Piran, Slovenia, 2016.
[109] Eswara, A.K., et al., Introduction to natural gas: A comparative study of its storage, fuel costs and emissions for a harbor tug, Annual Meeting of Society of Naval Architects & Marine Engineers (SNAME), Bellevue, Washington, USA, 2013
[110] Nett Technologies Inc., https://www.nettinc.com/information/emissions-faq/how-does-an-oxidation-catalyst-work
[111] Basshuysen, R., Schäfer F., Internal combustion engine handbook, SAE International, Warendalle, Pa, USA, 2004

Curriculum Vitae in English

Personal data

Name:	Mario Sremec
Address:	Radešić 43a, 42 225 Breznički Hum
Date and place of birth:	24th March 1990, Varaždin
E-mail:	sremec.mario@gmail.com

Education

11/2014 – 12/2018	Faculty of Mechanical Engineering and Naval Architecture, Zagreb Doctoral study Course: Theory of Structures
2/2012 – 7/2013	Faculty of Mechanical Engineering and Naval Architecture, Zagreb Graduate study Course: Design and Product Development Master degree in mechanical engineering (MEng Mech)
9/2008 – 2/2012	Faculty of Mechanical Engineering and Naval Architecture, Zagreb Undergraduate study Course: Design and Product Development Bachelor degree in mechanical engineering (BEng Mech)
9/2004 – 6/2008	Electromechanical school, Varaždin Course: Mechatronics technician

Work Experience

1/2015 –	Faculty of Mechanical Engineering and Naval Architecture, Zagreb Project Assistant
7/2014 – 1/2015	Wenker – Križanec d.o.o. (WE – KR d.o.o.), Ivanec Mechanical Engineer
4/2014 – 6/2014	IMG d.o.o., Zagreb Head of Technical Department and Production
9/2013 – 3/2014	Electromechanical school Varaždin Teacher of mechanical courses

Publications

- The list of publications: https://bib.irb.hr/lista-radova?autor=359014

Curriculum Vitae in Croatian

Osobni podaci

Ime i prezime:	Mario Sremec
Adresa:	Radešić 43a, 42 225 Breznički Hum
Datum i mjesto rođenja:	24. Ožujka 1990., Varaždin
Email:	sremec.mario@gmail.com

Obrazovanje

11./2014. – 12./2018.	Fakultet strojarstva i brodogradnje, Zagreb Poslijediplomski doktorski studij Smjer: Teorija konstrukcija
2./2012. – 7./2013.	Fakultet strojarstva i brodogradnje, Zagreb Diplomski studij Smjer: konstruiranje i razvoj proizvoda Magistar inženjer strojarstva
9./2008. – 2./2012.	Fakultet strojarstva i brodogradnje, Zagreb Preddiplomski studij Smjer: konstruiranje i razvoj proizvoda Sveučilišni prvostupnik inženjer strojarstva
9./2004. – 6./2008.	Elektrostrojarska škola Varaždin Tehničar za mehatroniku

Zaposlenje

1./2015. –	Fakultet strojarstva i brodogradnje, Zagreb Asistent – suradnik na projektu
7./2014. – 1./2015.	Wenker – Križanec d.o.o. (WE – KR d.o.o.), Ivanec Konstruktor metalnih konstrukcija
4./2014. – 6./2014.	IMG d.o.o., Zagreb Voditelj tehničkog odjela i proizvodnje
9./2013. – 3./2014.	Elektrostrojarska škola Varaždin Nastavnik iz strojarske grupe predmeta

Publikacije

- Lista publikacija: https://bib.irb.hr/lista-radova?autor=359014